An Investigation into Nanowire Formation via AFM, Neutron Scattering and various other methods [EDITED]

by

Adam Hobson

A thesis submitted in fulfilment for the

degree of Master of Philosophy in

Chemical Engineering and Physics and Astronomy

Department of Chemical and Biological Engineering

and

Department of Physics and Astronomy

September 2014

Dedicated to my late supervisor, mentor and friend,
Dr Tim Richardson.

For without him, and his passion for research, I would not be where I am today.

Abstract

The formation of nanowire structures from poly(3-hexylthiophene) (P3HT) in solution is of great interest in fields such as vapour sensing and organic solar cells. Being able to control formation, deposition and characterise these nanowires is therefore of great interest to maximise the potential of these devices. To this end this research investigates the growth of these nanowires in solution via small angle neutron scattering, and ultra-violet visible spectroscopy.

The ability to align these nanowires on a solid substrate is also of interest, as well as obtaining large quantities of aligned and densely packed nanowires. Therefore this thesis has investigated optimal processing conditions, deposition methods and post processing methods to get the optimal P3HT nanowires and nanowire alignment. Various methods of characterising the nanowires, such as ultra-violet visible spectroscopy, small angle neutron scattering, atomic force microscopy etc. have been used to characterise the nanowires that were created.

These nanowires were also tested for use in applications such as vapour sensing, by use in water-gated transistors and the effects of using nanowires, rather than a thin film of P3HT was also investigated.

In summary, various techniques for the production and optimisation of P3HT nanowire thin films were investigated, the growth of which was also carefully studied. Finally the nanowire films were characterised using various methods and applications tested to determine how to use nanowires to optimise these applications, namely for the purpose of vapour sensing.

Table of Contents

Table of Figures

1. Introduction

This thesis describes the author's contribution towards his degree of doctor of philosophy. The scope of the research was to investigate, using various characterisation methods (such as atomic force microscopy, ultra-violet visible absorbance measurements, current voltage probing, and neutron scattering) to probe nanoscale materials. The main material used by the author in this research was a carbon polymer known as poly(3-hexylthiophene) (P3HT). P3HT has interesting potential in applications such as solar cells [1] or toxic chemical detection [2, 3], and thus investigating the formation of nanowires from P3HT solutions could help improve such devices.

The main objectives of the research and thus the scope of the thesis are outlined below:

i. Investigate various processing and deposition methods of P3HT from solution as well as finding the optimal solvent for deposition.
ii. Investigate the growth of P3HT nanowires in solution and find optimal conditions.
iii. Optimise the alignment of P3HT nanowires on a solid substrate and remove amorphous molecularly dissolved P3HT.
iv. Characterise P3HT nanowires in solution and on a solid substrate using a variety of methods, mainly AFM and neutron scattering.
v. Explore applications of P3HT nanowires, such as in vapour sensing devices.

This thesis explains the basic theoretical concepts behind the materials, methods and classification methods used in the research. It goes on to explain the different methods in detail and the advantages and disadvantages of using them. It then describes optimisation and deposition techniques in order to find the optimal methods to align P3HT nanowires. Finally the nanowires are characterised via a variety of methods and applications such as water gated transistors are investigated.

Chapter 2 details the theory and background behind polymers and P3HT as well as the classification and deposition methods used throughout the research. It mainly focuses on P3HT itself as well as the deposition methods, the main two being atomic force microscopy (AFM) and Small angle neutron scattering (SANS).

Chapter 3 deals with the experimental methods and techniques, which discusses the actual process behind applying processing techniques, deposition techniques and the classification techniques discussed above.

Chapter 4 details a variety of topics, the first of which are the initial experiments to determine and classify nanowire growth in a variety of solvents. It goes on to discuss the nanowire formation at the smallest length scales, as investigated by small angle neutron scattering. Optimisation of the thin films is then discussed, discussing optimal solvent, solvent concentration, deposition and alignment methods. Finally characterisation of the P3HT nanowires in solution and in thin films is discussed.

Chapter 5 discusses the collaboration involving water-gating P3HT nanowires and discusses the advantage of using nanowires in vapour sensing transistors, over tradition P3HT thin films.

Chapter 6 discusses the final conclusions of this thesis and outlines any future work that this thesis could present.

2. Theory/Background

2.1. Basic Organic Chemistry

2.1.1. Carbon Bonding

There can be several definitions of an organic compound from a compound which contains only carbon and hydrodgen bonds to a compound to which contains large amounts of carbon.

The one defining factor in these is the element- carbon. Carbon is the base foundation for most organic compounds and understanding the carbon bonds is important to understanding all other organic chemistry [4]. The basics behind carbon start primarily with the three types of carbon bonds.

Carbon can form three different bonds, a single, double and triple bond. The electron structure of carbon is defined as having six electrons which means there will be a total of four electrons in the valence electron shell using the standard electron shell model. These four electrons can be uses for purposes of bonding. In the most common isotope of carbon (C^{12} the electron arrangement is given by $1s^2 2s^2 2p^2$ (vectorially splitting the p shell gives $1s^2 2s^2 2p_x^1 2p_y^1 2p_x^0$). [4, 5]

The accepted thought process by which carbon bonds is known as hybridisation, by which the wave functions of the four electrons in the valence band mix to form "hybrid orbitals" [4]. For this to occur the configuration of these electrons must be changed, in that a 2s orbital electron must be promoted into the empty $2p_z$ orbital [4, 6]. When this occurs there is a new orbital structure of $1s^2 2s^1 2p_x^1 2p_y^1 2p_z^1$ which allows hybrid carbon bonding. This is a commonly used thought processes used as a midway point between atomic and molecular orbitals. The actual way carbon knows in advance what type of bond will be created, and therefore which type of system to fall into is not known but in this case hybrid bonding is a useful thought concept to allow the process to be explained.

For a first order carbon bond the 2s orbital mixes with all three 2p orbitals to create four hybrid orbitals known as sp^3 orbitals, as shown in Figure 1. These orbitals form a tetrahedron whereby each bond is 109.5 degrees from the other.

When this system bonds with another sp^3 orbital carbon one of the sp^3 orbitals overlaps with the corresponding bond in the alternate carbon atom and forms a very strong and direction bond known as a carbon single bond (σ-bond).

Edited

Figure 1: Bond hybridisation for sp^3 orbitals [7].

Another carbon bond is shown in Figure 2 where we have mixing of only two of the three 2p bonds. This succeeds in creating three orbitals know as sp^2 orbitals, (b) lay flat in a plane at 120 degrees to each other. The un bonded remaining 2p orbital lays perpendicular to this plane [4].

In order for this to bond to another carbon there must be another carbon with an sp^2 bond available. These two bonds overlap (similar to the sp^3 bonding, however in this case the 2p orbital which did not hybridise still remain and overlap to produce a π-bond which is weaker and more localised than the σ bond). Combining these two bonds gives us the carbon double bond.

Edited

Figure 2: Bond hybridisation for sp^2 orbitals [7].

The final type of bond is the sp bond. In this case the 2s orbital mixes with a single 2p orbital to form two sp orbitals and two leftover 2p orbitals. These two orbitals lay along a single straight line and are therefore 180 degrees apart. The remaining 2p orbitals lay perpendicular to these orbitals in the x and y directions. This is shown in Figure 3.

Edited

Figure 3: Bond hybridisation for sp orbitals [7].

2.1.2. Conjugated Molecules

Carbon bonds can be used to explain systems such as conjugated molecules which are incredibly important to organic materials. The Benzene ring for example is a conjugated molecule and is one of the simplest to begin with. It has a hexagonal structure with six carbon atoms in the corners. This gives us an 120 degree angle between each side which is also the bond angle of an sp^2 orbital.

This therefore allows the ring to form two σ bonds with its neighbours and have a bond left-over for a hydrogen bond. The remaining p orbitals have two neighbouring carbon atoms with which to form π bonds. Since neither of these are more or less favourable the molecule chooses an intermediate superposition of both states (Figure 4).

Edited

Figure 4: Figure showing the benzene ring, a superposition of two equally favourable states [6].

This superposition allows the π electrons to become completely delocalised and form a π electron cloud around the molecule.

For a larger molecule such as a large chain polymer the π electrons are not delocalised along the length of the chain and reside around a finite area. These electrons contribute to the formation of nanowires as they allow the polymer chain to stack as discussed later in this manuscript.

2.2. Poly(thiophene)

2.2.1. Basics of Thiophenes

Thiophenes are a conjugated polymer system which allows high quality conductivity. This is due to delocalised π electrons allowing current to flow along the length of the polymer. Thiophenes themselves are a single repeat unit with the delocalisation coming into affect when chains are attached to form a poly(thiophene) polymer chain [9]. These poly(thiophenes) have a low density but a well defined direction of conductivity along the chain. They are a part of a group of well known conjugated polymers known as heterocycles, as they contain two different types of atom in the polymer backbone. They are useful due to their hole transporting capabilities and large relative stability.

The repeat unit of any poly(thiophene) is shown in Figure 5 with a simple repeat unit of a thiophene molecule containing four carbon atoms and a sulphur (chemical formula C4H4S) [10].

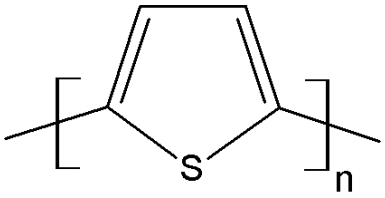

Figure 5: The polymer repeat unit of a poly(thiophene)

An addition of any side chain gives us specific polythiophenes with different properties and uses, one of which (poly(3-hexylthiophene) is discussed in the appropriate section.

2.2.2. Poly(3-hexylthiophene) (P3HT)

Poly(3-hexylthiophene) (P3HT) and other similar conjugated polymers have attracted a lot of research interest and are best known because they are effective electron donors and hole transporter [6, 11] materials in photovoltaic devices. They also have potential in other applications such as toxic chemical detection. Understanding the formation of nanocrystalline P3HT structures and knowing their electronic properties is therefore of considerable interest. The formation of crystalline P3HT within organic photovoltaics, for example, is known to improve device efficiencies.

For this reason P3HT was chosen as a suitable research material for creating nanowires to attempt to improve efficiencies of the above mentioned devices. P3HT is a long chain polythiophene with attached hexyl side chains (C_6H_{13}). The repeat unit of P3HT is shown in Figure 6.

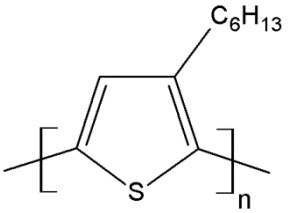

Figure 6: A P3HT repeat unit.

The alkyl chain of the P3HT allows an increase in solubility which allows thin film processing from solution which allows a lower cost and ease of sample creation.

2.2.3. Fibrilisation of P3HT

When P3HT is dissolved in a solvent it is allowed to reorganise to a more energetically favourable structure. The subject of this manuscript was the formation of crystalline nanowires when the polymer was allowed to fall out of solution. These nanowires form when the P3HT chains interact via the π electrons and stack in a lamellar structure as shown in Figure 7 [12, 13]. These sheets which come together due to interactions between the alkyl groups and form long nanowires via π-π stacking of the delocalised π electrons.

Due to the aligned nature of the nanowires, and as shown in various other scientific papers [5, 6, 14] this crystalline repeating structure allows the nanowires to have a large conductivity of holes. Control of the size, orientation and other properties of these nanowires is therefore an important topic of research.

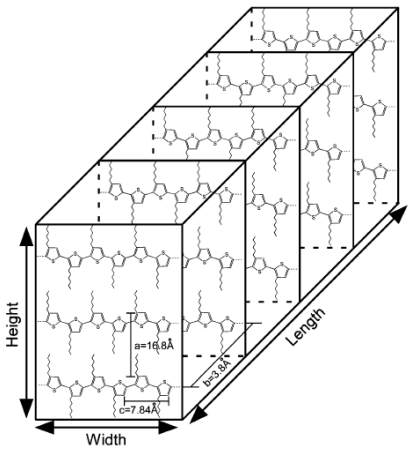

Figure 7: A schematic diagram of the structure of a P3HT fibril. Information from GIXD and TEM/XRD studies. Reprinted (adapted) with permission from [13]. Copyright 2004 American Chemical Society.

2.2.4. Processing methods of P3HT

Various methods for processing P3HT from solution exist. These methods are discussed in more detail in their relevant theory and experimental methods sections but will be briefly detailed here.

Drop casting is on of the simpler methods whereby the solution is applied dropcast to a substrate and allowed to either dry naturally in air or in a sealed container. This typically produces thicker films due to the slower drying times of other methods.

Another methods similar to drop cast would be spin casting whereby a substrate is rotated at high speeds [15] (for example between 1000-5000rpm) and the P3HT solution is dripped onto the substrate either before or during spinning. The spin speed can be altered to change the thickness of the film (as well as the viscosity of the solution) and generally produces more uniform films.

Langmuir Blodgett [16] and Langmuir Schaefer [16] films both involve applying the solution to a water surface and allowing the solvent to evaporate, leaving a thin, uniform layer of P3HT on the water surface. The methods differ in the extraction of the layer as the Langmuir Blodgett method requires the substrate to be dipped into the water perpendicular to the substrate surface, whereas the Langmuir Schaefer method has a parallel substrate coming down into contact with the water surface. Both methods have their merits but unless the material has highly hydrophobic and hydrophilic parts it is generally found the Langmuir Schaefer gives the best results [16, 17].

Other methods include different solvents and types of P3HT which are covered later in the manuscript in the experimental methods and results section. It is also possible to have post creation methods of modifying films such as solvent annealing and heat annealing. Heat was not used in this research however solvent “washing” both in solution and on substrate whilst spinning was tested and is mentioned later in the manuscript.

2.2.5. Uses of P3HT

There are many uses of P3HT as it is a very useful and versatile material. It has been used for many years in organic semiconductors as it is a very good hole conductor, especially when paired with an equally good and similar electron conductor (PCBM) to produce a relatively efficient photovoltaic device. P3HT would also be useful in the new field of organic lighting as well as various other new organic devices [6].

P3HT has also shown considerable promise in vapour sensing devices (especially polar organic compounds) [2, 18]. From previous literature it has been used to sense hydrazine, monomethylhydrazine, methanol and hexane etc. [2, 17-19]. Improving the sensitivity and selectivity of these devices would therefore be of great use.

Nanowires may allow this to occur by increasing the surface area for sensors or also increasing the interfacial mixing in solar cells.

2.2.6. Alignment

Various methods exist to attempt to align nanowires. This would be beneficial to allow a higher density of nanowires to exist for the purposes of vapour sensing, or a possibility of higher charge running down one axis of a nanowire film.

The first method to attempted to align nanowires could be via the drop cast method and simply allowing the solution to run down an incline. Thermal and solvent annealing can also either align nanowires or improve nanowire alignment and clean up any amorphous material [5, 20].

Another novel way of aligning fibrils would be to use micro-contact printing to deposit the layer directly onto the substrate [21]. A pattern can be imprinted on the stamp which will then give rise to an ordering in the film itself.

A method tested in this research was to float off nanowires from a solid substrate onto a water surface, The material would then either be vibrated or compressed

(or a mixture of both methods) to try to align the nanowires in a preferential direction .

Brush painting is also a novel method of aligning nanowires and would simply require a polymer brush to align nanowires along it's direction of movement [22].

Finally, spinning a nanowire solution at high enough speeds should force the nanowires to align radially along the spin axis and therefore substrates placed at the edges of the spin device would allow for a large parallel alignment [15].

2.3. Langmuir Films

The two Langmuir methods are the Langmuir Schaefer and the Langmuir Blodgett methods, they both start with the same basic principles when a thin film is required on a solid substrate. The solution is added dropwise to a water surface in a PTFA coated trough[16]. This allows the meniscus of the water to rise above the level of the trough and a PTFE barrier to compress any material on the surface. The solution is added to the surface and the solvent allowed to evaporate. The barrier is then compressed to the desired pressure (usually enough to enter the solid regieme but not enough to cause the film to collapse) [17].

For Langmuir Blodgett deposition a hydrophobic substrate (usually a cleaned glass slide treated with HMDS) is held perpendicular to the subphase surface and slowly plunged into it. Due to its hydrophobic nature it can be submerged relatively far into the subphase without breaking the surface. If the substrate is then retracted, two layers of our material are applied to the substrate. As seen in Figure 8, Repeated dipping allows multiple layers of material to be applied to the substrate [16].

Edited

Figure 8: Diagram of the Langmuir Blodgett method [17].

The Langmuir Schaefer technique is similar up to the point where the substrate is dipped into the water subphase. For this method the substrate is parallel to the water surface and is brought down into contact with the layer and brought up again. In this action only one layer of the material is added. Multiple layers can be added by moving the substrate to a different area and dipping again. This method is useful for materials that are more rigid and cannot bend for the Langmuir Blodgett method. Instead the layer simply adheres to the substrate and is ripped off the water subphase [16]. This is shown in Figure 9.

Edited

Figure 9: A diagram of the Langmuir- Schaefer method [17].

2.4. AFM

The basic concept behind AFM is that it is a type of scanning probe microscopy, but does not require the surface to be charged (unlike Scanning tunnelling microscopy) and can thus be used to scan a wider variety of surfaces. It is especially useful in the non-contact and tapping modes for surfaces that would normally be destroyed by full contact mode scanning (such as soft polymers).

The basic principle of AFM is a simple one, a sharp, nanoscale tip which is attached to a cantilever is scanned across the sample surface. The interaction with the tip and the surface is measured, as well as the position of the tip in order to get a topographical view of the sample surface. These height images are an improvement on a simple microscope as we get a 3d image and have improved resolution (typically optimal sample conditions and tops at around 0.1 to 1nm in the x-y resolution and 0.01nm in the z direction).

In simple terms, when the AFM tip glides across the surface, the force between the sample surface and the end of the tip causes the cantilever to be deflected slightly, this deflection causes a laser which is reflected off the tip onto a photodetector array to also be deflected

As the tip and laser are calibrated we can then use this laser deflection to determine the height of the cantilever as shown in Figure 10 .

Figure 10: A schematic diagram of an AFM [23].

There are three basic AFM modes that can be used:

- Contact mode (<0.5nm probe-sample separation)
- None contact mode (0.1-10nm probe-sample separation)
- Tapping mode AFM (0.5-2nm probe-sample separation)

Contact as it suggests is a full contact mode where the tip is drawn across the surface of the sample, for this mode the tip can either be set to keep a constant height, or (more commonly) a constant force mode. Conversely the non-contact mode uses the attractive forces between the sample and tip to create a topographical map of the surface. These three modes are shown in Figure 11 as a function of the separation between the cantilever and sample[24].

Edited

Figure 11: Force as a function of probe-sample separation [25]

Tapping mode is extremely useful to scan soft surfaces such as polymers, which would otherwise be destroyed using a full contact mode.

Tapping mode works by having the cantilever oscillate at its resonance frequency. In this way the tip will only lightly tap the surface when scanning along it. The AFM is set to keep a constant oscillation amplitude then the information in height changes to maintain the oscillation will present the height scan of the sample [25-27].

The main limiting factor in the resolution of the AFM is usually the tip. It is recommended that an AFM session is begun by scanning a relatively small area to begin with then switch to larger and larger area as the tip "blunts" on the surface. The sharpness of the tip will determine the maximum resolution unless an amount of material adheres on the end of the tip. Larger images can still be captured however with a slightly lower resolution if you simply re-tune the tip for the extra weight on it from the material.

AFM is an incredibly versatile technique probing a sample surface. There are a few disadvantages however such as the long scan time compared to a UV-Vis spectrometry measurement and that AFM is only a surface measurement and cannot probe deeper into the surface [27-29].

2.5. Small Angle Neutron Scattering

2.5.1. Basic Concepts

A few basic concepts of small angle neutron scattering (SANS) will be mentioned in this section. The section will not go into a great detail as neutron scattering was not the main scope of the investigation but a summary will be provided as the technique was very useful in probing growth at the shorter length scales of growth (approximately 0.5-100 nm [30]).

The SANS technique was used for this research due to the fact that it can probe such small length scales. This was particularly useful as techniques such as AFM could not allow us to detect growth in the very early stages of nanowire growth, especially as a large amount of amorphous material is also present, making it difficult to ascertain the size of the forming nanowires.

The basic principle of neutron scattering is that the thermal neutrons are scattered elastically by whatever sample the beam is incident on, this sample can be solid or liquid and the scattering pattern that results on the target can be analysed to provide a wide range of information about the sample, such as size, shape and other factors dependant on the sample in question [31].

SANS was also useful for this research as x-rays do not distinguish between deuterated and non deuterated substances. Therefore x-ray scattering of carbon based chlorobenzene and chloroform versus P3HT would give very little contrast. In contrast to this, there is a large difference in scattering length density between deuterated solvent and non deuterated P3HT [31-33] which means we get a good contrast and strong signal when scattering. This allows us to differentiate between solvent and P3HT.

Another advantage is that, for other techniques such as light scattering, or UV-Vis, for a sample that is opaque, as not enough light can pass through to get an

adequate sampling [33]. However the solutions may not be opaque to neutrons which can therefore be used to probe these opaque solutions.

The typical wavelengths of neutron radiation are between 0.01 and 3nm [33]. This is useful when we wish to probe small length scales, as visible light can only probe length scales around 400-700nm).

When neutrons are incident on for example, a suspension of particles in a liquid, these nuclei (due to them being smaller than neutron wavelengths) act like point scatterers, meaning neutron scattering remains constant as angle increases. Meaning scattering patters can be taken over a range of angles [31].

Another advantage, but also potential disadvantage of neutron scattering is that neutrons, compared with x-rays are very weakly interacting with matter. This means that neutron radiation can penetrate deep into a material (which is beneficial) but also means that it takes a substantially longer time to collect enough neutron scattering data, compared to the relatively quick collection rate of x-rays [32, 33]. This also means however that the sample is less likely to be damaged via exposure to neutron radiation than it is of x-ray.
For SANS a beam of collimated neutrons is directed at the sample, a small area is passed through, as with light scattering an amount of the neutron radiation will be transmitted, an amount absorbed and amount scattered [31]. The detector, placed at some distance away, will record the flux of the radiation scattered (as well as direct beam) and angle away from the detector [33]. This gives us the differential cross section of the neutron scattering with respect to intensity, from this we can get all the information about the size shape and interactions of the scattering objects [33].

It is important for each experiment to ensure the detector has the correct "Q-space) range which is as reciprocal of the length scales of the scatterer. Thus the Q-range of the instrument must encompass the expected size of the scatterer or no useful data will be found due to the range laying outside the range of the instrument [31].

When the data is reduced from the detector into a format which has the Intensity versus Q, this can then be modelled depending on expected size and shape of the scatterer in order to find important information about the scattered. This obviously will depend on the expected scatterer and model in order to determine what properties can be found from modelling.

2.5.2. Porod Guinier Model

The Porod-Guinier model was chosen for the neutron scattering experiments as it encompasses the expected states of the nanowires in solution. The Guinier model is a standard model used for determining the size of dilute, monodisperse spheres, this is known as the Guinier regime [34]. The porod model on the other hand is used for elongated objects like chains, as well as lamellar structures. Combining the two gives the Porod-Guiner model which includes a porod exponent to determine the degree of elongated chains and can thus determine the structure of the nanowires [34]. The Guinier regime should be seen when the nanowires have not yet formed and thus the P3HT is almost like small point like objects, as nanowires grow the Porod regime comes into effect as the P3HT nanowires grow into the elongated chains. There may also be some lamellar effects due to the stacking of the chains which would mean a lamellar porod regime would be seen [34]. Information about the equations used in the model can be found at the corresponding information file from SAS view [35] but was beyond the scope of what was needed for this research. The parameters of the model will however be briefly described. The scale factor and background adjust the scale of the model due to different intensity, and the background noise of the instrument respectively. There is also a radius of gyration and a porod exponent which determines the type of porod shown and the important factor which is the dimensionality factor (s). This factor was what was needed as it gives information on the regime the sample is in. An S value of 0 shows that there are only 3D globular objects such as spheres in the solution, an S value of 1 shows 2D symmetry such as long chains or rods, finally an S value of 3 shows 1D symmetry such as lamellae or platelets [34]. Of course in the actual measurements it is expected that the value given from the

model will not be an integer and will in fact show combined states between these three regimes.

2.6. UV-Vis spectroscopy

UV-Visible Spectroscopy is a fairly simple technique for looking at the absorbance spectrum of solution or substrate with thin opaque film. At its most basic it works by measuring the absorbance of a range of wavelengths of light that pass through the sample.

When white light is passed through the sample certain wavelengths of light will excite systems in the sample and cause excitation of electrons by promoting them to a higher energy level. Not all light can do this however so only a specific wavelength of light will excite a specific electrical system[36].

In this case the photon of light that caused the light will be absorbed and the spectrometer at the other end of the sample will register a lack of that wavelength. Thus by comparing a reference sample's transmission (for example an empty curette if we are using a solution) to that of the actual sample we can ascertain what wavelengths are being absorbed in the sample and thus compare to theory and literature [37]. Figure 12 shows the UV-Vis setup, comprising of a white light source, a cuvette station which will hold slides also (with a station cover to block out any ambient light that may affect measurements) and a spectrometer to measure the light transmitted through the sample.

Edited

Figure 12: A photograph of the UV-Vis setup [17]

Via this method very dilute solutions (or less dilute solutions with a smaller path distance) and thin films can have their absorbance measured in real time. This makes it an interesting technique to study nanowire growth in solution as well as to characterise nanowire and non nanowire thin films [36, 38].

For P3HT nanowires specifically, there is an absorbance peak at 450 nm for non-nanowire, molecularly dissolved P3HT whereas if nanowires are present there will also be peaks at 550nm and 600nm due to the electronic π-π stacking interaction, and the vibronic replicas [39].

3. Experimental Methods and Techniques

3.1. Clean-room facilities and working practices

The facility in which most of this research was performed (especially sample preparation) was a clean room. The advantage of using such an area is that work areas are kept free from dust and dirt that could contaminate any samples or solutions being created, which would in turn invalidate any sensitive measurements taken of the sample.

The room features an outer lab where experiments and preparation that does not need a clean environment can be performed. The inner room is sealed off from the outer lab and does not allow any air that is not filtered to pass inside. There is a two door “airlock” system which prevents a flow of dust into the clean room. The user must never open both doors at the same time and an overpressure created by a fan ensures any dust is blown out through vents on the door.

Figure 13: The clean room "airlock", this features a changing area with over boots, hats/hairnets and coats. There is also a dust vent which allows the overpressure to remove dust from the room.

Figure 13 shows the clean room airlock which is equipped with over boots to prevent dust being brought in on shoes, as well as coats and hairnets to prevent hair and dust from clothing entering the room.

The clean room is equipped with an over pressure fan and a HEPA filter box (both shown in Figure 14) which creates an overpressure to prevent dust from entering, and filters to remove as many particulates as possible. The room also features an air purifier with the same filters as the filter box to maximise particulate removal (also shown in Figure 14).

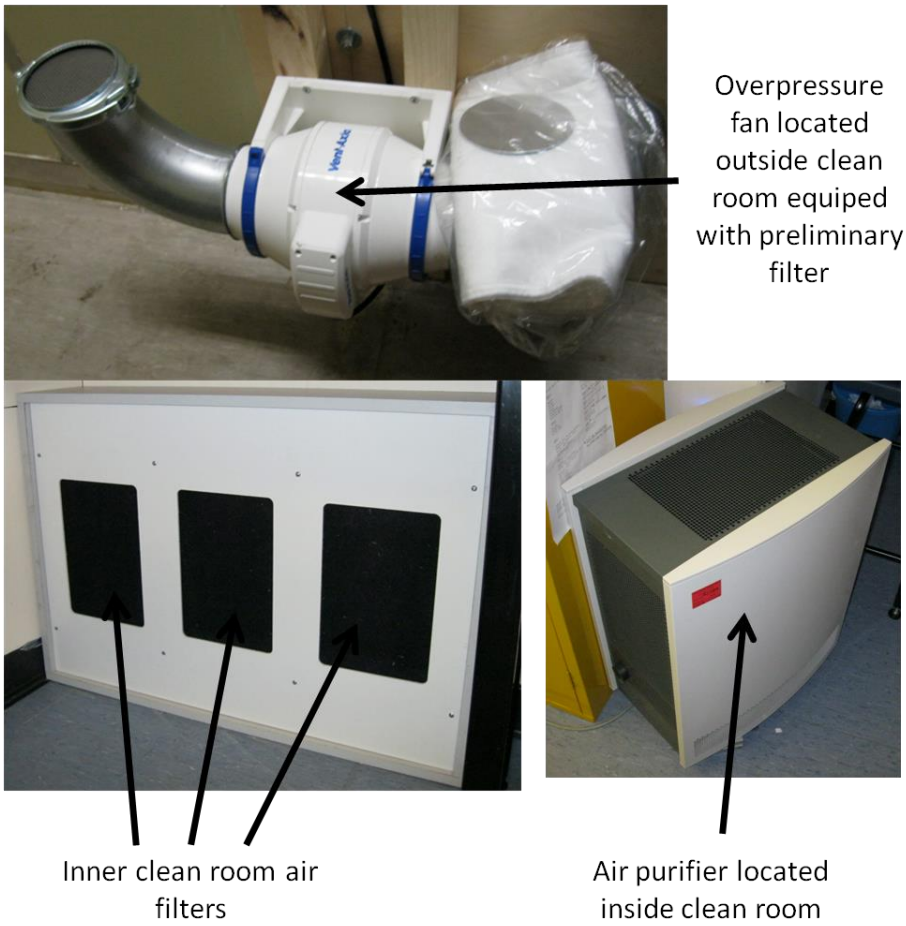

Figure 14: The overpressure fan located outside of the clean room to provide a suitable overpressure for dust removal as well as the filter box and air purifier to ensure minimal dust inside the room.

The room features a large fume hood in order to create a safe working environment by extracting and filtering dangerous vapours from experiments, it is advisable to do preparation in the fume hood, shown in Figure 15).

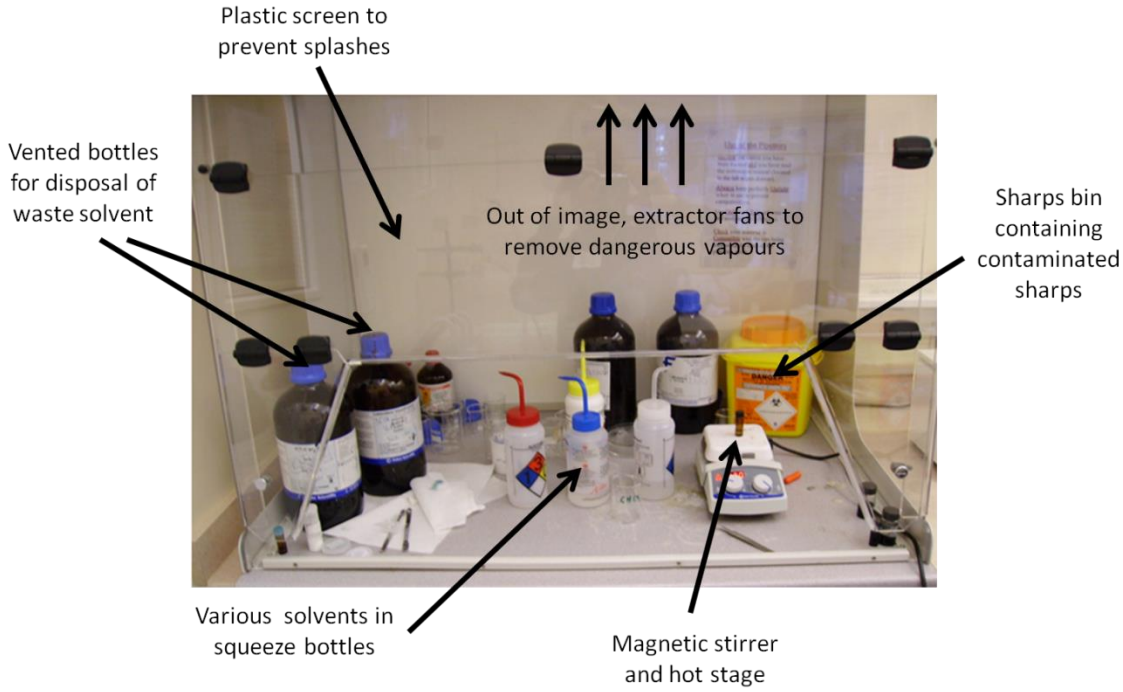

Figure 15: The in clean room fume hood, which allows solutions to be prepared with fumes extracted and filtered. Also extracts fumes from vented waste bottles.

The clean room also includes a sticky mat to remove any residual dirt from the over boots and it is advised to wear disposable nitrile gloves to prevent skin from accumulating, as well as to prevent hands becoming contaminated.

In order to ensure results produced using the facility are consistent, the clean room is equipped with an air conditioning device that allows the room to be maintained at 18 degrees constantly, with temperature and humidity monitors in place to ensure optimal conditions.

The clean room features surfaces which must be kept clean with solvent based cleaners and wiped down with specially designed lab wipes which limit the fibres

that can be released in comparison to non clean room wipes. The paper used in the clean room is also tear proof so that particles from torn paper are not introduced into the clean room environment.

The clean room also has a Purelab ELGA DV25 water purification system which provides de-ionised water which has been cleansed of bacteria and ions. This is especially useful as it is essential to have the purest water possible when working with the Langmuir techniques (as discussed later in this thesis). The ELGA water system is shown in Figure 16.

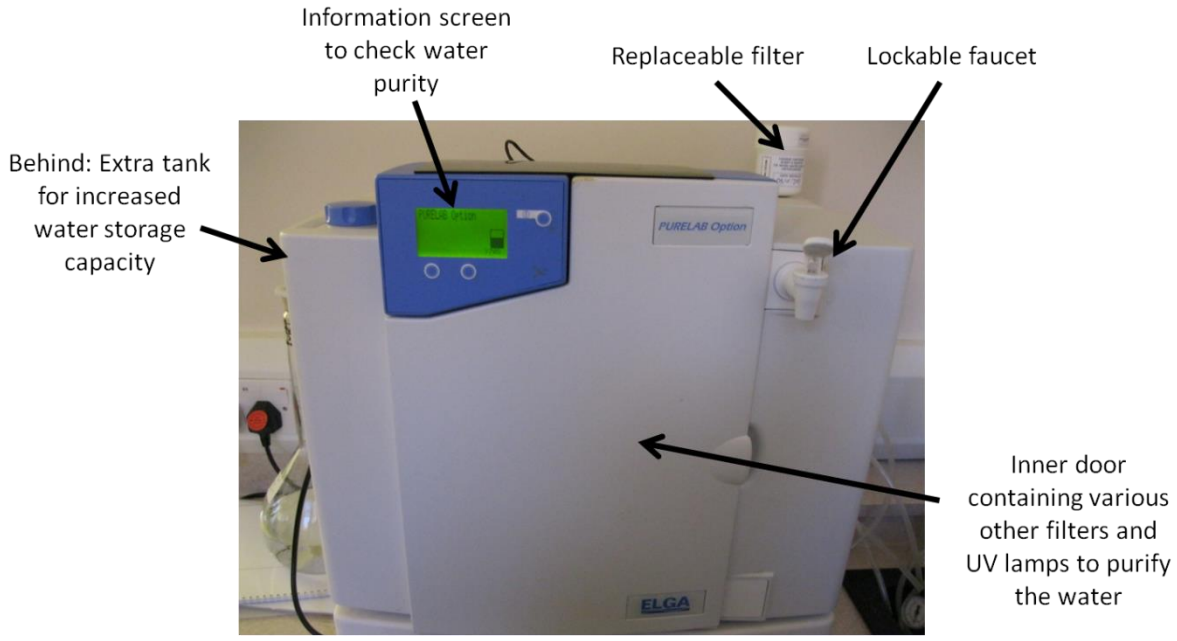

Figure 16: The de-ionised water system.

The clean room also features a variety of clean glass ware, as well as a glassware oven to thoroughly dry the glass after cleaning. Generally the glassware is all cleaned in the same fashion; however it is common practice to have glassware for use with one solvent only, and to have a designated "clean solvent" beaker and another for waste only. This helps prevent contamination which could alter results and reduces the need for cleaning between uses.

To clean glassware after use it is generally accepted to place them in the sink with diluted Helmanex solution and gently clean them with a cloth. After a thorough rinse of pure water the glassware can be placed in the glassware oven to thoroughly dry (shown in Figure 17).

Another method used to clean glassware before use is to swill with chloroform, then IPA to remove any residual chloroform then water to remove any IPA. The nitrogen gun can then be used to remove any water left behind. The two methods both produce clean glassware however the chloroform-IPA-water method seems to be preferred for a better clean overall.

Figure 17: The glassware oven used to thoroughly dry glassware.

Finally the clean room is also equipped with various other pieces of equipment to assist research such as a microbalance, IPA reflux unit for glass slide cleaning (discussed later in this section), pipettors for measuring out solvents, a sonic bath for cleaning substrates and possibly glassware, and several chemical cabinets and a fridge for storage of solutions. Any specialist equipment in the clean room which

was not mentioned here and is relevant to this thesis is discussed in the appropriate section.

3.2. Making Solutions

The primary solutions used for this research were solutions of P3HT dissolved in various solvents, mainly chlorobenzene for the majority of the studies as it was found to produce optimal nanowires (as discussed in the results chapter). It was also found that optimal concentrations for creation of nanowires were between 5-10 mg/ml. Generally with around 5-10ml of solvent and thus 25-50mg of P3HT powder respectively. The P3HT used in the majority of the experiments was from Ossila [40] and was the M101 96.6% regioregular P3HT, unless stated otherwise).

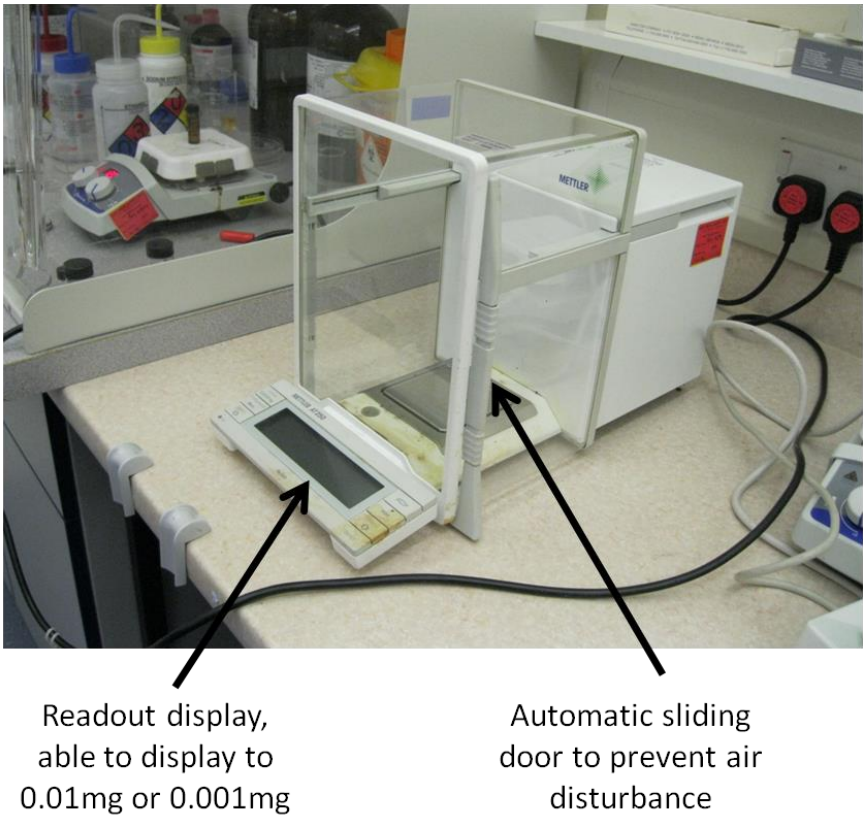

Figure 18: The Mettler AT250 microbalance used to weigh P3HT powder for solution creation.

The first step in solution creation was to take an amber vial (amber as it is possible that the light sources in the clean room may affect the solution, therefore amber vials were used with foil around to limit light exposure) and place it on the microbalance shown in Figure 18. A small spatula (PTFE coated as P3HT is attracted more to metal spatulas) was used to carefully scoop P3HT into the vial which was then weighed. When the desired amount of P3HT was weighed out, the corresponding amount of solvent was extracted from a clean beaker via an appropriate pipettor Figure 19 and carefully added to the P3HT vial.

Figure 19: A set of pipettors used with disposable PTFE to measure and dispense pure solvents.

A small magnetic stirrer pip was then added to the bottle and the lid tightly screwed on. The bottle was then left for 10 minutes on a hotstage/stirrer to make sure the

P3HT dissolved in the solvent. The temperature used depended on the solvent used and was always below the boiling point to prevent explosion. The magnetic stirrer/hot plate can be seen in Figure 15 at the front right of the hood.

After the solution is thoroughly mixed the magnetic stirrer pip is removed via a PTFE coated magnetic wand and left to stir in a vial of clean solution so it may be re-used. The solution is then poured into a syringe and slowly pushed through a 5μm Whatman PTFE filter into another clean amber vial. This is to remove any un-dissolved P3HT in the solution.
The vial is then wrapped in foil and is ready for use or to be left to grow nanowires.

3.3. Substrate Preparation and Cleaning

During the course of this research two main substrates were used. During the initial research whole glass slides were used and for that the IPA reflux method was ideal, when silicon and smaller glass pieces were used it was no longer possible to perform the IPA reflux and thus the oxygen plasma cleaner method was used instead.

3.3.1. IPA reflux method

The IPA reflux method is ideal for cleaning long glass slides as it employs a slide holder to work. When handling the glass slides it is always necessary to wear clean disposable nitrile gloves in order to not contaminate them with oils and skin from fingers. The first step to cleaning was to place the slides into the slide holder which was then lowered into a beaker and fill until the slides are covered with pure di-water. After this a small amount of Helmanex solution was added and the beaker lowered into a sonic bath and left to vibrate for 10-15 minutes. This allows any dirt to be dislodged from the slides (sonic bath is shown in Figure 20.

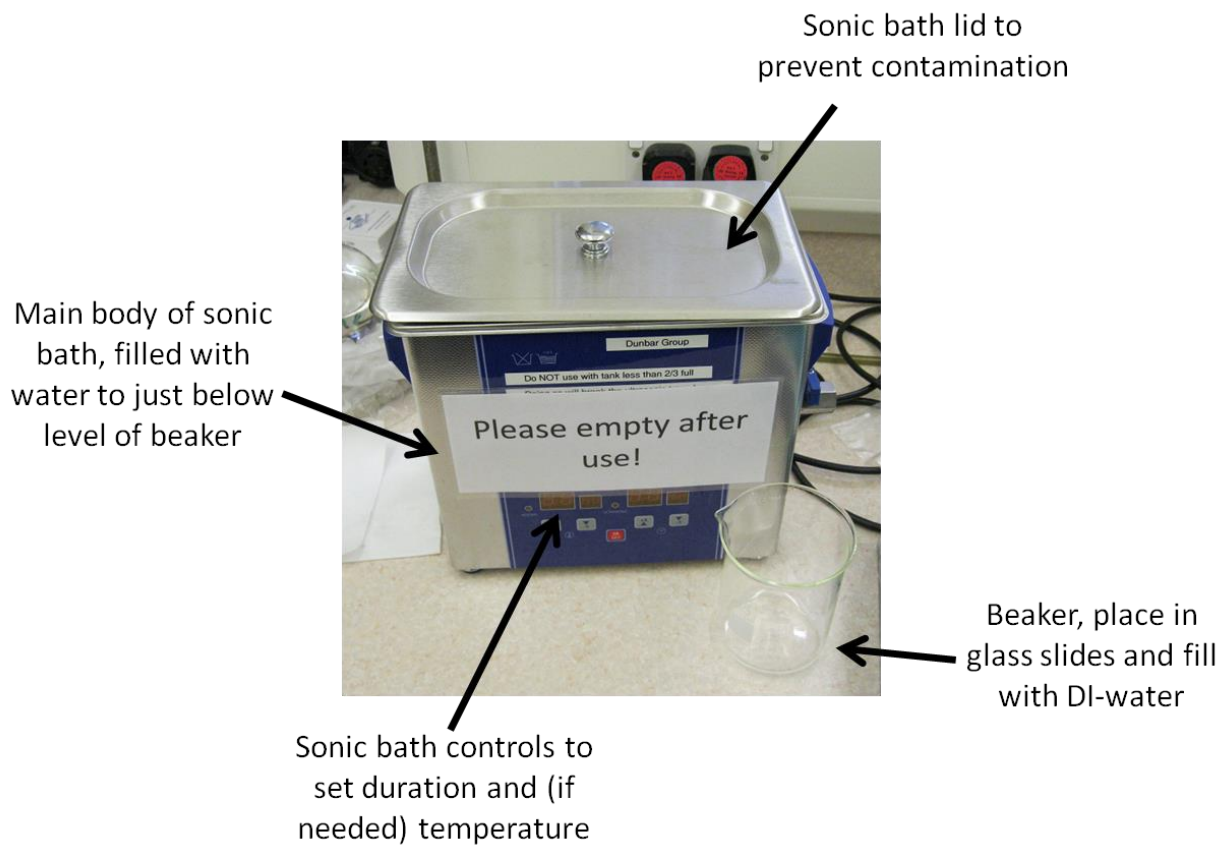

Figure 20: Sonic bath used to pre-clean glass slides.

After removing the slide holder from the beaker they were rinsed in di water until all traces of the Hellmanex were removed. The slides and holder was then lowered using tweezers into the vessel of the IPA reflux and the lid replaced. After ensuring an adequate amount of IPA in the bottom of the reflux unit and that the water cooling was switched on (in order to condense the IPA) the reflux unit was switched on and left for 2 hours (IPA reflux unit is shown in Figure 21).

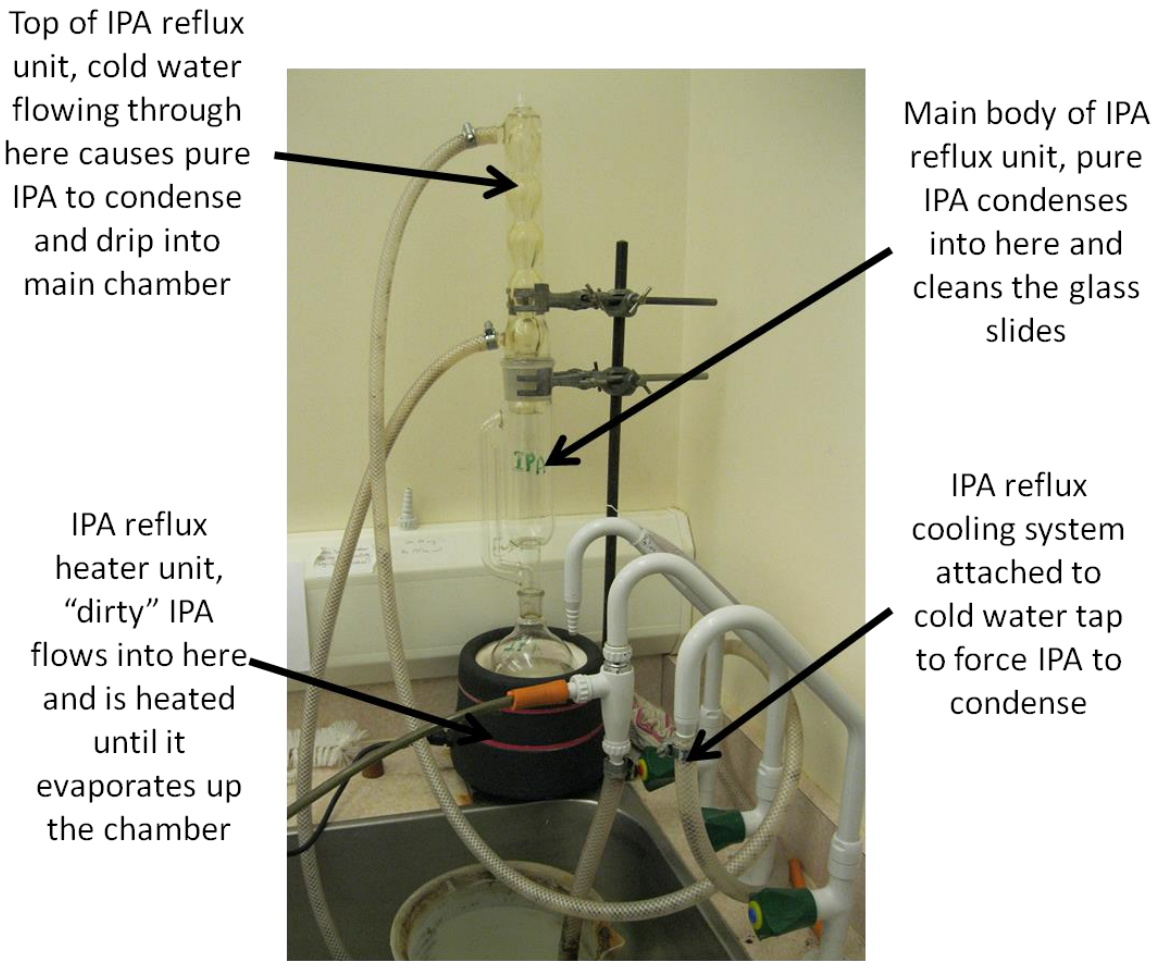

Figure 21: The IPA reflux unit which uses pure IPA to flush and clean glass slides.

The reflux unit works by heating up IPA so that it evaporates, leaving any impurities in the lower part of the chamber, this is then condensed in the top via the water cooling and pure heated IPA drips into the central chamber, washing the glass slides. When the IPA reaches a certain level it drops back into the bottom to be evaporated again.

When the cycle has been allowed to run for the desired time the glass slides are removed after the unit has cooled and they are then considered clean and ready to use.

3.3.2. Oxygen Plasma Cleaning

If smaller pieces of substrate are required, it is necessary to use a different technique. This is especially useful since in this research small (approximately 2cm by 2cm) pieces of silicon were used as substrates.

The first step was to prepare the glass or silicon by cutting it to the desired size by using a graphite or diamond scribe, being careful not to shatter the substrate or touch without wearing disposable nitrile gloves. After the substrates are the desired size they were cleaned of any residual shards by use of the nitrogen gun. These substrates were then chemically cleaned before the Oxygen Plasma cleaner to remove any large deposits of dirt on the surface.

First the substrates were dipped into a petri dish of acetone to start the cleaning process and then lifted out using tweezers and dried using the nitrogen gun. As acetone is miscible in IPA the substrates are then dipped in IPA for further cleaning, and again dried using a nitrogen gun. Finally they were dipped into clean acetone and blown dry for a final time using the nitrogen gun.

The substrates were then taken to the oxygen plasma cleaner and loaded onto a large glass plate and placed inside the chamber. The oxygen plasma cleaner works in two ways, first of all the UV light breaks most organic bonds on the surface to remove and break apart and residual contamination. The oxygen plasma created inside then react with the organic contaminants which are then removed by the vacuum pump. This leaves a clean, contaminant free and uniform surface.

After inserting the substrates into the chamber the front window was placed securely on and the oxygen cylinder opened a quarter turn. The machine was turned on and the chamber is pumped to as low a vacuum as possible and then flushed with oxygen. This process was repeated 3-4 times in order to remove any contaminants from the chamber.

After this has been performed the pump button was pressed which allows a steady stream of oxygen whilst maintaining some vacuum suction. The UV bulb was then turned on and the power adjusted as well as the amount of oxygen in order to create

a grey plasma (oxygen plasma) a pink plasma usually indicates too much nitrogen in the chamber so should be avoided.

Finally adjustments were made to ensure the UV light is not too bright that it will pit and damage the surface, but also that it is steady and not flickering. The substrates were left in the chamber for 20 minutes and then the chamber is flooded with oxygen and the substrates removed. They are now cleaned and ready for use.

3.4. Deposition Methods

3.4.1. Langmuir Preparation

In order to spread a Langmuir film the trough was first cleaned via a woven fibre lab wipe and clean chloroform. After the chloroform has had time to evaporate the barrier can be lowered and moved to a far position. Figure 22 shows a typical Langmuir trough setup, with two barriers instead of a more common one. The troughs used in this research mostly had one barrier; some may have two barriers for more uniform compression or may even have a circular barrier.

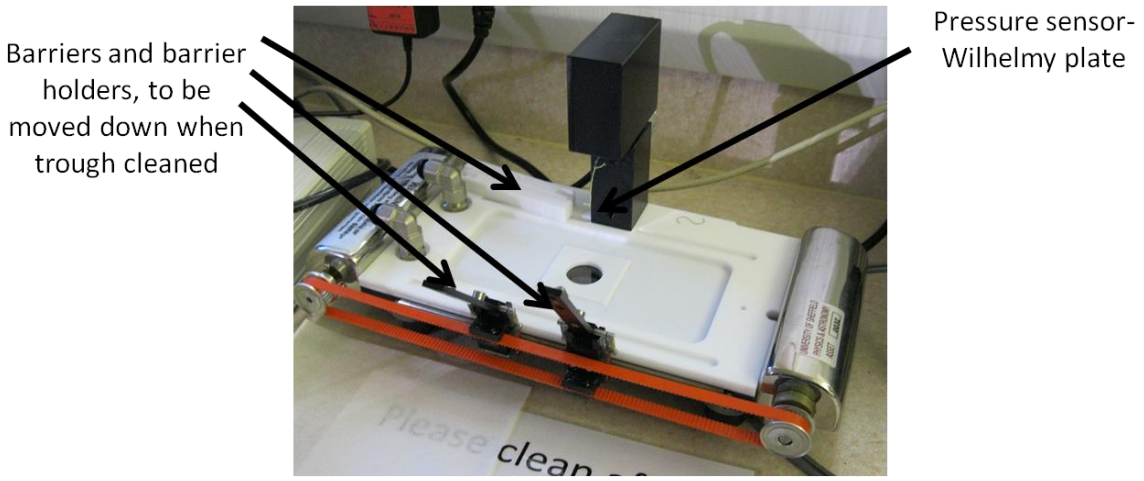

Figure 22: A clean room Nima 601M Langmuir trough, used for mainly isotherms and Langmuir Schaefer deposition.

After the barrier has been lowered, DI-water is poured slowly on the side of the trough away from the channel. This is done until the water level is above the barrier but is not in danger of spilling over the edge of the hydrophobic surface. After this is done the barrier can be opened fully and the non used part of the trough cleaned by using a suction device attached to a mains tap. This device creates suction with running water and a glass pipettor attached to the pipe allows precise cleaning.

The non used area is cleaned first to ensure no floating dirt accidentally falls into the water subphase and rises back up to the deposition side. Once this is done the barrier is closed and the wilhelmy plate lowered into the subphase. The deposition side is then cleaned thoroughly, opening and closing the barrier to test if the water is sufficiently free of debris (this is when the zeroed surface pressure stays constant when opening the barrier).

After the water is clean the barrier is opened and the solution to be either deposited or studied is deposited dropwise via syringe evenly onto the water subphase. In order to allow time for the film to spread evenly and the solvent to evaporate, around 30 minutes (dependant on solvent and material dissolved) is usually the average for a chloroform based solution. (Figure 23 shows the solution being added dropwise to the water subphase).

Edited

Figure 23: A solution added dropwise to a langmuir trough, to then be compressed to form a compact film [17].

After the time has elapsed the trough barrier can be set to compress to the desired pressure, which is does so as the water can pass under the barrier but the film cannot, and thus is compresed (usually an isotherm is performed beforehand as discussed in the theory section, in order to determine the solid region and not to destroy or compress the film to collapse). Once the film has reached the desired pressure it is ready to be deposited onto a substrate.

3.4.2. Langmuir Schaefer

For Langmuir Schaefer the substrate is brought into contact with the Langmuir layer, parallel to the water subphase. This is performed by attaching the substrate

to the automated dipping arm shown in Figure 24 which is programmed to contact the water subphase, but not penetrate the meniscus of the water. The substrate is then brought back up and may either be removed carefully via tweezers and allowed to dry, or the dipping arm may be moved in order to create multiple layers on the substrate.

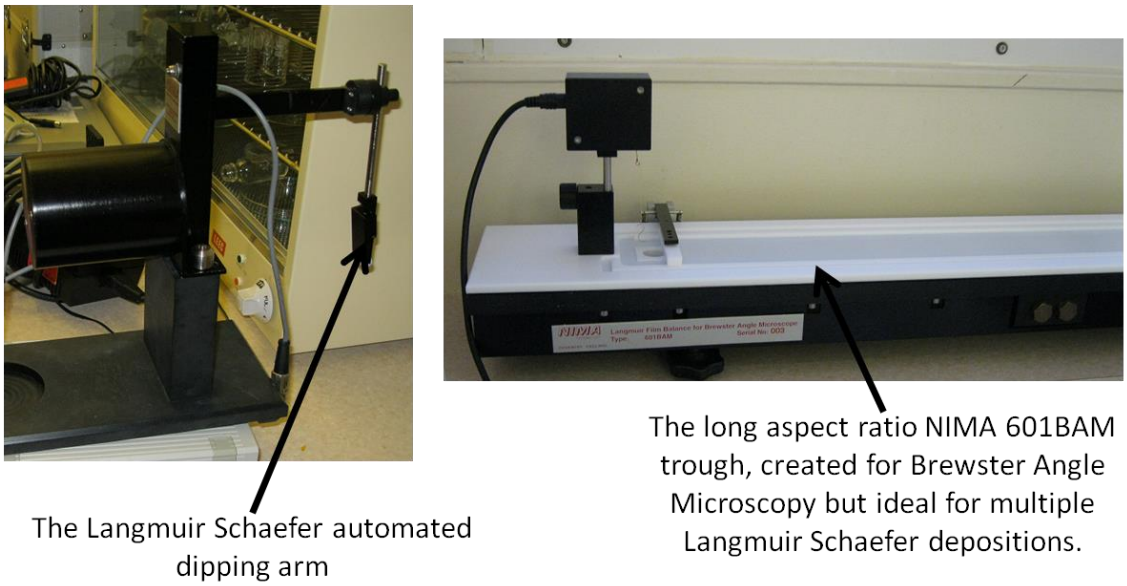

Figure 24: The Langmuir Schaefer automated dipping arm and the long aspect ratio NIMA 601BAM trough, most commonly used for Langmuir Schaefer deposition as well as isotherms due to the aspect ratio.

Langmuir Schaefer works best when it is needed to simply shear the film off the surface and works well for less polar materials which may not want to adhere using Langmuir Blodgett methods.

3.4.3. Langmuir Blodgett

For the Langmuir Blodgett method, the substrate is usually treated with Hexamethydisilazane (HMDS) in order to make the surface more hydrophobic. The substrate is then lowered into the water via the automated dipping arm shown in Figure 25. This is done with the substrate perpendicular to the water subphase.

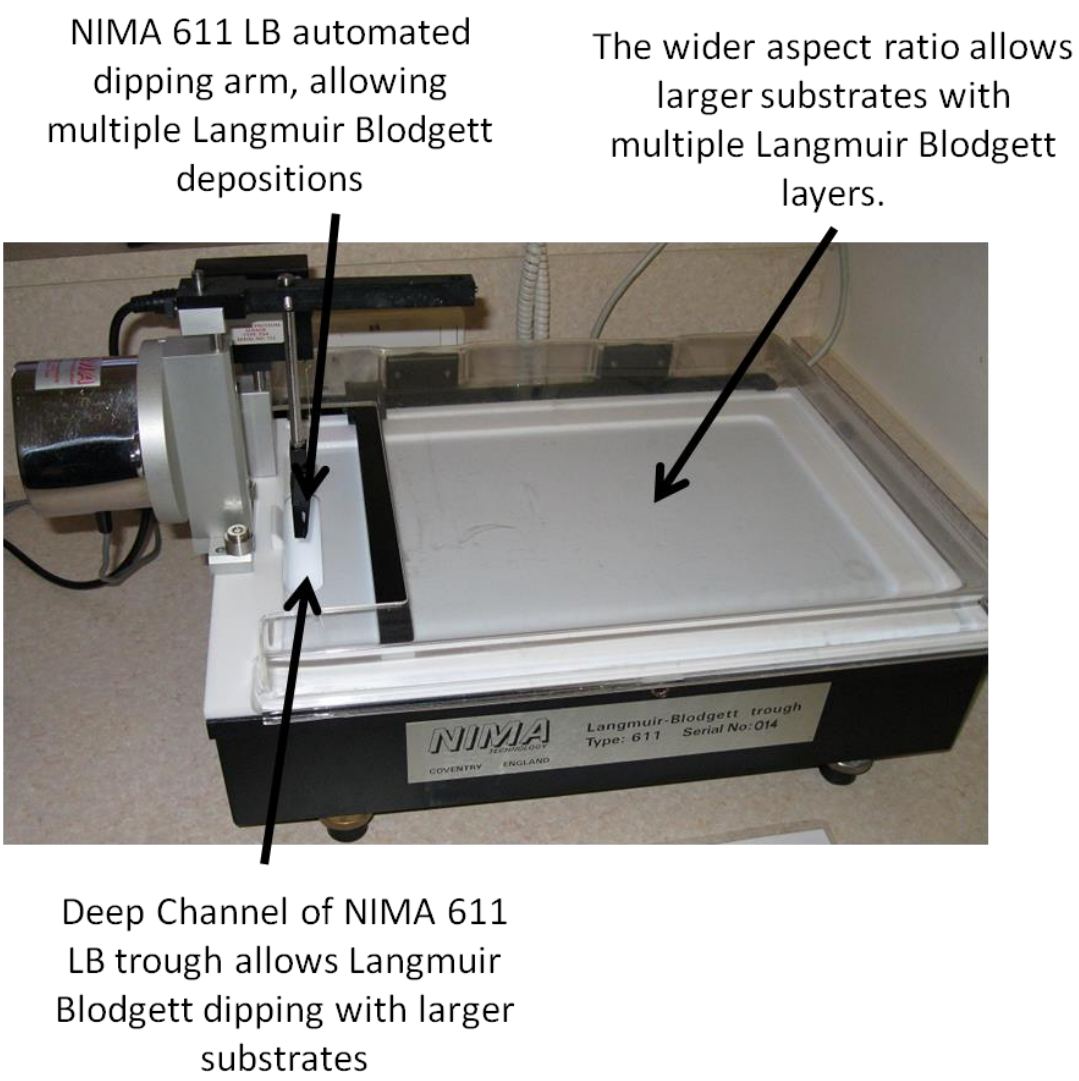

Figure 25: Nima 611 LB trough which allows multiple Langmuir Blodgett depositions, creating multiple layers on a single substrate.

This method generally works well with polar materials as the hydrophilic parts will be close to the water, and the hydrophobic parts will be attracted to the substrate as it enters the water. The substrate is then removed from the water which causes another layer to be deposited on top. The substrate can then be dipped multiple times as long as the barrier is set to maintain the desired surface pressure.

The substrate can then be carefully removed and dried.

3.4.4. Spin Casting

The spin coater was used to make quick, uniform thin films on solid substrates. In order to use the spin coater the substrate must be placed on the vacuum chuck as shown at the centre of the spin coater in (#). The pump is then turned on and a test run can be performed to ensure the substrate is properly secured. If there is any leakage the spin coater will not function until an acceptable vacuum is created.

Figure 26: The "home made" spin coater complete with control box and (out of picture) vacuum pump.

After the substrate is secured the spin coater can be programmed using the control box shown to the left of the spin coater, the acceleration, constant speed and deceleration can all be programmed in, as well as the time spent in all of these phases. Once the spin coater is programmed it is possible to apply the solution to the substrate (usually via a pipettor or syringe) either with the substrate at rest or when it is in motion. The film will differ depending on which option is taken. Generally depositing when the substrate is already moving gives more uniform films, however in our case it seemed to make thinner and less adhered films. The

spin speed and acceleration also has a large impact on the thickness and quality of the films.

The green button shown in Figure 26 can be used to start the program and the red as an emergency stop. Once the program has stopped on its own it is advisable to wait for the substrate to dry before removing it from the chuck. It is advisable to wear goggles and ensure the protective shield is secured as the spin coater is capable of very high speeds and could cause injury if the sample was ejected off the vacuum chuck. It is also good laboratory practice to clean the spin coater after use to remove any solution before it dries.

3.4.5. Drop Casting

The drop casting method was one of the simplest sample preparation techniques. It simply requires a substrate cleaned by the methods mentioned previously, placed into a clean petri dish. The solution is then added dropwise to the centre of the substrate via pipettor or syringe and simply allowed to dry either in air or in a sealed environment. The nature of the drop casting means it will usually be a thicker, less uniform film than one that has been spin cast (although this may not always be the case. The thickness of the film will depend on the viscosity of the solution and the evaporation rate of the solvent itself.

3.5. Characterisation Methods

3.5.1. Atomic Force Microscopy

Atomic force microscopy formed an integral part of characterising a variety of nanomaterial films, such as P3HT nanowires, gold nanoparticles and various transistor devices. AFM was particularly useful as it allows us to view the length scales of the nanowires without having to infer their presence from UV-Vis data or electrical measurements.

The AFM used for most of the characterisation was a Veeco Dimension 3100 with a Nanoscope IIIa controller and basic extender. These were used only in tapping mode due to the delicate nature of the samples and the specific tapping cantilevers used were Bruker's TESPA cantilevers with spring constant and resonant frequencies of 42 N/m and 30 kHz respectively.

As explained in the theory section, the AFM tip touches the surface of the sample and taps at a specific frequency depending on the cantilever used. This creates an oscillation with an amplitude that the device attempts to keep constant. If the topography of the sample changes, the waveform's amplitude does too and height of the tip must also change. This directly corresponds to the height change in the sample. The oscillations are observed via a laser diode being reflected off the tip onto a photo-detector.

Figure 27: An image of the Dimension 3100 AFM [41] .

The first step in setting up the Dimension AFM is to obtain and align a cantilever, the AFM head Figure 27 can be removed from main device and the cantilever holder

also removed (Figure 28) and placed on a separate stand, ready to accept a cantilever. Care must be taken when handling the cantilever as it is very easy to damage or destroy the tip. It is advisable to check that the main cantilever arm is still visible in a microscope before attempting to align the AFM.

Figure 28: The AFM head, including cantilever holder attached at the bottom [41].

Figure 29 shows the cantilever holder with a cantilever inserted into it, be careful to insert the correct way around and keep tweezers away from the triangular end to avoid damaging or destroying the tip. After the cantilever is loaded the holder can be re-attached to the AFM head which can then be locked into the main instrument and plugged in to the laser power source.

Figure 29: The Dimension 3100 AFM cantilever holder stand [41].

Load the current version of the AFM software and wait for the laser to turn on. Remove the AFM head from the stand and use the laser alignment screws to centre the laser on the tip of the cantilever. Once the laser is incident on the tip, place the afm head back onto the main device.

Carefully adjust the laser alignment screws until the signal level is at its highest. The red dot should then be centred on the crosshairs of the detector by using the detector alignment screws on the left side of the head (see Figure 28).

Lock the lock screw to secure the AFM head to the main instrument. The next step is to use the find tip button to find the tip and the Optical camera adjustment screws as shown in Figure 27 to ensure proper alignment in the centre of the cantilever tip. A trackball can be used by holding down the focus button in order to ensure the image of the tip is sharp, ensure the tip is still aligned at the centre of the crosshairs.

Again the focus button and trackball can be used to focus and find some feature on the surface of the substrate, taking care not to get too close to the substrate as to drive the tip into it. It is possible however to focus on dirt on the microscope lens so it is always advisable when a focus has been found to use the provided AFM stage controls to move the sample, if the image on screen also moves, you are focussed on the sample, otherwise you are focussed on something else, such as the lens.

The cantilever tune icon should then be pressed and a start frequency of 50 kHz and end frequency of 500 kHz input. The auto tune button. If the graph shows a drive frequency of around 300 kHz and no error message is detected, the tip has been successfully tuned. Ensure the peak offset is 10% and zero the phase. Then exit the tuning window.

The most important settings are having a reasonable initial scan size (usually 5-10 μm in the case of this research) and Integral gain to 0.3, proportion gain to 0.6, scan rate to 1 Hz. It is also important to ensure the AFM is set to tapping mode, as contact mode would destroy the types of sample used for the majority of this research.

The engage button should be pressed and it will take a couple of minutes for the tip to engage onto the surface. When this happens the AFM will start to show an image.

Once an image has been started the graph button should show the AFM trace and re-trace (#). After this has been loaded the amplitude setpoint must be adjusted to as high as possible without broadening of the AFM trace and re-trace. If the trace and re-trace are in good agreement then the eye button can be pressed to bring the image back. For further adjustments the integral and proportional gain can be adjusted, however this is not always necessary. It is also important to now adjust the data scale in order to have the majority of the AFM data within range, otherwise the false colour scale will not show any meaningful data.

Once the AFM is capturing data and the image looks acceptable, press the capture button and enter a file name. The AFM will wait until a full scan has been performed before taking an image. Each successive image will have an increasing number appended to the file name until it is changed, which is useful for multiple areas on the same sample. It is important to note down the file names for future reference.

When the images have been taken the tip should be retracted from the surface, the sample removed and the cantilever carefully removed from the holder by again using the cantilever holder stand. The AFM images can now be exported and analysed using various AFM programs, the one used in the case of this thesis was a free to use software known as Gwyddion.

3.5.2. Neutron Scattering

Small angle neutron scattering was used on P3HT solutions made in chlorobenzene, deuterated chlorobenzene (d5) and deuterated chloroform (the specifics of each sample is mentioned in the neutron scattering results section). The instrument used was the Sans2d small-angle diffractometer at the ISIS Pulsed Neutron Source (STFC Rutherford Appleton Laboratory, Didcot, UK) [42, 43] (shown in Figure 30).

Figure 30: The Sans2d small angle neutron scattering instrument [43].

The vials used were 2mm quartz banjo vials and were placed in a water bath to allow temperature to be controlled precisely. A simultaneous Q-range of 0.0045 to 0.75 was achieved utilizing an incident wavelength range of 1.75 – 16.5 $Å^{-1}$ was achieved by using a wavelength range of 1.75 – 1.65 Å and using an instrument setup of L1=L2=4m, with the 1 m^2 detector offset vertically 150mm and sideways 180mm. The samples used were all prepared in deuterated solvents, except for the chlorobenzene based sample. The deuterated solvent provided a large contrast between scattering length density as mentioned in the theory section.

The diameter of the beam was 12mm. Each raw data set was corrected for the efficiencies of the detector, transmission of the sample and background scattering and converted to cross sectional scattering data (intensity vs Q) using the Mantid reduction software [44]. These data were plotted on an absolute scale (cm^{-1}) which was determined by comparing with a standard sample (a solid blend of hydrogenous and perdeuterated polystyrene) in accordance with established procedures [45].

3.5.3. UV-Visible Spectroscopy

UV-Vis spectroscopy was used both on solutions and on solid substrates. As described in the theory section the absorbance of the nanowires and the P3HT itself

allows us to obtain data on the composition of samples or solutions. We can measure the relative absorbance of the wavelengths of light associated with fibrillar and amorphous P3HT and thus compare various ages of samples or samples from different conditions.

Edited

Figure 31: UV-Vis setup with the Ultraviolet/visible light source, cuvette/sample holder and USB spectrometer [17].

Figure 31 shows the UV-Vis setup used for the research. This includes an Ocean Optics USB 2000 spectrometer, a cuvette/sample holder and a Mikropack Mini D2 UV-vis-IR light source (wavelength between 350-850nm).

Once the software has been loaded it is necessary to take a reference spectrum as the absolute transmission through the solid or liquid is not important, it is the relative decrease in transmission (ie the amount of light of the specific wavelength absorbed) that shows us the absorbance spectrum of the sample.
The reference sample depends on the sample in question. For example for a liquid sample an identical cuvette with only the solvent used is appropriate. For a solid sample on glass for example would need an identical but clean glass slide as a reference sample.

First a darkness spectrum where no light is present is taken and then a reference sample is needed as stated above.

Once the reference sample is loaded and the station cover is over to reduce external light affecting measurements, the initial reference is taken and then the actual sample is placed in the holder. If the mode is switched to absorbance rather than transmission (which, relative to the reference sample will always be lower in places) the relative intensity of the peaks shows how different wavelengths of light are absorbed by the sample. The spectrum can then be saved and analysed later. It is important to note that as this is relative intensity the actual heights of the peaks are not important, it is the relative heights of the peaks on the same spectrum, as well as the actual wavelengths of light absorbed that is important.

3.5.4. Electrical Measurements

For the electrical measurements of the gold electrodes with nanowire films across them a pair of Keithley 2400s were used. Two Suss microtec PH100 probe heads (three if using transistors rather than chemiresistors) were attached via coaxial cables to the Keithleys and the tungsten probe heads (seen in Figure 32).

Edited

Figure 32: A pair of Keithley 2400s with attached tungsten probeheads [46].

The probeheads were then brought into contact with the gold electrode pads, using a small magnifying glass to ensure they were indeed making contact with the electrodes. By using the software shown in (it is possible to set a voltage sweep (either one way or if using all 3 sections from zero to a required positive voltage, then down to a negative and finally back to zero. The software will allow a number of types of sweeps. This sweep can then be initiated, at which time the keithley takes over the program and when finished outputs the data to the program which can then be saved as a .csv file.

4. Analysis of P3HT Nanowires

4.1. Initial Experiments

4.1.1. Primary experiments

The preliminary aims of the P3HT growth studies was to create nanowires through a variety of different methods and study them with various techniques. Then attempt different methods to deposit and align nanowires.

Different methods were also examined to try to tailor the properties of the nanowires and P3HT films so that the processing could be adjusted to tailor films to any number of applications. For example creating an optimal blend of nanowires in amorphous P3HT so this can simply be added to PCBM in the exact quantities needed for maximum device efficiency, rather than annealing a mix of P3HT and PCBM to a balance point whereby there is a trade off between maximum nanowires formed and not having the structure too phase separated that charge transfer cannot occur.

A large amount of the literature that was reviewed tended to involve creating a solution of P3HT in a solvent and immediately spinning or spreading the solution, annealing afterwards in order to create and align nanowires. Therefore this research has different in its approach as it has mainly investigated forming nanowires by leaving a solution of P3HT to age and thus form nanowires actually in the solution. These nanowires were then processed from solution to create films.

As stated above the preliminary aims of the research were to create and identify nanowires in thin films. The first experiments that were carried out were of 1 mg/ml of the 96.6% regioregular P3HT (M101 rrP3HT) in chlorobenzene (CB) (which was chosen due to being a different solvent from a lot of the literature that was known to dissolve P3HT well. In future research, changing the solvent should also provide another variable that can be used to modify the properties of the nanowires) which

was spread on the Langmuir trough (150 μl of solution) immediately after the solution was created and 20 hours afterwards. Figure 33 shows a comparison between clean silicon and hydrophobic silicon and 20 hour old LS dipped samples.

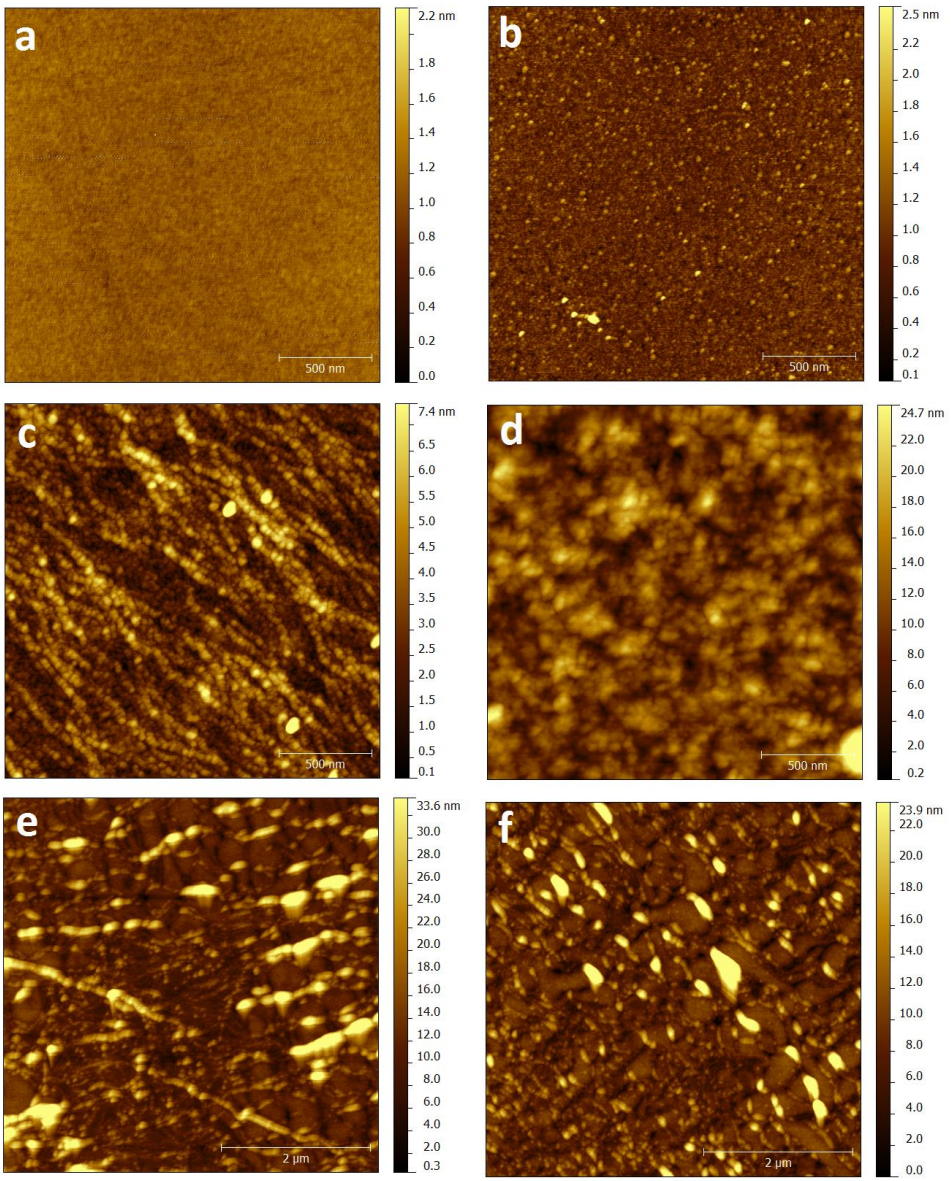

Figure 33: Tapping mode AFM images of: a) Cleaned silicon. b) Hydrophobic silicon, c) 1 mg/ml 20 hr old rrP3HT/CB solution, spread and compressed once before LS dip on hydrophobic silicon. d) 1 mg/ml 20 hr old rrP3HT/CB solution, spread and compressed twice before LS dip on hydrophobic silicon. e) 1 mg/ml 20 hr old rrP3HT/CB solution, spread and compressed four times before LS dip on hydrophobic silicon. f) 1mg/ml 20 hr old rrP3HT/CB solution, spread and compressed eight times before LS dip on hydrophobic silicon.

The films from Figure 33 were compressed eight times to determine if any ordering or alignment of the nanowires could be obtained but this was not clear from the AFM images. However it is possible to see clear evidence of nanowires as well as “ripped” and amorphous areas of rrP3HT which show a good mixing of domains even in the preliminary AFM images.

After the first batch of experiments a lower concentration of rrP3HT in chlorobenzene was tested to try to obtain more isolated nanowires that could be categorised more easily. For this a solution of 0.1 mg/ml rrP3HT in chlorobezene was made and a different trough used to get a better aspect ratio for compression.

The solution was spread on the Langmuir trough immediately after creation and also 11 days after creation in order to compare the two isotherms. Unfortunately the isotherms were very similar but due to trough problems (a motor would continually compress the films, forcing them to collapse rather than stopping at the desired pressure) the isotherms were unable to be properly compared. The isotherms did however appear to be similar in the stages before the film collapsed, suggesting that perhaps the lower concentration was not producing a significant amount of nanowires (or that packing did not affect the isotherm).

UV-Vis spectroscopy was performed on the solution in order to ascertain if nanowires were present at all at this concentration. The 0.1 mg/ml solution was first diluted to 0.05 mg/ml so that sufficient light could pass through and the absorbance could be measured accurately. The solution was left in the cuvette for a period of 190 minutes. As can be seen from Figure 34 there is no visible change in the spectrum unlike in the literature, which observes peaks appearing at 550 and 600 nm when nanowires are present. The peak from the bulk P3HT dissolved in solution is however clearly present centred on a wavelength of 450 nm.

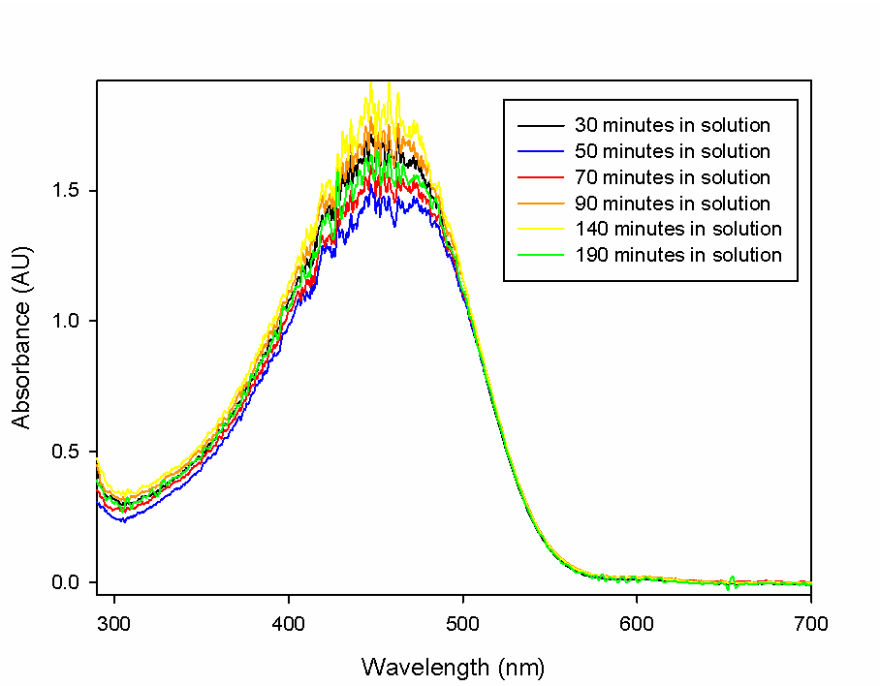

Figure 34: 0.1mg/ml rrP3HT in CB diluted to 0.05mg/ml and measured in UV-Vis spectrometer over 190 minutes. Normalised to a spectrum taken of the solution immediately after creation when no nanowires are present.

A possible problem that was discovered after this experiment was that leaving the diluted solution in the spectrometer would further retard any possible nanowire formation. To solve this problem a new 0.1 mg/ml solution was created and left to age for 48 hours. Samples were taken after 30 minutes, 24 hours and 48 hours which were then diluted to 0.05 mg/ml for use with the spectrometer. From the data shown in Figure 35 there appears to be very little change in the spectrum after 48 hours which suggests that the initial solution concentration is too low for sufficient nanowire formation.

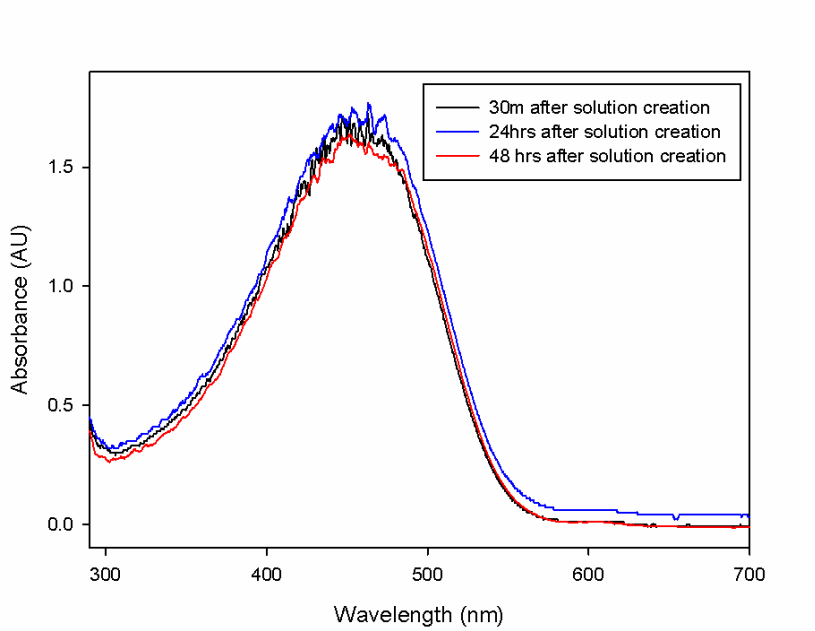

Figure 35: 0.1mg/ml rrP3HT in CB. Left for 48 hours and diluted to 0.05mg/ml for UV-Vis spectroscopy

4.1.2. 13 day nanowire growth experiments

To ensure sufficient concentration of P3HT so that nanowires would form a new solution of 10 mg/ml rrP3HT in chlorobezene was created which from literature was known to be a high enough concentration for nanowires to form. This solution was left for a period of 13 days, with UV-Vis measurements, isotherms and LS dips taken every day over this period.

Firstly for the isotherms the stock solution was diluted to 0.5 mg/ml as 10 mg/ml was too concentrated to sufficiently spread on the trough. 100 µl of this 0.5 mg/ml solution were spread on the Langmuir trough. The isotherms for the 13 day period are shown in Figure 36.

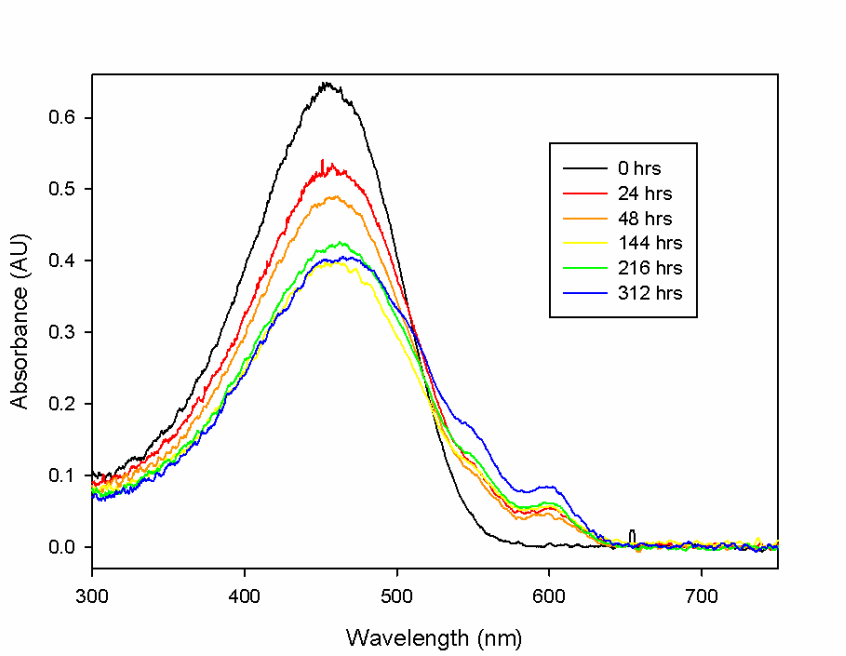

Figure 36: UV-Vis Spectroscopy over 13 days on 10mg/ml rrP3HT in CB diluted to 0.02 mg/ml for spectroscopy.

From these UV-Vis spectra it can be seen that after 24 hours we can see well defined nano wire peaks at 550 and 600 nm. After 24 hours from these measurements it does not seem like there is much change in these peaks, which would suggest that most nanowire formation occurs within the first 24 hours. In order to confirm this the AFM images of the LS dips of these films must be examined, which are shown in Figure 37, Figure 38 and Figure 39.

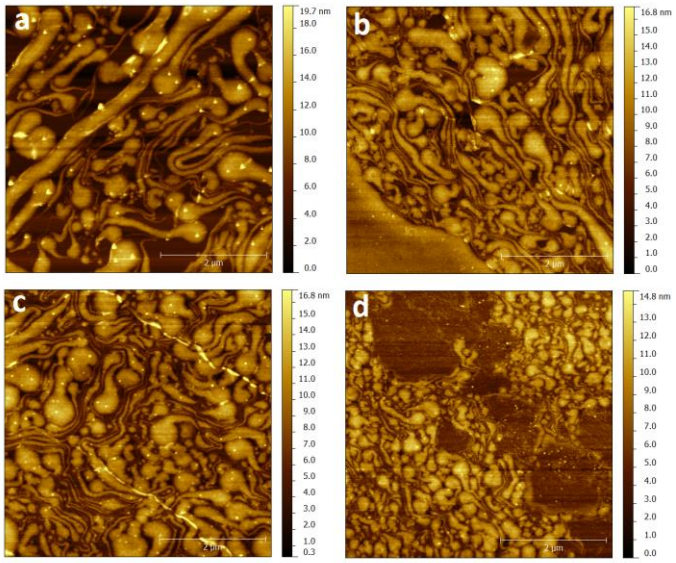

Figure 37: AFM images of 10mg/ml rrP3HT in CB (diluted to 0.5mg/ml) LS dipped films spread 2 hours after solution creation, taken at a pressure of: a) 1mN/m, b) 6mN/m, c) 12mN/m, d) 18mN/m.

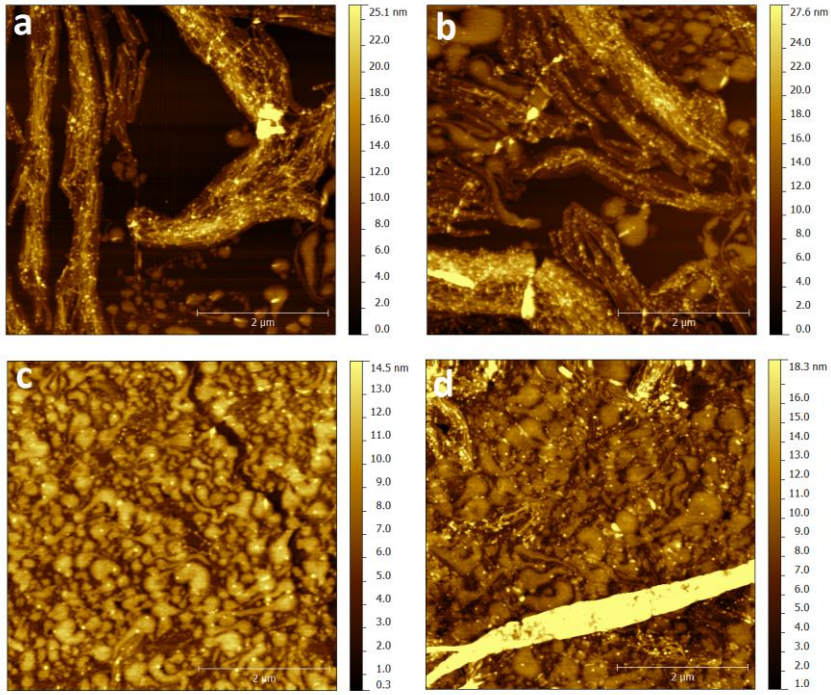

Figure 38: AFM images of 10mg/ml rrP3HT in CB (diluted to 0.5mg/ml) LS dipped films spread 25 hours after solution creation, taken at a pressure of: a) 1mN/m, b) 6mN/m, c) 12mN/m, d) 18mN/m.

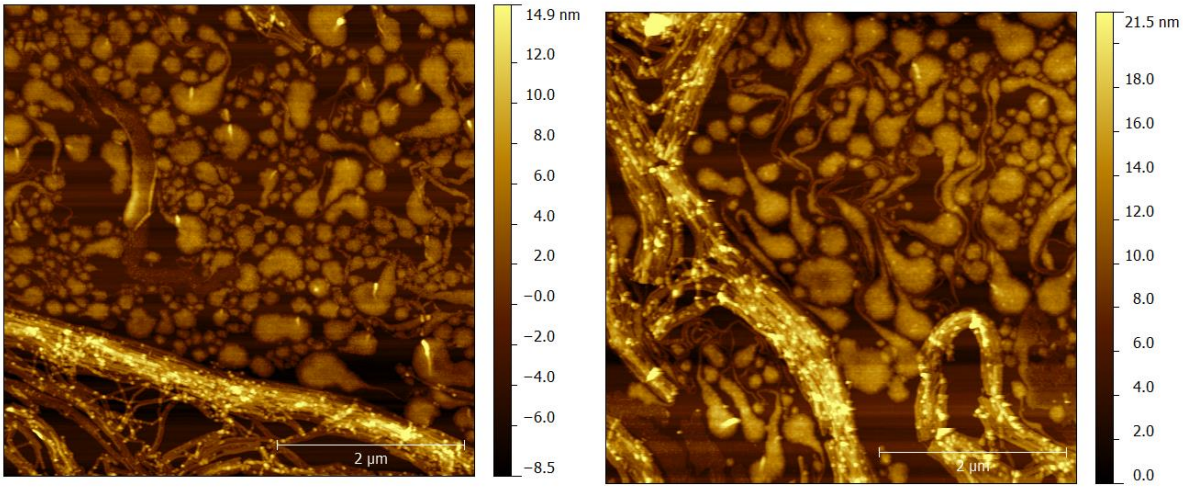

Figure 39: AFM images of a 10mg/ml rrP3HT in CB (diluted to 0.5mg/ml) LS dipped film, spread 49 hours after solution creation, taken at a pressure of 6mN/m. These two images show different areas of the same LS dipped film.

These images suggested that an optimal pressure for observing nanowires appears to be at 6 mN/m as at higher pressures the film seems to collapse (this was also verified visually as the film appeared to collapse at the barrier at higher pressures). These images also confirm that most nanowire formation had already occurred in the first 24 hours. However even after 48 hours amorphous areas of P3HT can still be seen alongside the nanowires. The theory behind this is that these areas are occurring due to the volatile nature of the solution and the fact that dilution is required for spreading. The addition of extra solvent increases the solubility of the solution which causes some nanowires to be re-dissolved. When spread on the surface a reaction occurs where little droplets of solution energetically and randomly move around on the surface until the solvent has fully evaporated. These dried areas could be what is being seen as amorphous areas of P3HT.

From analysis of these AFM images a nanowire width of (60±8) nm was calculated with a height of (5±2) nm. Comparing these values to values from literature, Oosterbaan found nanowires of heights between 2 to 5 nm with a width of (20±5) nm. This information helps to reaffirm the configuration of the nanowire as previously described, as the molecular weight of these 20 nm nanowires was a third

of the molecular weight used in this research and thus the chain length (and from this the nanowire width) is a third smaller.

4.1.3. 24 hour nanowire growth experiments

As can be seen from the data in section 4.1.2, most of the nanowire formation appears to take place in the first 24 hours, and thus it was decided to examine this 24 hour period more closely with isotherms and LS dips taken at 1 hour intervals over the 24 hour period.

The isotherms differed from the previous ones in that at hourly periods the 10 mg/ml solution was diluted to 0.2 mg/ml for spreading purposes rather than 0.5 mg/ml. This was because at a lower concentration, more solution could be spread (250 µl in comparison to the previous 100 µl) which meant a lower error in the amount of solution added as well as more solvent to allow for better spreading. The results of the isotherms are shown below in Figure 40.

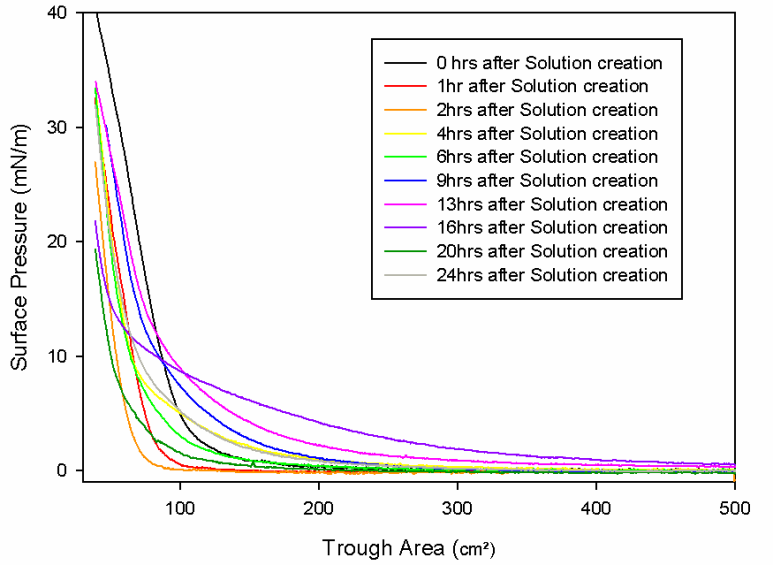

Figure 40: 10mg/ml rrP3HT in CB diluted to 0.2mg/ml (250ul spread) over 24 hours, isotherms taken.

Again, the isotherm shows very little information about what is occurring over the 24 hours, due to the previously mentioned formation of macroscopic domains on the water subphase. A better indication of the nanowire growth over the 24 hours was shown in UV-Vis spectroscopy taken at hourly intervals. An error in the dilution process however meant that instead of the 10 mg/ml solution being diluted to 0.02 mg/ml for UV-Vis measurements, it was diluted to 0.005 mg/ml which meant there would be a lower contribution from the nanowires in the peaks as well as possible nanowire dilution due to the large amount of extra solvent added. The UV-Vis of the solution over 24 hours is shown in Figure 41.

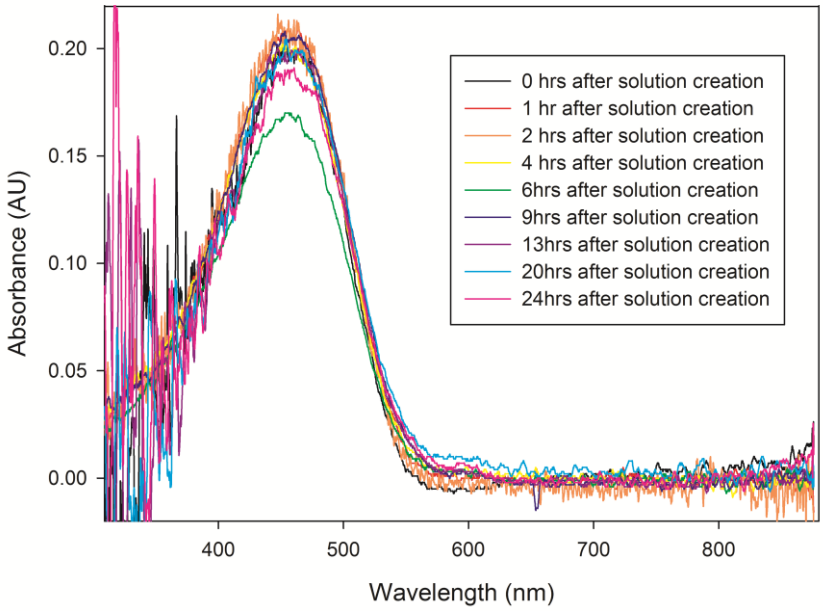

Figure 41: 10mg/ml rrP3HT in CB UV-Vis over 24 hours. Solution diluted to 0.005mg/ml for spectroscopy.

Due to the extra dilution compared to previous UV-Vis images the two peaks at 550 and 600 nm corresponding to nanowires being present were harder to see. The data did show however that there looked to be a peak at 24 hours but was hard to ascertain at what time that peak began to appear. Again the AFM data must be examined to ascertain what was occurring in the solution over 24 hours. The images that were taken are shown in Figure 42.

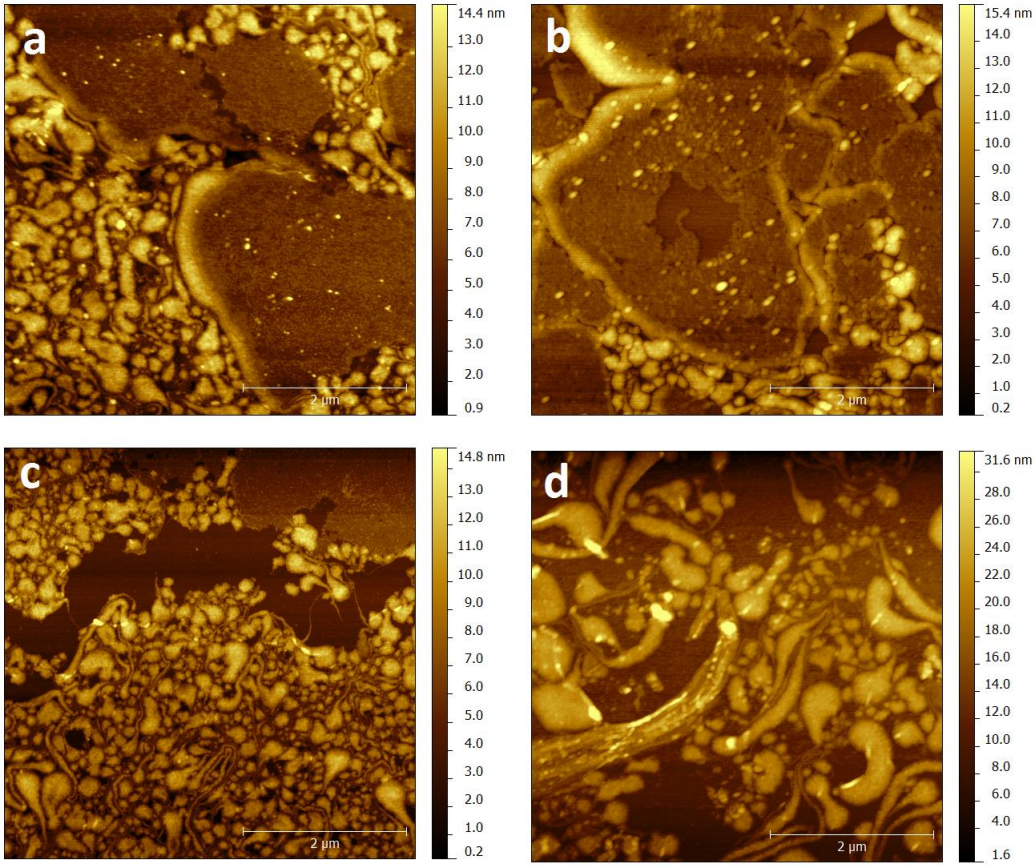

Figure 42: AFM images of 10mg/ml rrP3HT in CB (diluted to 0.2mg/ml) LS dipped films, spread a) 0hrs, b) 1hr, c) 2 hrs and d) 24 hours after solution creation. LS dips were taken at a pressure of 6 mN/m.

Again these AFM images were of LS dips taken over various hours in the 24 hour period. At each of these points where a measurement was required, the aged stock solution of 10 mg/ml rrP3HT in chlorobenzene was diluted to 0.2 mg/ml and spread at 250 µl for the reasons stated previously. From these images it is clear that after 1 hour nanowire like structures are starting to form (image b(ii) top right corner) , becoming even more prominent after two hours (image c(ii) along the right hand side). After twenty four hours there are a lot more nanowires but still large amount of amorphous areas. Again this is likely due to dissolving of nanowires when the solution is diluted for spreading.

4.2. Dynamic P3HT Nanowire Growth Studies in solution, via Small-Angle Neutron Scattering

4.2.1. One week old P3HT in deuterated chlorobenzene

This sample was made by creating a 5 mg/ml solution of the M101 rrP3HT in deuterated (d5) chlorobenzene, which was left for one week to allow nanowires to grow and then added dropwise to a 2mm path length banjo cell. This sample was kept at 25°C in the water bath for the duration of the experiment, except for the end where it was dropped to -2°C to see if further nanowire growth could be promoted. The purpose of this experiment was to determine the dimensionality factor for solutions which already had nanowires present.

The first set of data for this sample was taken over 22 minutes of the sample being held at 25°C. The data and fit are shown in Figure 43.

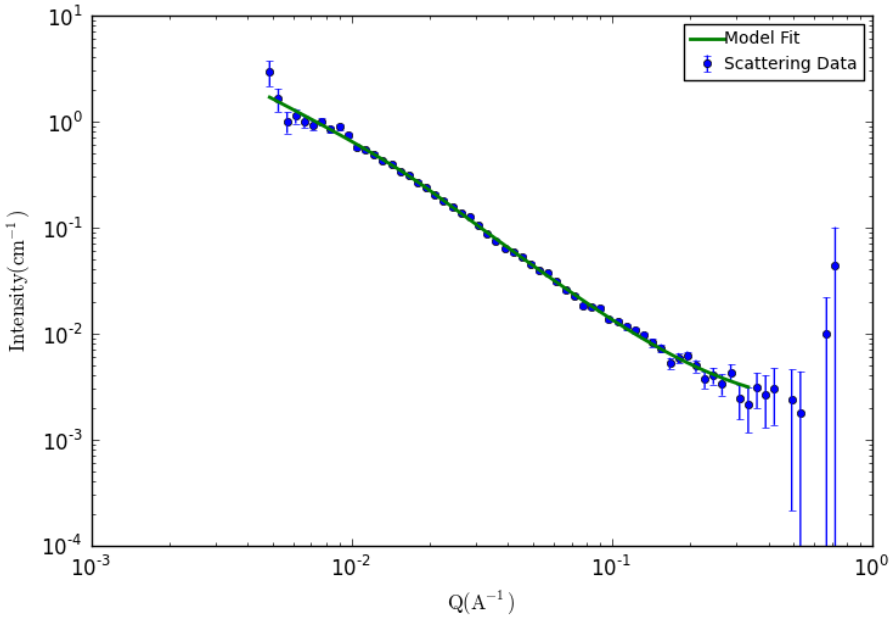

Figure 43: Neutron scattering data of the sample after 22 minutes at 25°C

The dimensionality factor from this fit was found to be 1.25±0.11. Which shows that the regime has 2D symmetry, suggesting nanowires as well as some lamellar aspect. Which is as expected as this is an aged sample.

The sample was then left for a further 68 minutes then recorded for 31 minutes in order to check results. The data and fit are shown in Figure 44.

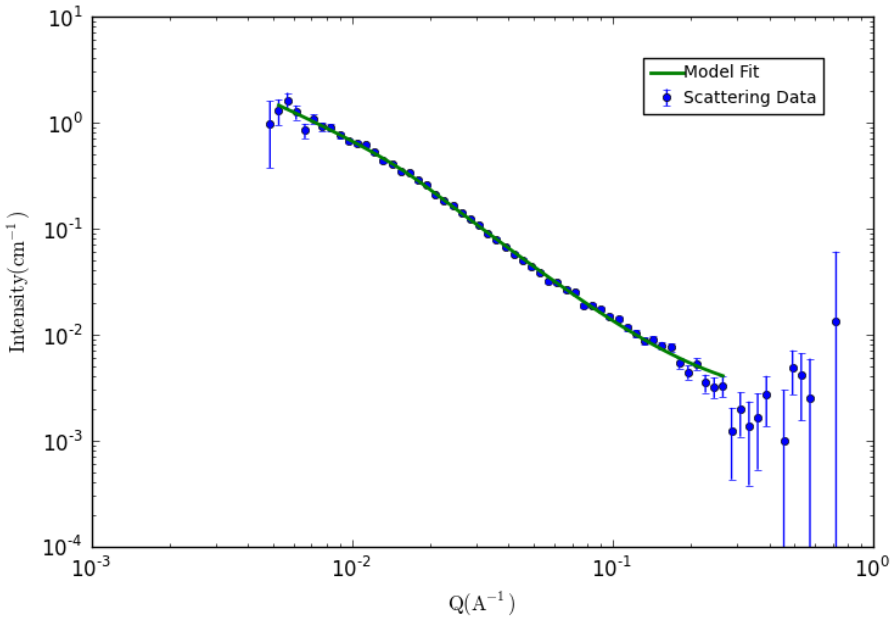

Figure 44: Neutron scattering data of the sample after a further 68 minutes at 25°C then recorded for 31 minutes at that temperature.

These data give a dimensionality factor of 1.09±0.13 which again is within the previous range and shows that there is a mixed regime, made up mainly of the already formed nanowires with some lamellar structure.

Finally the sample was left for 11 hours at 25°C then cooled to -2°C for 33 minutes and allowed to rise to 25°C again. The sample was then recorded at 25°C for 22 minutes, as shown in Figure 45.

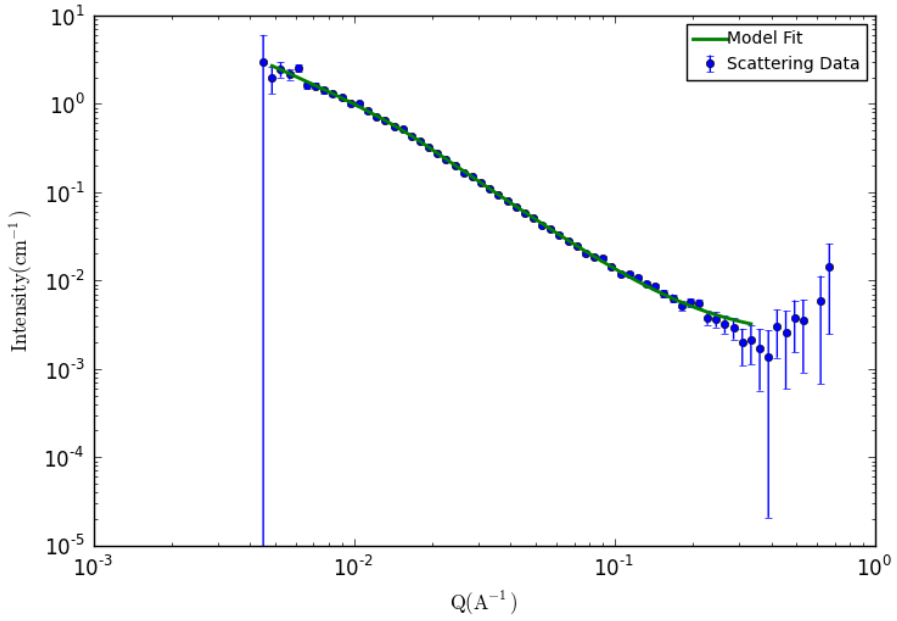

Figure 45: Neutron scattering data of the sample after being cooled to -2°C for 33 minutes then recorded for 22 minutes at 25°C.

The dimensionality factor from these data was 1.39±0.19 which suggests that more of the P3HT has switched to a lamellar regime due to the cooling process.

4.2.2. 9 months old P3HT in chlorobenzene

This sample was made by creating a 5 mg/ml solution of the M101 rrP3HT in chlorobenze, which was left for 9 months to allow nanowires to grow and then added dropwise to a 2mm path length banjo cell. This sample was also kept at 25°C in the water bath for the duration of the experiment. The purpose of this experiment was to see if the dimensionality factor was different for older nanowires, and also in chlorobenzene, if the scattering length density has a large enough contrast between P3HT and solvent.

The first set of data for this sample was after the sample had been held in the water bath at 25°C and was recorded for 22 minutes, the data and fitting is shown in Figure 46.

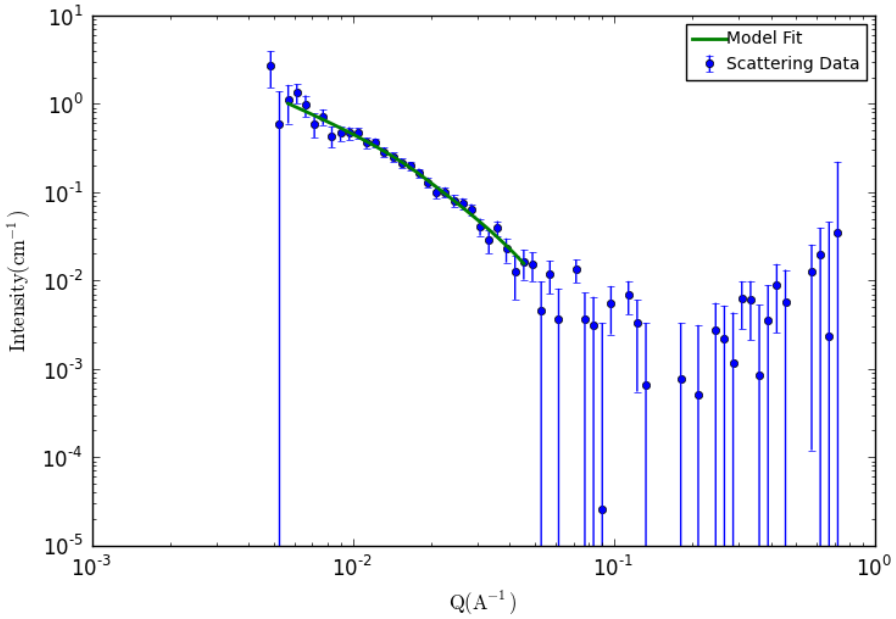

Figure 46: Neutron scattering data of the sample after being held at 25°C and recorded for 22 minutes.

The dimensionality factor from these data was found to be 1.23±0.14. Which is between the rod like regime and lamellar. Meaning again that nanowire were present as well as some stacking in this sample, as expected from a previously aged sample.

The sample was left for 3 hrs 25 minutes at 25°C and then recorded at that same temperature for 22 minutes. The data is shown in Figure 47.

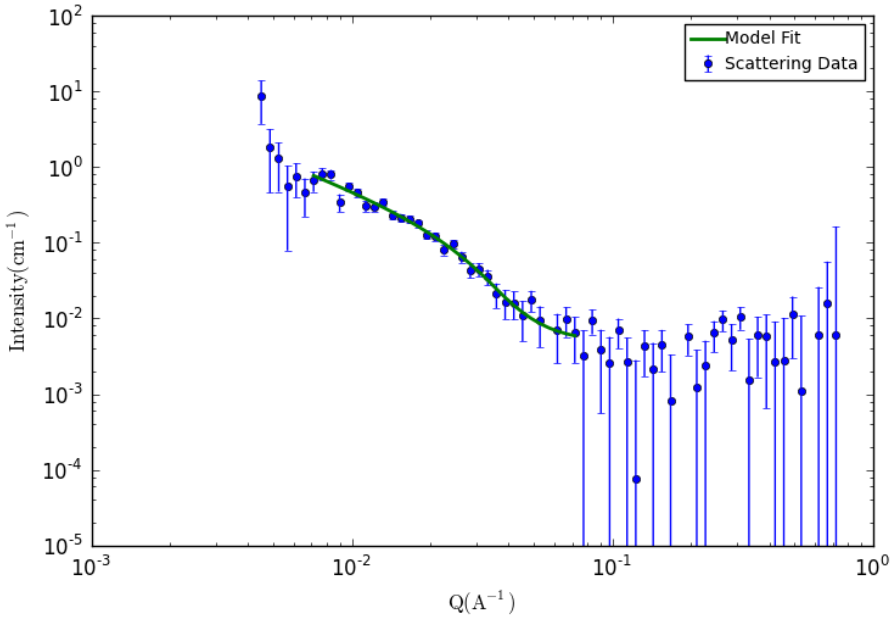

Figure 47: Neutron scattering data after the sample was held at 25°C for 3 hours 25 minutes then recorded for 22 minutes at that temperature.

The dimensionality factor for these data was found to be 1.34±0.21. Which again shows that potentially more nanowires have become lamellar stacked but undoubtedly shows nanowires are present within the system.

Finally, the sample was held at 25°C for a further 2 hours 21 minutes then cooled to -2°C for 33 minutes and allowed to warm to 25°C. The sample was then recorded for 24 minutes at this temperature, as shown in Figure 48.

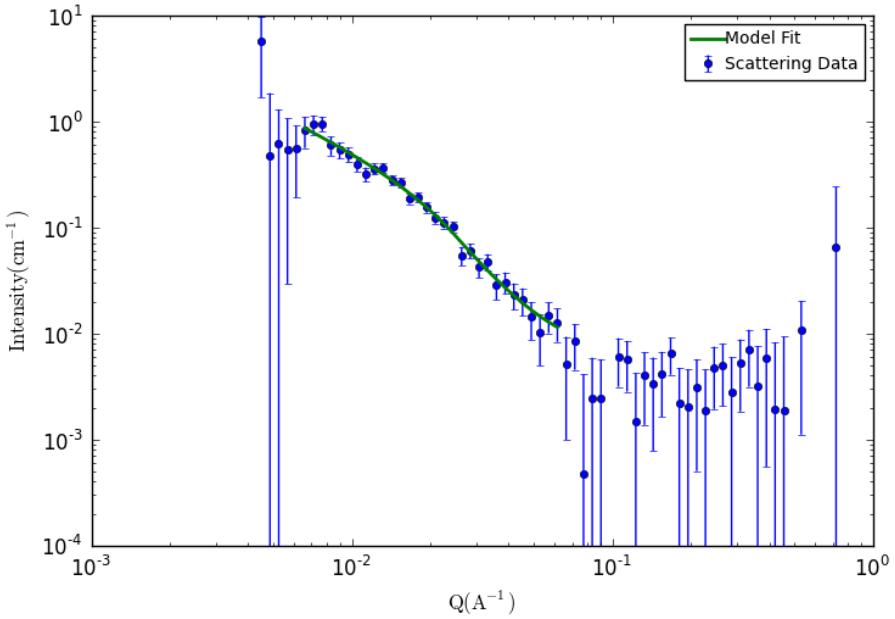

Figure 48: Neutron scattering data after the sample was held at 25°C for 2 hours 21 minutes then cooled to -2C°C for 33 minutes and finally recorded for 24 minutes at 25°C.

The dimensionality factor here was found to be 1.20±0.27 which is within error of the other values and does suggest that not many more nanowires have formed, perhaps due to the long 9 month period at which nanowires were created.

4.2.3. Fresh P3HT sample in deuterated chlorobenzene (nanowires formed then re-dissolved)

This sample was made by creating a 5 mg/ml solution of the M101 rrP3HT in deuterated (d5) chlorobenzene, this was heated for 10 minutes at 80°C at the ISIS facility and kept in the water bath in a 2mm banjo cell at 74.8°C at the start of the experiment for around 7.5 hours. The temperature was then dropped to 4°C over 1 hour and then held at that temperature for a further 20 hours. After which it was heated in 20 degree increments and recorded until it reached 80°C. The purpose of this experiment was to determine the dimensionality factor as the nanowires formed whilst cooling, and to see the change in regime. It was also to see if, as predicted, the

nanowires would re-dissolve when heated and thus the dimensionality factor would get closer to zero once again.

The first set of data was from the fresh sample before it had been allowed to cool. It was kept at 74.8°C in the water bath and recorded for 45 minutes at this temperature. The data is shown in Figure 49.

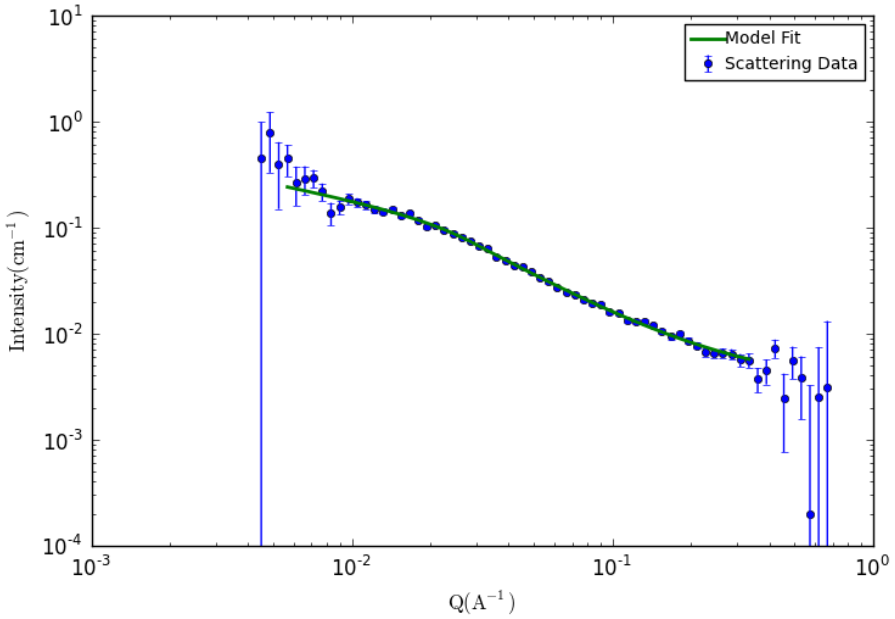

Figure 49: Neutron scattering data showing the sample after it had been held at 74.8°C for recording over 45 minutes.

The dimensionality factor from these data was found to be 0.5±0.12 which suggests a regime between that of globular or spherical scattering objects, and that of rods or long chains. This fits with what was expected as the nanowires have not had chance to form as they have been kept at a high temperature for these data.

The sample was held at 74.8°C for a further 2 hours 33 minutes before again being recorded for 45 minutes at this temperature to ensure there will still a regime between nanowires and spherical objects. The data is shown in Figure 50.

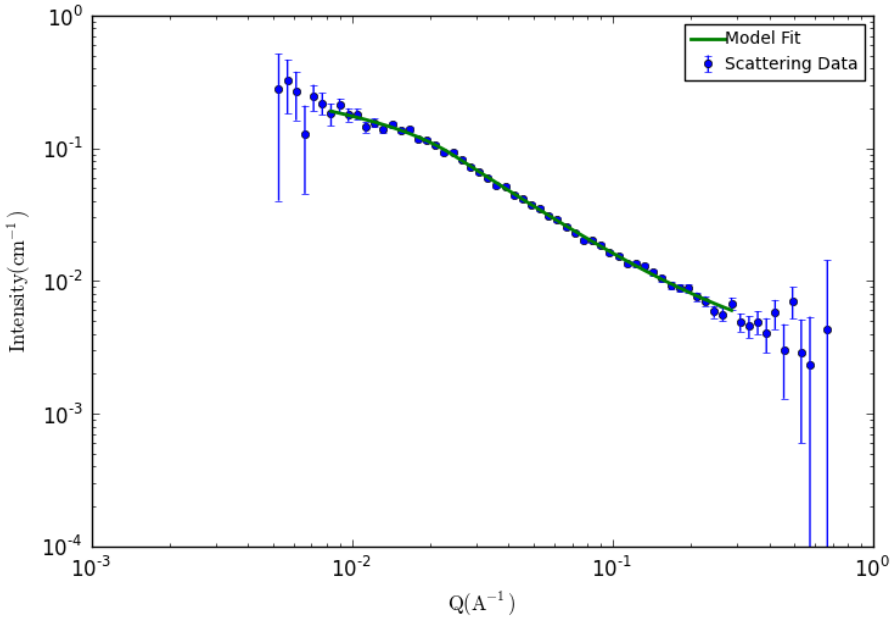

Figure 50: Neutron scattering data showing the sample after it had been held at 74.8°C for a further 2 hours 33 minutes, then recorded at this temperature for 45 minutes.

The dimensionality factor of these data was found to be 0.33±0.19 which again shows that there is a regime where nanowire formation has not properly begun and is somewhere between spherical objects and rods.

The sample was then cooled to 4°C over an hour and then held at 4°C for a further hour and recorded. These data are shown in Figure 51.

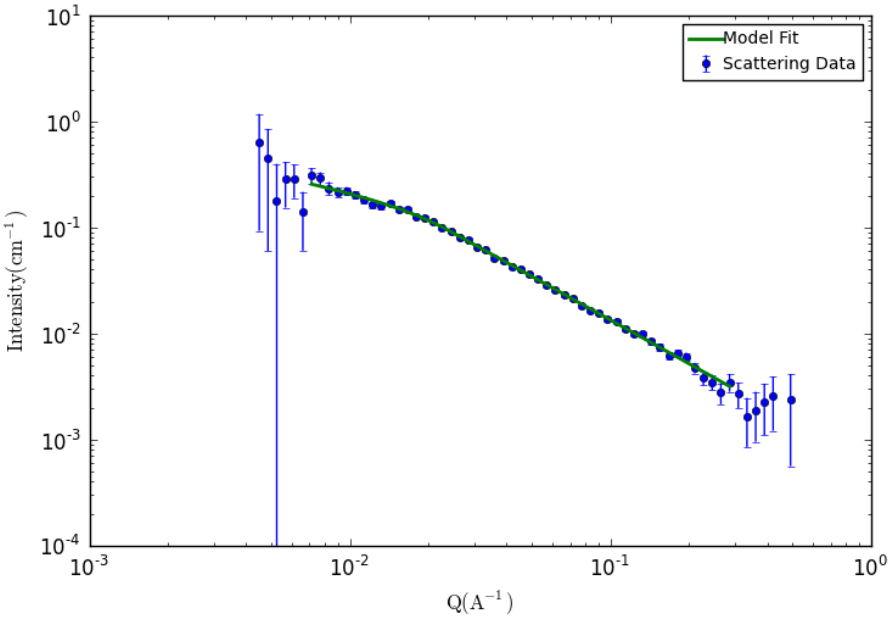

Figure 51: Neutron scattering data after the sample was cooled to 4°C over 1 hour then recorded at this temperature for a further hour.

The dimensionality factor here was found to be 0.512±0.15 which may be suggesting nanowire formation is occurring. In order to determine this, the sample was left at 4°C for a further 7 hours and then recorded at this temperature for an hour. These data are shown in Figure 52.

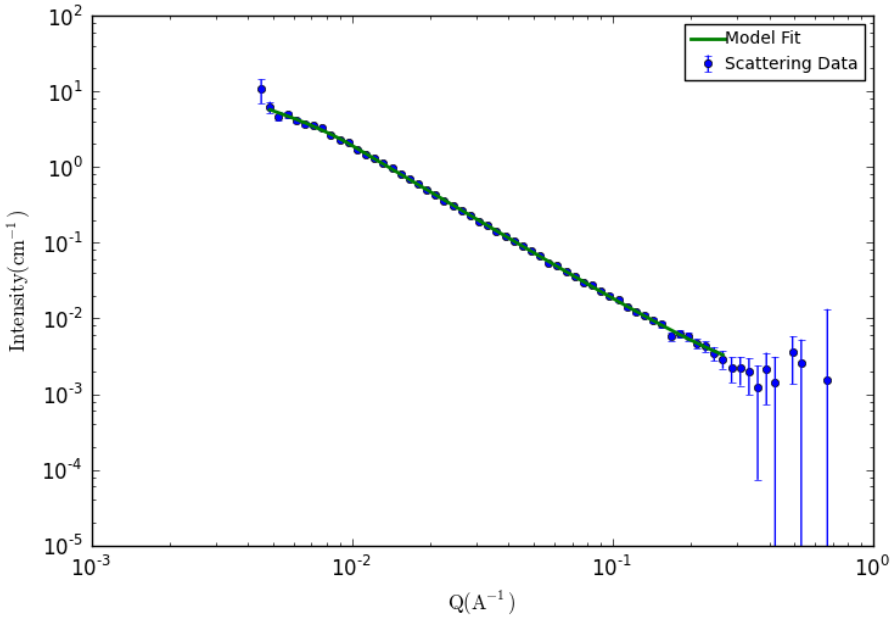

Figure 52: Neutron scattering data after the sample was held at 4°C for a further 6 hours and then recorded at this temperature for an hour.

The dimensionality factor here was found to be 0.94±0.19 which suggests that indeed nanowire formation has occurred due to the cooling of the solution from 74°C where the nanowires cannot form as the solubility of the solution is increased, to 4°C where the P3HT can drop out of solution and form nanowires.

The sample was then held at 4°C for a further 18 hours and then recorded at this temperature for 52 minutes, the data are shown in Figure 53.

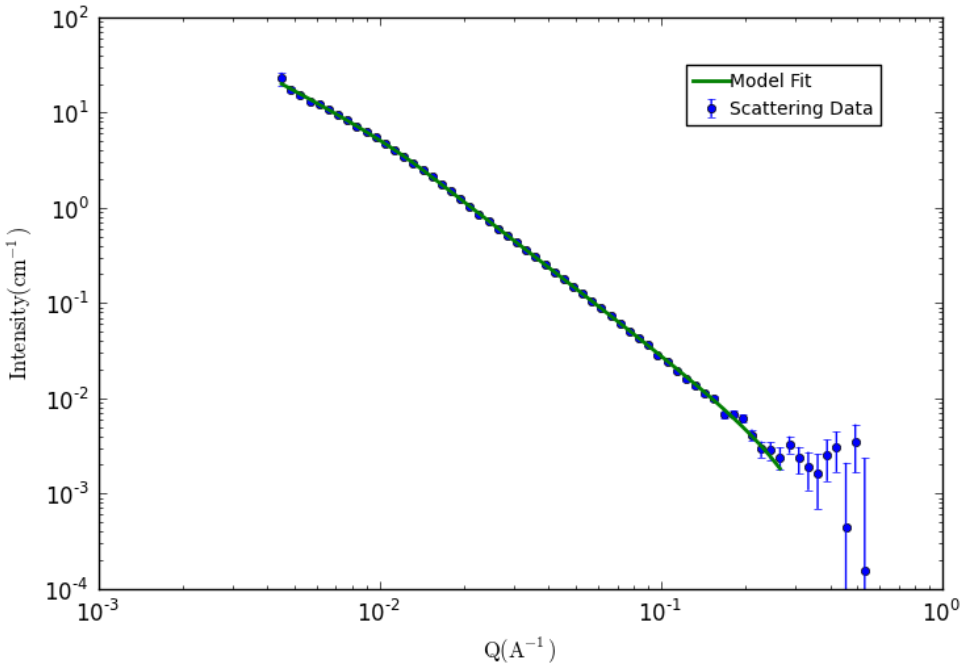

Figure 53: Neutron scattering data after the sample was held at 4°C for a further 18 hours, then recorded at this temperature for 52 minutes.

The dimensionality factor for these data was found to be 1.52±0.05 which shows that after a long period of time at this reduced temperature, the regime has shifted to one between long rods, and some lamellar structure. Indicating that significant nanowire formation has occurred.

The sample was then kept at 4°C for 56 minutes before being heated in order to ascertain if the nanowires could be re-dissolved and thus lower the dimensionality factor again. Figures Figure 54, Figure 55 and Figure 56 show the heating steps, which involved heating to 20°C, 40°C, 60°C and 80°C in that order, taking 600 seconds to heat. The sample was then held at each temperature respectively for 55 minutes in order to record for the temperature increase.

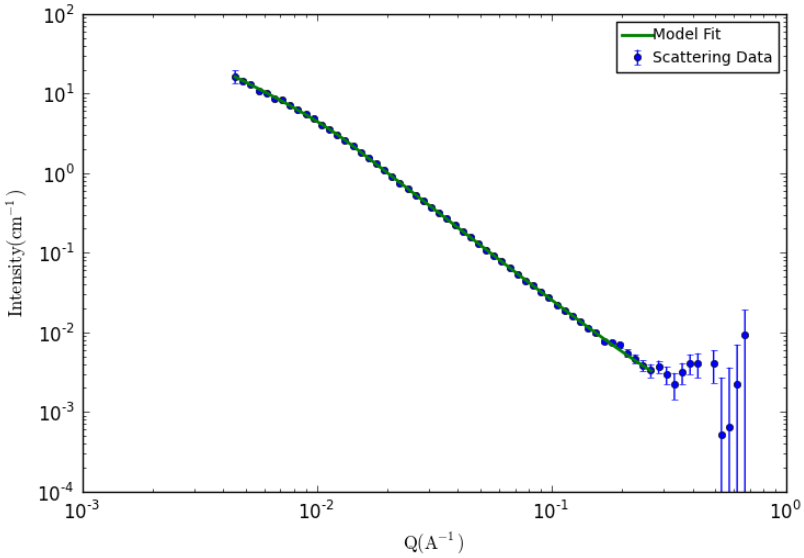

Figure 54: Neutron scattering data showing the sample after heated to 20°C over 600 seconds, then held and recorded at this temperature for 55 minutes.

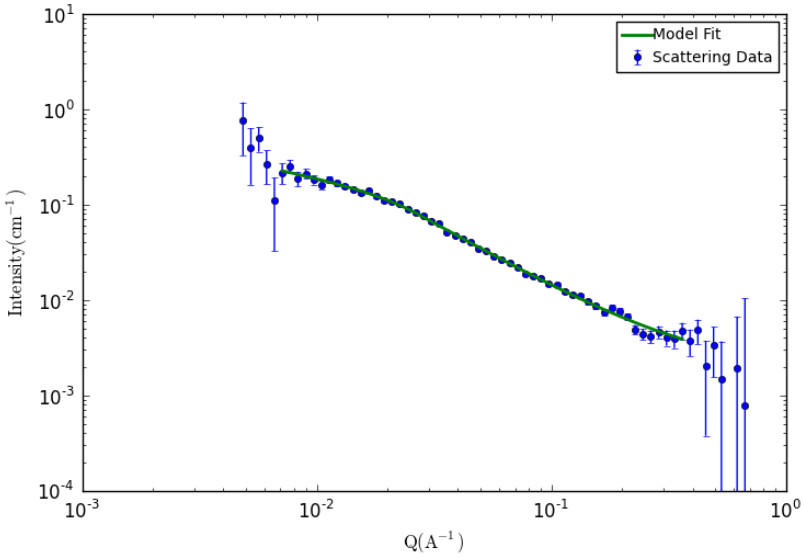

Figure 55: Neutron scattering data showing the sample after heated to 40°C over 600 seconds, then held and recorded at this temperature for 55 minutes.

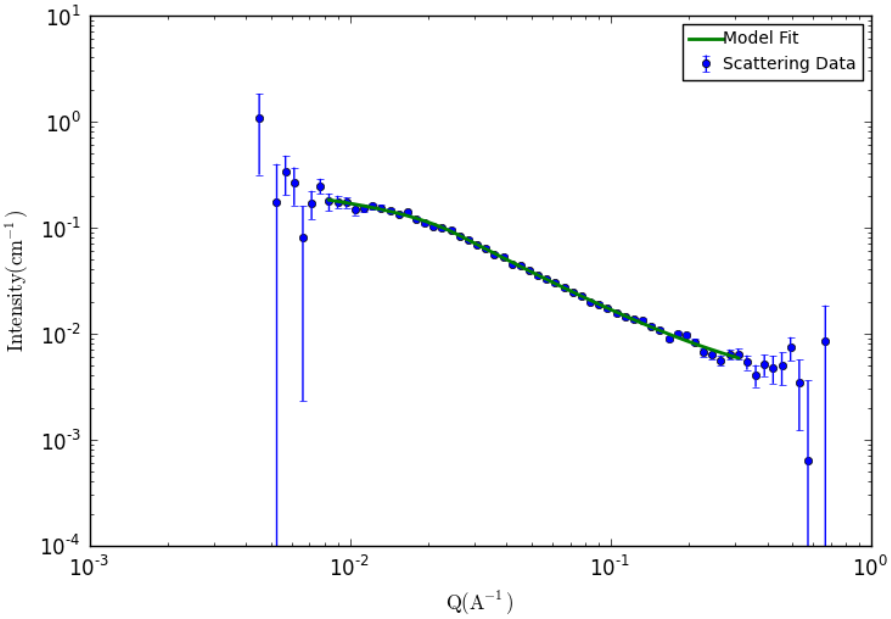

Figure 56: Neutron scattering data showing the sample after heated to 80°C over 600 seconds, then held and recorded at this temperature for 55 minutes.

The beam was down for the 60°C period and thus it has not been included. For the 20°C period the dimensionality factor dropped to 1.39±0.05 which shows the nanowires are starting to re-dissolve and thus go back to the more spherical regime. The 40°C period had a further drop in dimensionality factor to 0.49±0.13 which again is a large jump to between spherical objects and long rods, indicating nanowires have been re-dissolved due to the temperature increase.

Finally, for the 80°C period the dimensionality factor had dropped to 0.28±0.16 again further adding to the evidence that the temperature was causing the nanowires to re-dissolve back into solution.

4.2.4. Fresh P3HT sample in deuterated chlorobenzene (seeded then re-dissolved)

This sample was made by creating a 5 mg/ml solution of the M101 rrP3HT in deuterated (d5) chlorobenzene, this was then immediately placed in a freezer (-18°C) for 13 hours. It was then seeded with 50 µl of the one week old P3HT mentioned above in order to promote nanowire growth. The sample was agitated and then left in the same freezer for a further 13 hours. This sample was then added to a banjo cell and heated, again in 20°C increments up to 80°C. The purpose was similar to the previous experiment but was designed to quickly create a large amount of nanowires then watch the dimensionality factor change as they were heated and re-dissolved.

The first recorded set of data for this sample was after the seeding process had occurred and the sample was removed from the freezer. The sample has held at 3C straight from the freezer and was recorded at this temperature for 55 minutes. The data is shown in Figure 57.

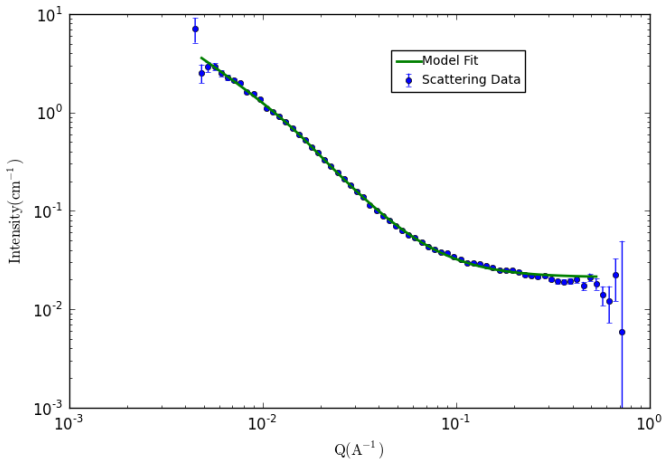

Figure 57: Neutron scattering data showing the sample after it had been taken out of the freezer, 13 hours after seeding and recorded at 4°C for 55 minutes.

The dimensionality factor was found to be 1.33±0.08 which shows that the freezing and seeding process accelerated nanowire growth in the solution and thus after this relatively short period of time the regime was already that of a sample between spheres and long rods, hence a significant amount of nanowire formation had occurred.

Like the previous (unseeded) sample, the sample was heated to 80°C in 20 degree increments, in order to attempt to re-dissolve the nanowires. Again, the sample was heated to 20°C, 40°C, 60°C and 80°C and held there for 600 seconds. After which at each stage, the sample was recorded at the respective temperature for 55 minutes. Figures Figure 58, Figure 59, Figure 60 and Figure 61 show these data.

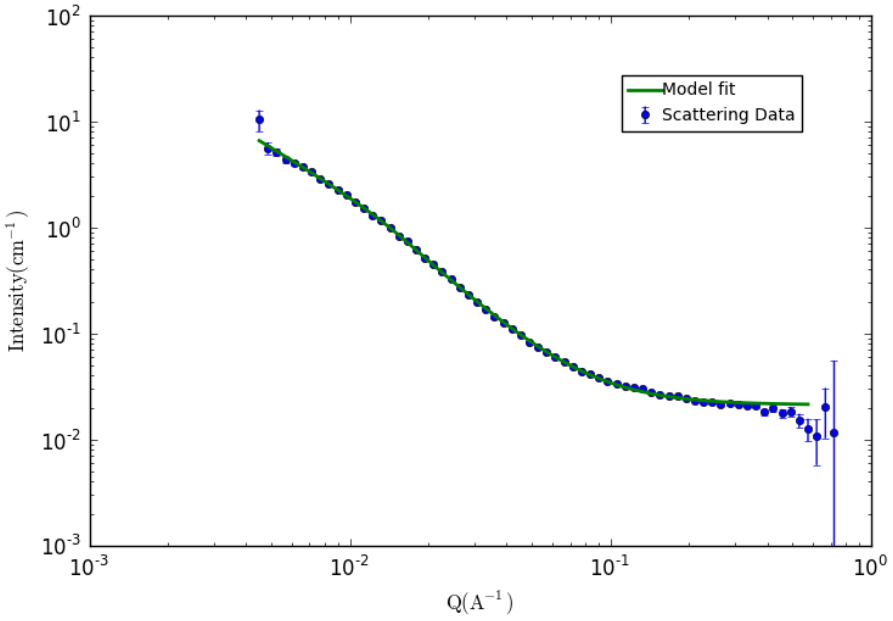

Figure 58: Neutron scattering data showing the sample after heated to 20°C over 600 seconds, then held and recorded at this temperature for 55 minutes.

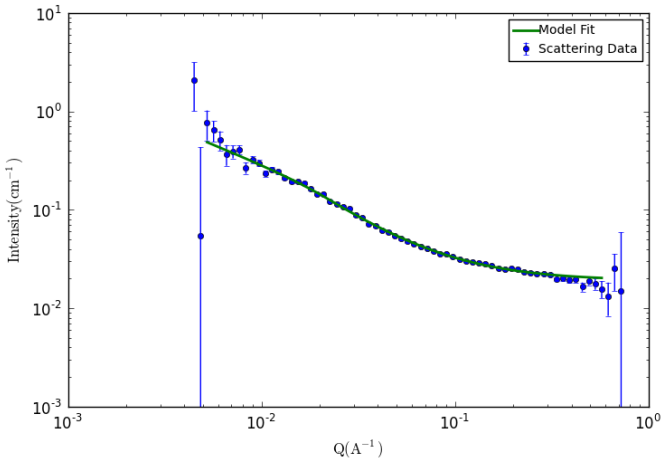

Figure 59: Neutron scattering data showing the sample after heated to 40°C over 600 seconds, then held and recorded at this temperature for 55 minutes.

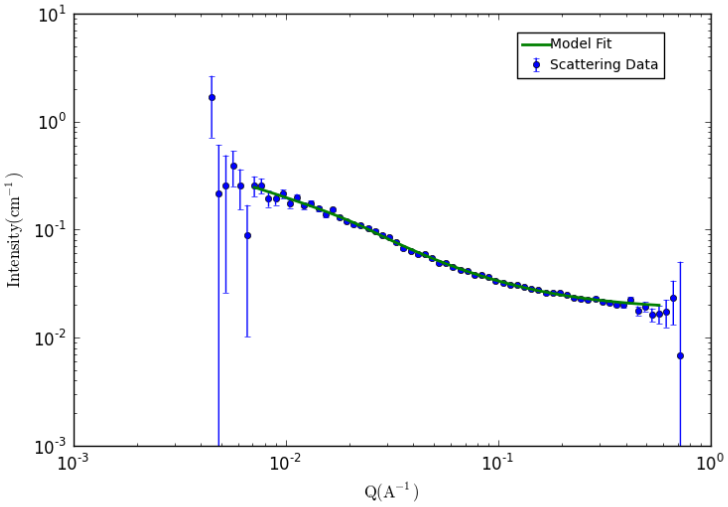

Figure 60: Neutron scattering data showing the sample after heated to 60°C over 600 seconds, then held and recorded at this temperature for 55 minutes.

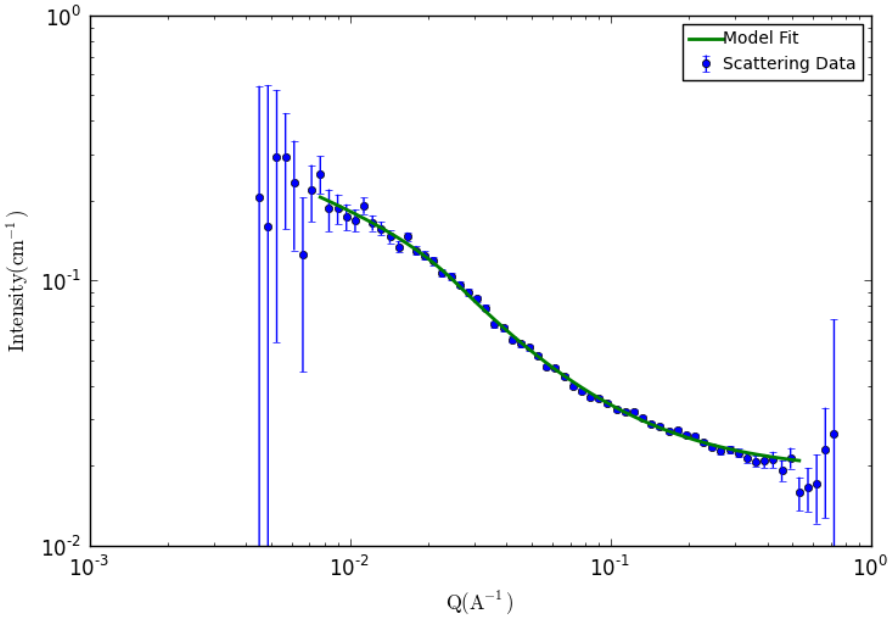

Figure 61: Neutron scattering data showing the sample after heated to 80°C over 600 seconds, then held and recorded at this temperature for 55 minutes.

The dimensionality factor from the 20°C period was found to be 1.43±0.06 which is slightly higher than the previous factor. This may simply indicate that the nanowires have not yet begun to re-dissolve, as 20°C is not sufficiently high enough to significantly re-dissolve the nanowires.

For the 40°C the dimensionality factor had dropped to 0.82±0.14, indicating that at this temperature the nanowires had started to re-dissolve back into solution. This was further supported by the 60°C dimensionality factor, which had again dropped to 0.63±0.15.

Finally, the 80°C was the lowest, at 0.43±0.17. Indicating that the nanowires had significantly re-dissolved into solution, leaving a regime that was partly spherical in nature and partly long rods.

4.2.5. Fresh P3HT sample in deuterated chloroform

This sample was made by creating a 3 mg/ml solution of the M101 rrP3HT in deuterated chloroform. This was then placed in a 2mm banjo cell and then into a water bath at 25°C. This sample was held at 25°C for over 18 hours in order to watch nanowires grow in solution over a long time scale. As well as investigating nanowire growth in a chloroform solvent rather than the usual chlorobenzene.

The first set of data for this sample was taken after the sample was created and then held at to 25°C. The sample was kept at this temperature and recorded for 22 minutes. The data is shown in Figure 62.

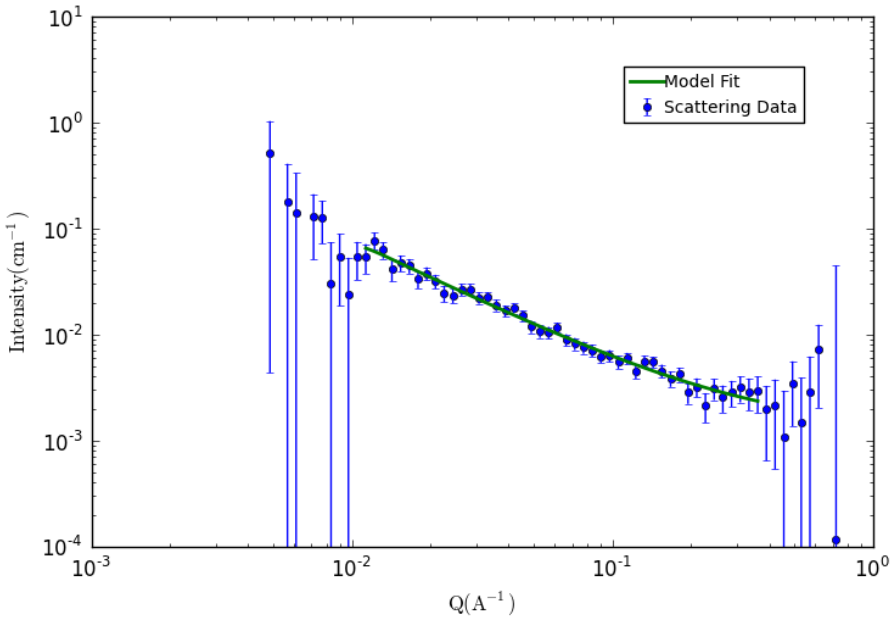

Figure 62: Neutron scattering data showing the sample after creation, sample held at 25°C for 22 minutes.

The dimensionality factor from these data was found to be 0.034±0.005 which indicates the sample is close to simply having globular or spherical objects. This could lower than previously created samples as the concentration of the P3HT is almost halved.

This sample was then held at 25°C for 17 hours 53 minutes and then recorded at this temperature for 1hr 25 minutes, as shown in Figure 63.

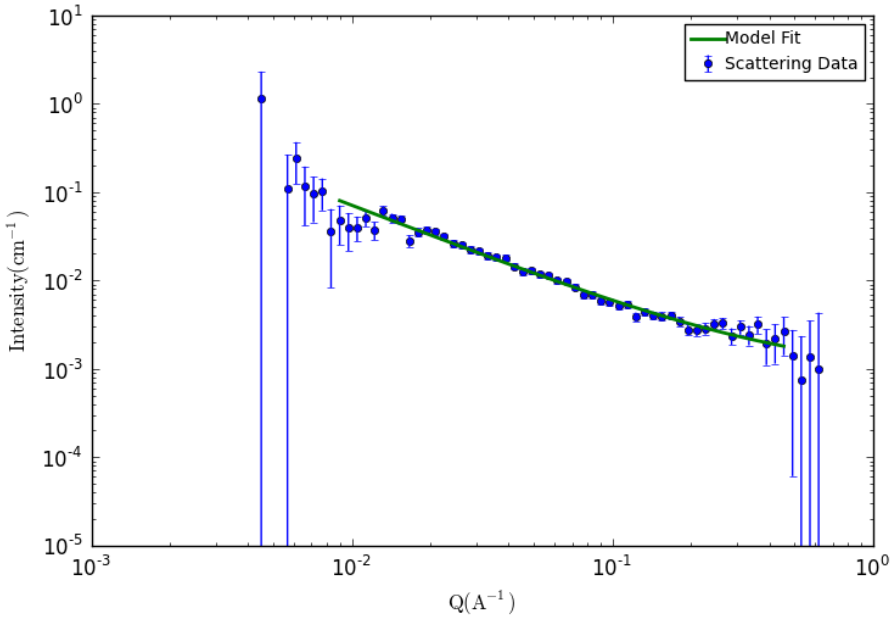

Figure 63: Neutron scattering data showing the sample after it has been held at 25°C for 17 hours 53 minutes, and then recorded at this temperature for 1 hour 25 minutes.

The dimensionality factor for these data was found to be 1.01±0.02. This shows that nanowire formation has occurred, and is very close to the long rod regime. This is lower than the previous experiments, again likely due to slower nanowire growth from a lower concentration, as well as the fact that the solvent is chloroform which, as shown in the AFM analysis section, produces shorter nanowires over a longer time period.

4.2.6. Fresh P3HT sample in deuterated chlorobenzene

Finally this sample was made by creating a 3 mg/ml solution of the M101 rrP3HT in deuterated (d5) chlorobenzene. This was placed in a 2mm path length banjo cell and then into a water bath at 25°C. This was also held at 25°C for over 15 hours in order to watch nanowires grow in solution over a long time scale.

The first data from this sample was taken after the sample was created and held at 25°C and recorded for 1 hour 52 minutes. The data is shown in Figure 64.

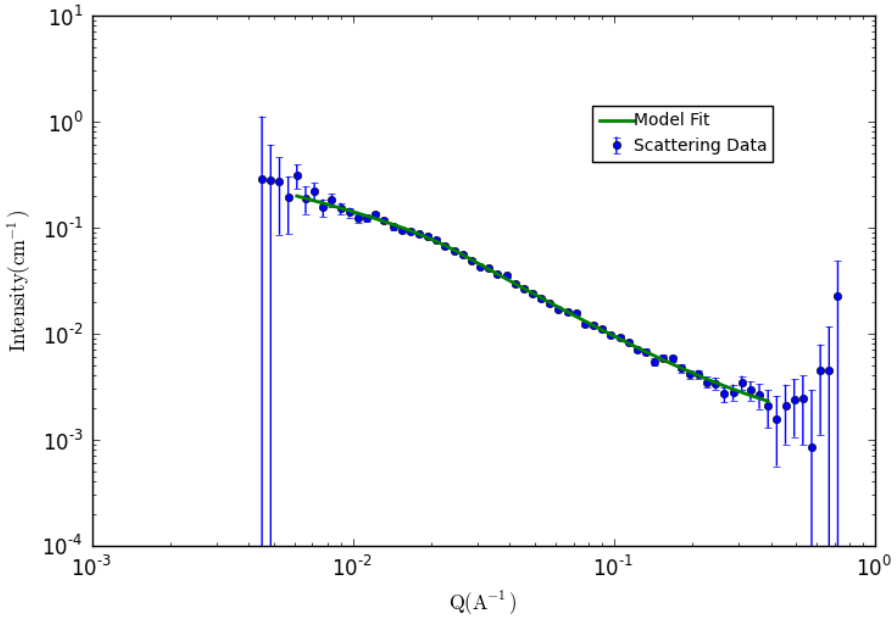

Figure 64: Neutron scattering data showing the sample after creation, held at 25°C for 1 hour 52 minutes and recorded for this period.

The dimensionality factor for these data was found to be 0.62±0.14 which shows that again, the solution is between a spherical regime and long rod.

The sample was then held at 25°C for 7 hours 27 minutes and recorded at this temperature, for 1 hour 4 minutes. The data is shown in Figure 65.

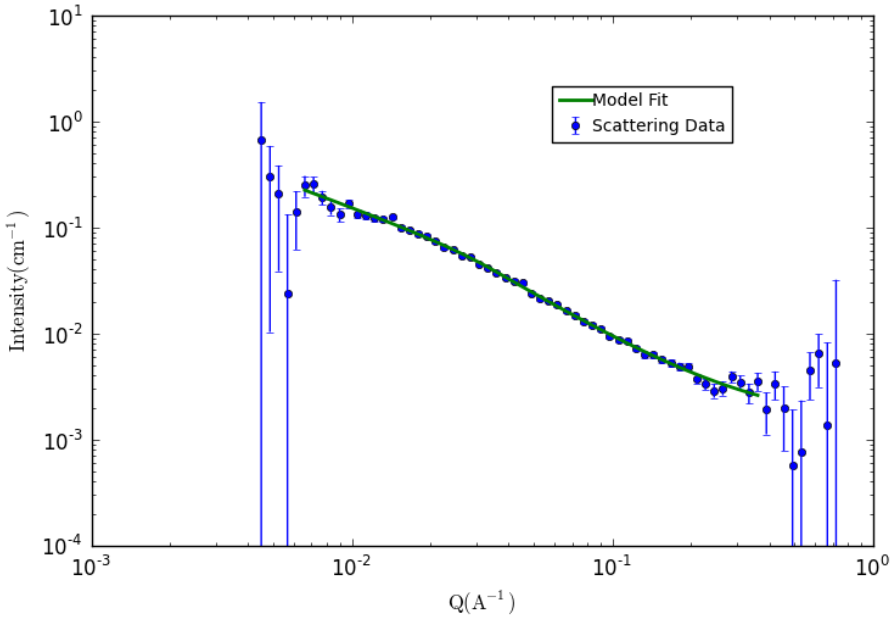

Figure 65: Neutron scattering data after the sample was held at 25°C for 7 hours 27 minutes and recorded at this temperature for 1 hour 4 minutes.

The dimensionality factor after this period of time had increased to 0.90±0.07, again demonstrating nanowire formation has occurred over this time period, but at a slower rate due to the lower concentration of P3HT in d5 chlorobenzene.

To ascertain if further nanowire formation would occur, this sample was held at 25°C for a further 6 hours 18 minutes, and then recorded at this temperature for a final 1 hour and 1 minute. The data is shown in Figure 66.

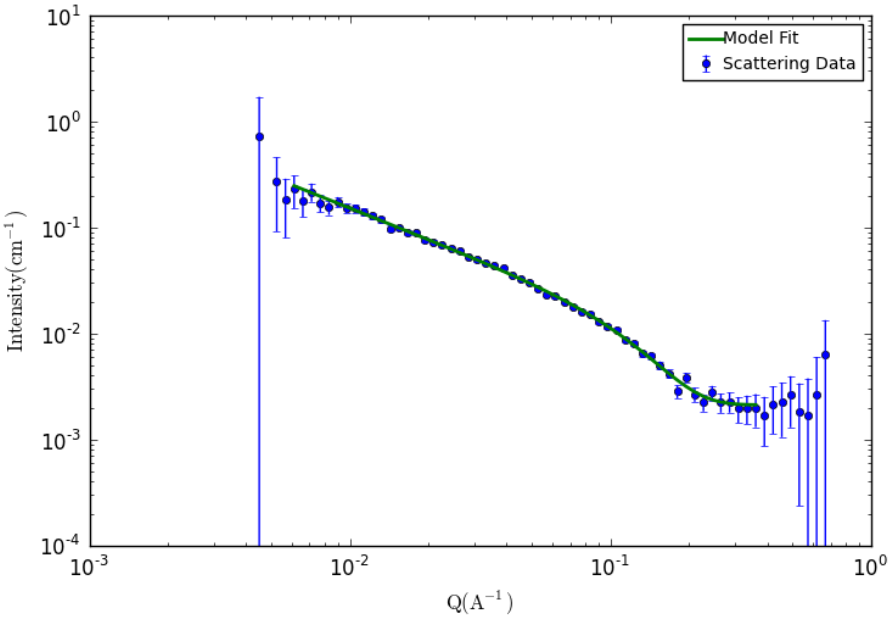

Figure 66: Neutron scattering data after the sample was held at 25°C for a further 6 hours and 18 minutes, then recorded at this temperature for 1 hour 1 minute.

The dimensionality factor here has risen to 0.99±0.08, again showing that although slower than higher concentrations, nanowire formation has continued over the 6 hour 18 minute period.

4.2.7. Results and conclusions

To conclude, the neutron scattering data of the six samples was vital in confirming the predicted behaviour of P3HT nanowires in solution, which was previously difficult to ascertain due to the opaque nature of the solution and the similarity between the solvent and P3HT.

The experiments confirmed that P3HT nanowire growth does occur, albeit at smaller length scales that is accessible via tapping mode AFM, within a few hours of sample creation. They also confirmed that by heating the solution, the nanowires re-dissolve into the solution. Additionally, a lower concentration of P3HT in solvent, produces

slower forming nanowires. Finally, chloroform also produces nanowires, but like a lower concentration, they have form slower, as well as having a different structure.

Finally, the experiments also proved that seeding a sample as well as freezing it, dramatically increases the speed of nanowire formation, but these nanowires can still be re-dissolved by heating the solution.

4.3. Optimisation of thin films

4.3.1. Optimal solvent and solution concentration

The primary source of optimisation for the P3HT nanowires was to first obtain the optimal solvent and concentration parameters to produce long nanowires in a large volume that possessed a mobility to be aligned along a desire direction. An optimal time period for growing the nanowires was also needed, however previous studies in this research found that at least 24 hours are required for sufficient growth.

After consulting literature four different solvents were selected, these were chloroform, chlorobenzene, dichlorobenzene and trichlorobenzene. Previous experiments were performed using chlorobenzene due to the price and previous knowledge from fellow researchers about its effectiveness at producing nanowires. It was necessary to ascertain if this was the most efficient and optimal solvent for the task.

These solutions were mixed with the previously mentioned P3HT at a concentration of 10mg/ml as per the previous experiments. These were heated after mixing to 80 degrees for 15 minutes for chlorobenzene, dichlorobenzene and trichlorobenzene and 60 degrees for chloroform (due to the low boiling point). The solution was also stirred using a magnetic stirred on a hotplate whilst being heated. The solutions were then left for 22 days in order to grow nanowires. After which time the samples were spun again.

The figures below, Figure 67 to Figure 70 show a comparison between the four solvents.

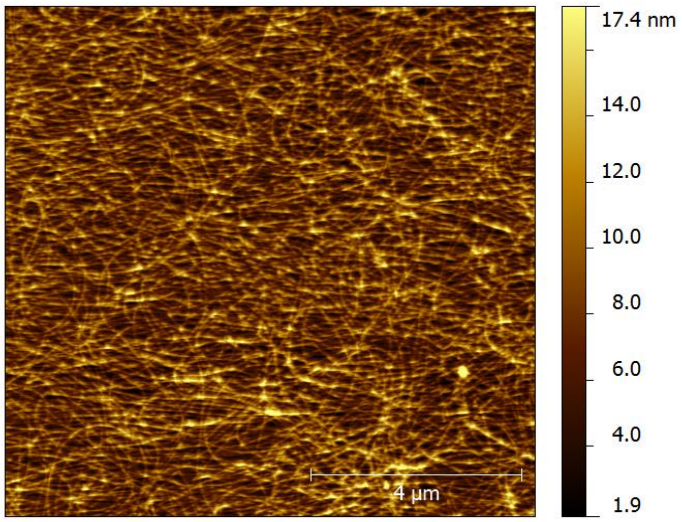

Figure 67: P3HT nanowire growth in chlorobenzene after 22 days. 10mg/ml concentration.

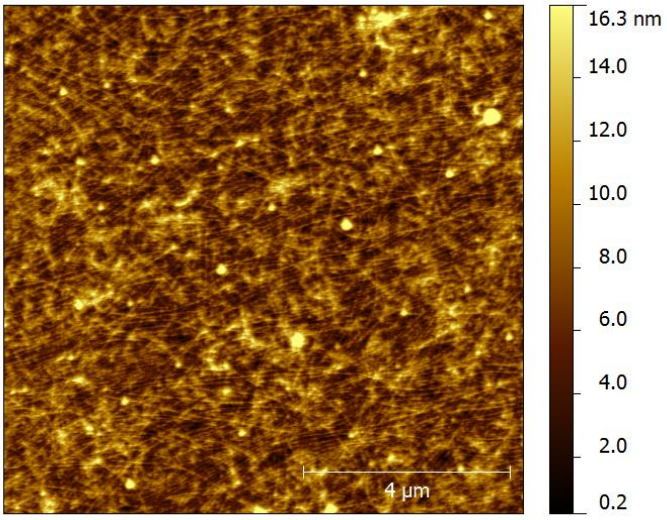

Figure 68: P3HT nanowire growth in dichlorobenzene after 22 days. 10mg/ml concentration.

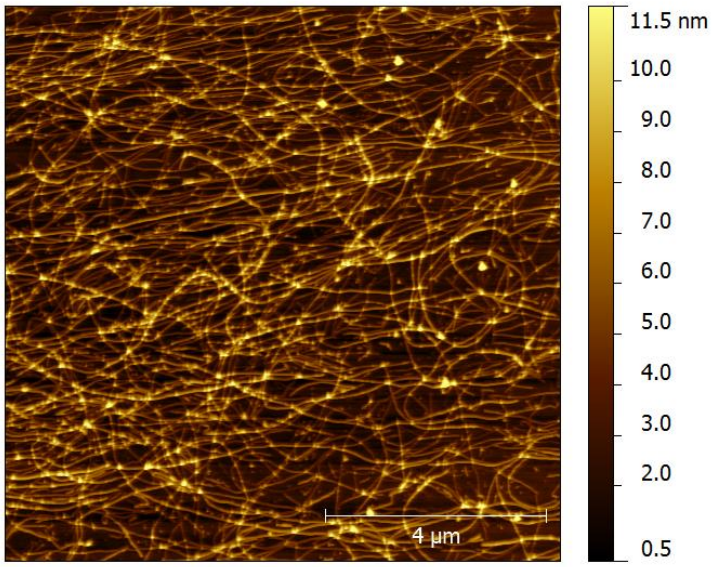

Figure 69: P3HT nanowire growth in trichlorobenzene after 22 days. 10mg/ml concentration.

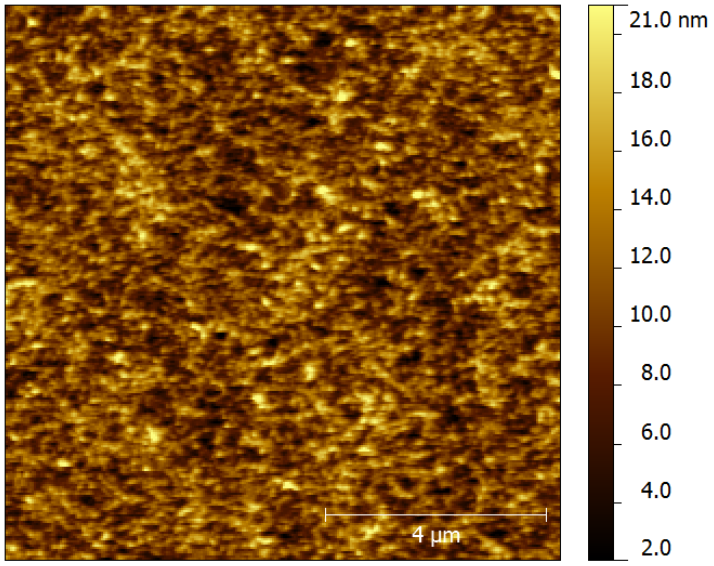

Figure 70: P3HT nanowire growth in chloroform after 22 days. 10mg/ml concentration.

By comparing these figures it was found that chloroform did not appear to form long nanowires, and instead formed shorter structures as seen in Figure 70. Dichlorobenzene produced nanowires however there was a lot of amorphous material surrounding them (Figure 68). Finally, from figures Figure 67 and Figure 69 we can see that chlorobenzene produces the most densely packed nanowires;

however trichlorobenzene seems to give slightly cleaner wires. Due to the small difference however it was decided to continue using chlorobenzene for the remainder of the research.

The second parameter to optimise was the concentration of the solution. By searching literature a range of difference concentrations were decided on, these were 0.1, 0.2, 0.5, 1, 5 and 10mg/ml of P3HT in chlorobenzene. These were left for 30 days in solution before being spun at 2000rpm for 60 seconds.

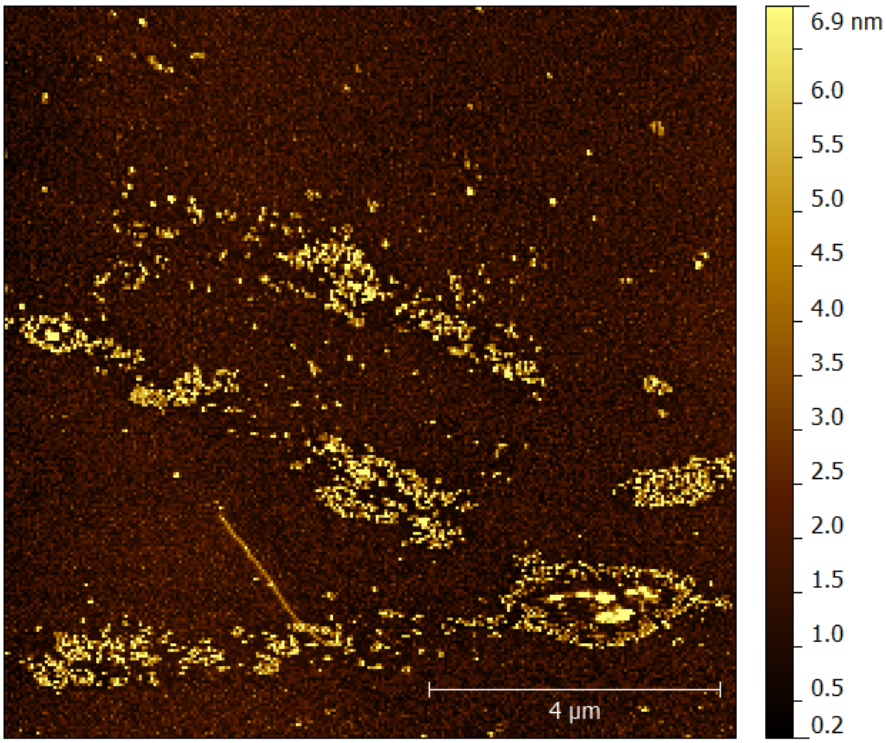

Figure 71: 0.1 mg/ml P3HT in chlorobenzene, spun at 2000rpm onto silicon after 30 days growth.

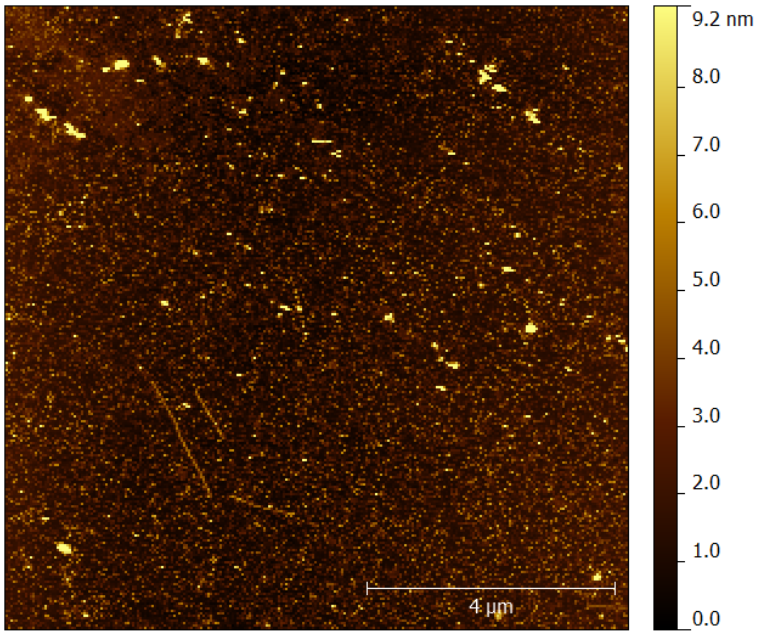

Figure 72: 0.2 mg/ml P3HT in chlorobenzene, spun at 2000rpm onto silicon after 30 days growth.

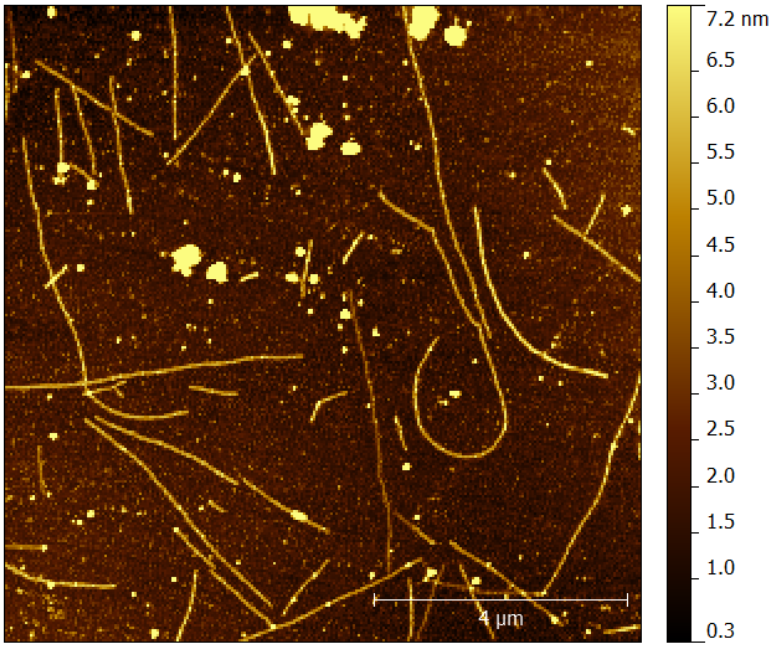

Figure 73: 0.5 mg/ml P3HT in chlorobenzene, spun at 2000rpm onto silicon after 30 days growth.

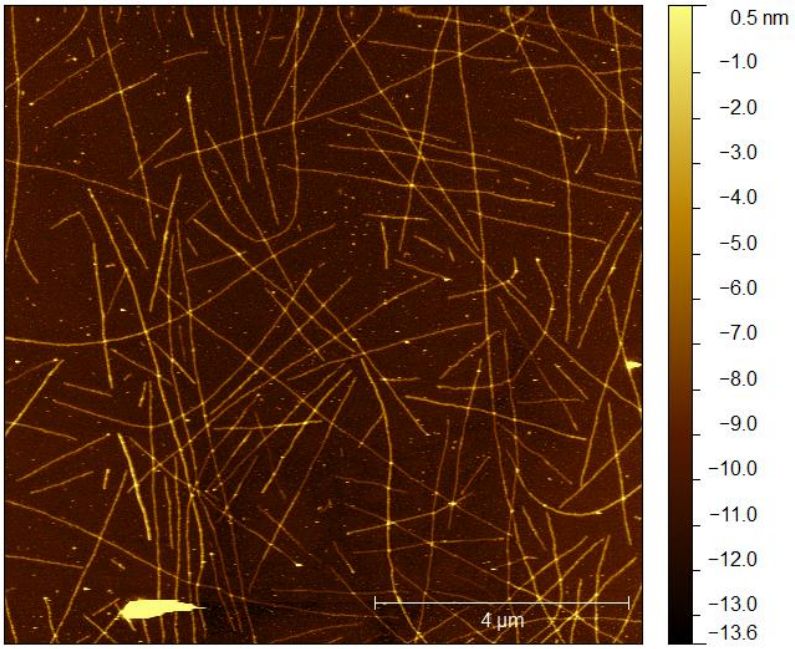

Figure 74: 1 mg/ml P3HT in chlorobenzene, spun at 2000rpm onto silicon after 30 days growth.

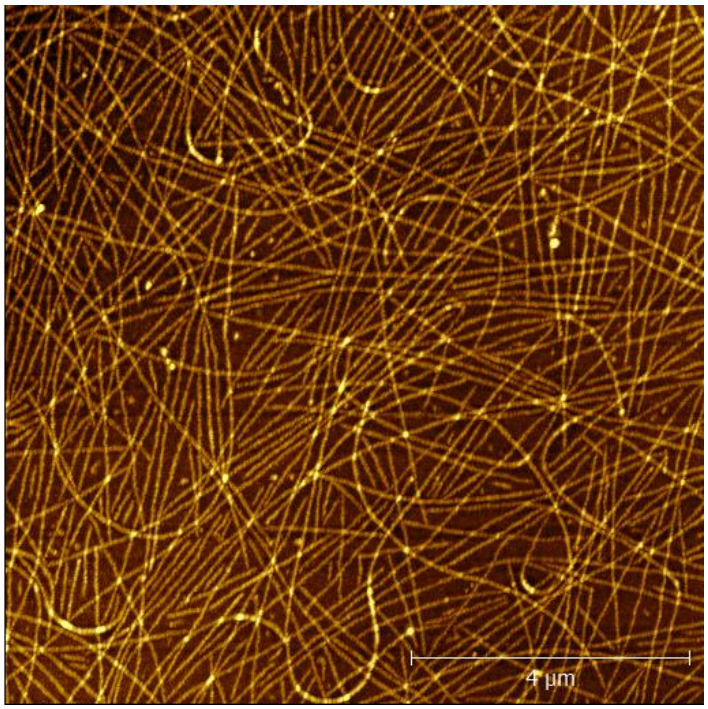

Figure 75: 5 mg/ml P3HT in chlorobenzene, spun at 2000rpm onto silicon after 30 days growth.

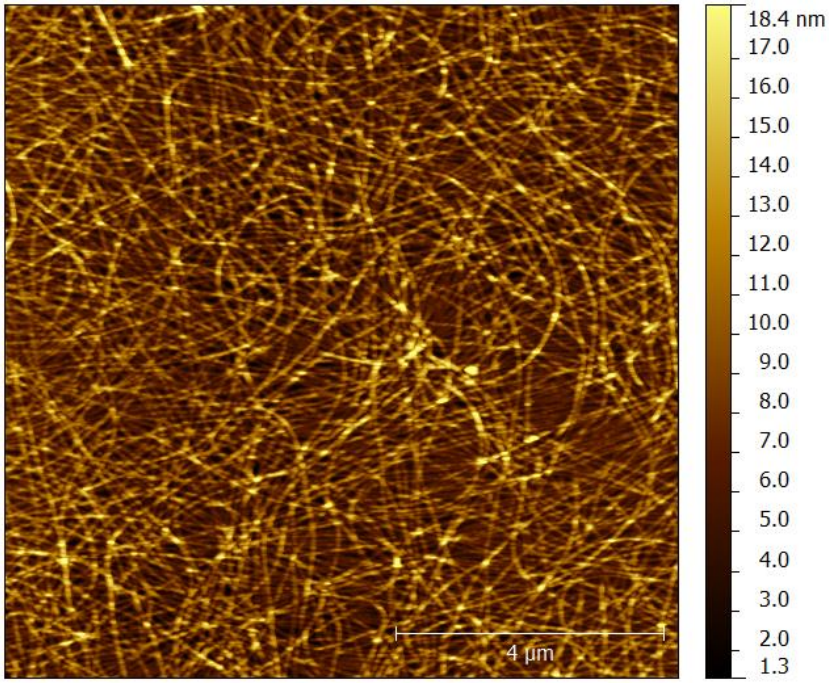

Figure 76: 10 mg/ml P3HT in chlorobenzene, spun at 2000rpm onto silicon after 30 days growth.

From figures Figure 71 to Figure 76 it can be seen that for concentrations below 1 mg/ml very few nanowires are actually present in the solution when spun. Only a few shorter nanowires can be seen on the AFM. 1 mg/ml produces more nanowires but mostly short, sparsely packed wires. For the optimal densely packed long nanowires 5 mg/ml or 10 mg/ml are seen to be optimal from Figure 75 and Figure 76. This is because both of them have large numbers of nanowires of lengths exceeding 1µm, they are also densely packed. The 10 mg/ml looks to be packed more densely than the 5 mg/ml but the 5 mg/ml itself looked to be cleaner nanowires. Both were chosen to be used in the nanowire cleaning methods discussed in section 4.3.

4.3.2. Deposition methods

Several methods were used to try to obtain more uniform, densely packed and aligned nanowire films. The techniques tested were Langmuir films (with multiple compressions and vibrations to promote alignment), drop casting and spin coating. The initial experiments were done using the Langmuir trough stated in the experimental methods section and involved spreading a Langmuir layer of P3HT in chlorobenzene on the water surface, then either performing multiple compressions to attempt to align the nanowires, or vibrating the trough with a sonic probe to do the same. Two concentrations were used on the trough, both were of 30 day old 10 mg/ml solution, one was spread via a few drops directly on the trough, the other was diluted to 0.5 mg/ml, an optimal spreading concentration found in literature. These were then LS dipped onto clean silicon.

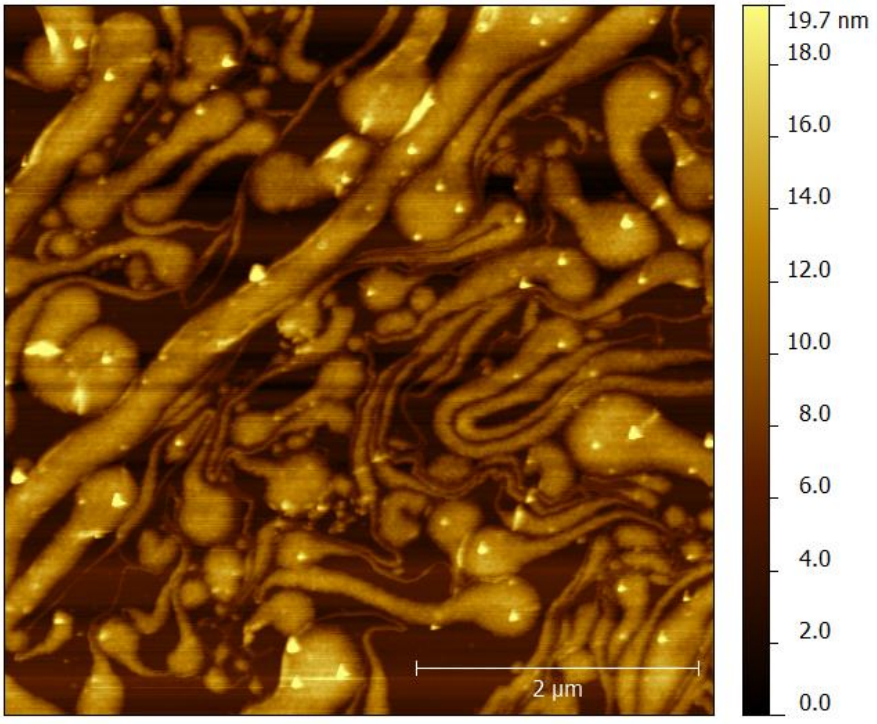

Figure 77: AFM Image of 10mg/ml P3HT diluted to 0.5 mg/ml then spread on a water subphase and LS dipped onto clean silicon.

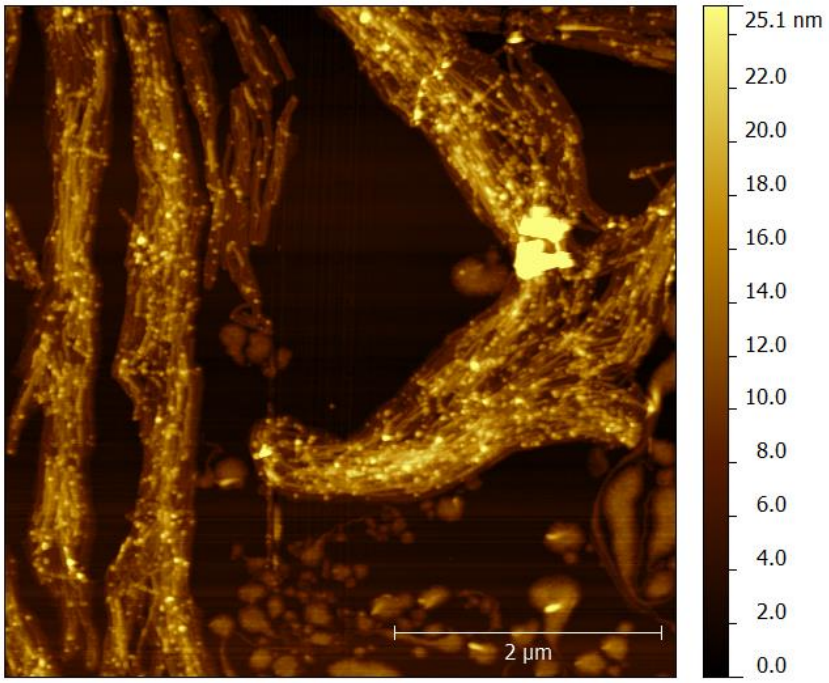

Figure 78: AFM image of 10mg/ml P3HT diluted to 0.5 mg/ml then spread on water subphase and LS dipped onto clean silicon, compressed and expanded 20 times.

From figures Figure 77 and Figure 78 we can see that a large area of the sample is "amorphous" molecularly dissolved P3HT. It was thought that this was either down to insufficient time for a large enough amount of fibrils to form in solution, or that the dilution process was redissolving a large amount of nanowires, causing a lot of amorphous material.

To test this, a sample which was aged for 3 months was LS dipped using the same conditions as above. As seen in Figure 79 and Figure 80.

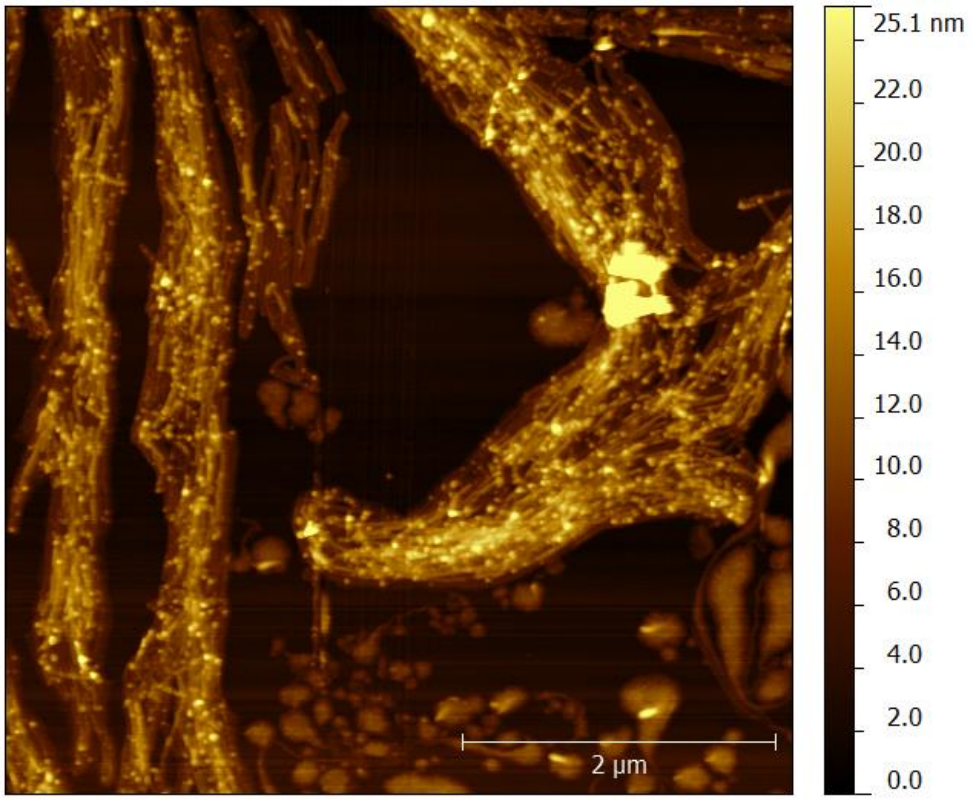

Figure 79: AFM image of 3 month old P3HT in chlorobenzene, 10 mg/ml, diluted to 0.5 mg/ml then spread on water subphase then LS dipped onto silicon after 10 minutes of sonic vibration.

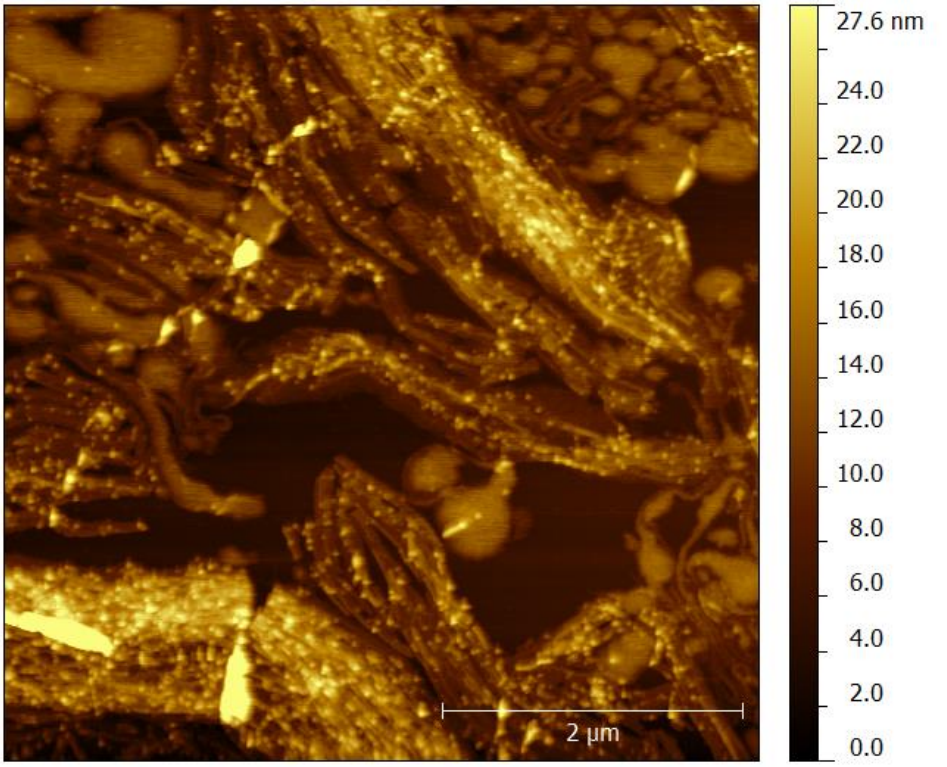

Figure 80: AFM image of 3 month old P3HT in chlorobenzene, 10 mg/ml, diluted to 0.5 mg/ml then spread on water subphase then LS dipped onto silicon after 20 barrier compressions and expansions.

Even after 3 months of growth, the dilution process can still be seen to dissolve a large number of nanowires. It was decided therefore to attempt to drop a few droplets of the 1 month old 10mg/ml solution onto the trough, which was left for 1 hour to allow time to spread evenly. This was then vibrated via ultrasonic probe for 10 minutes and compressed and expanded 20 times.

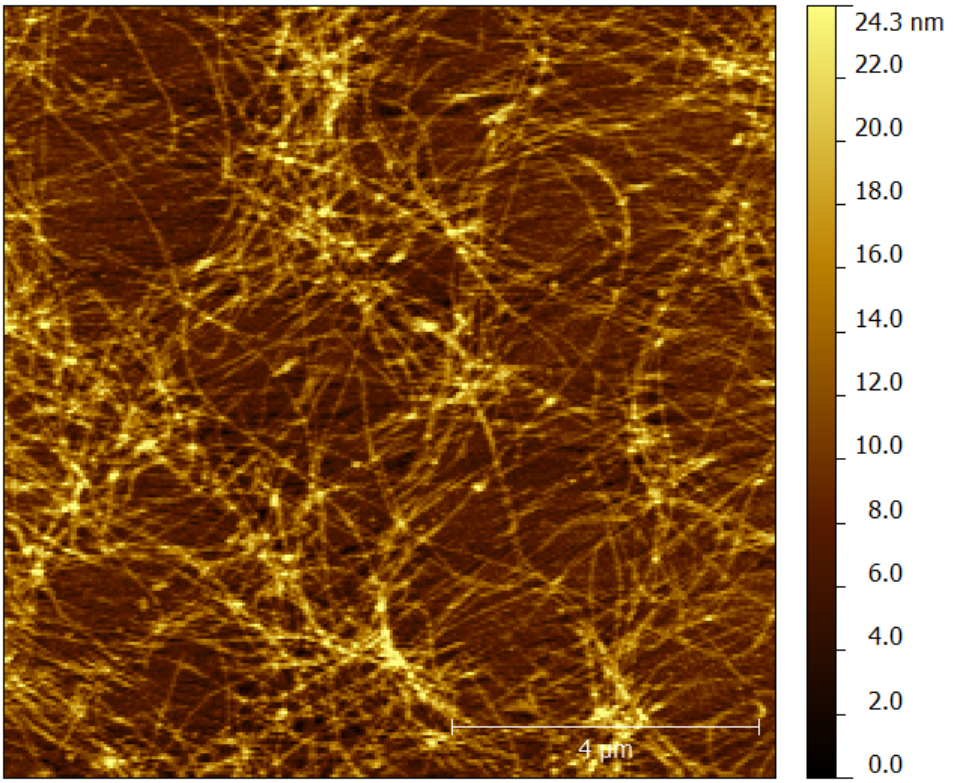

Figure 81: AFM images of 1 month old P3HT in chlorobenzene, spread dropwise onto water subphase then vibrated for 10 minutes and compressed 20 times before being LS dipped onto clean silicon.

From Figure 81 and subsequent data it is seen that the dilution is the main cause of the amorphous P3HT on the LS dipped samples, unfortunately the dense packing of the dried 10 mg/ml film on the water subphase meant that it was not possible to align the nanowires even using both vibration and compression methods.

Another deposition method that was tested was to drop cast the 1 month old solution onto clean silicon, this simply involved applying a small amount of solution onto cleaned silicon via a syringe and covering or being left open to air, allowing the solvent to slowly evaporate, leaving only nanowires on the surface. This was done with the 10 mg/ml P3HT in chlorobenzene solution.

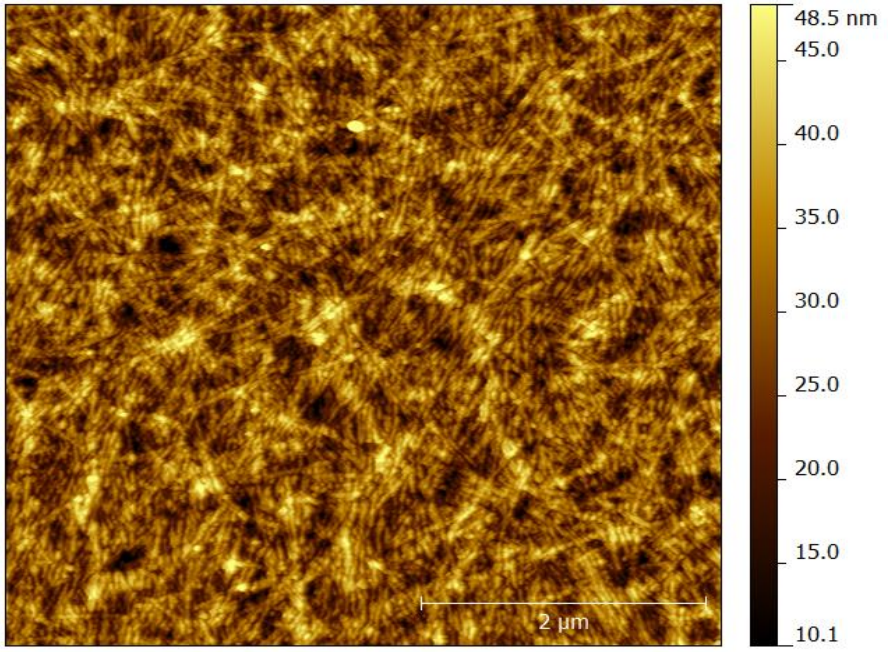

Figure 82: AFM of 1 month old 10 mg/ml P3HT in chlorobenzene, drop cast onto clean silicon then left open to air to dry.

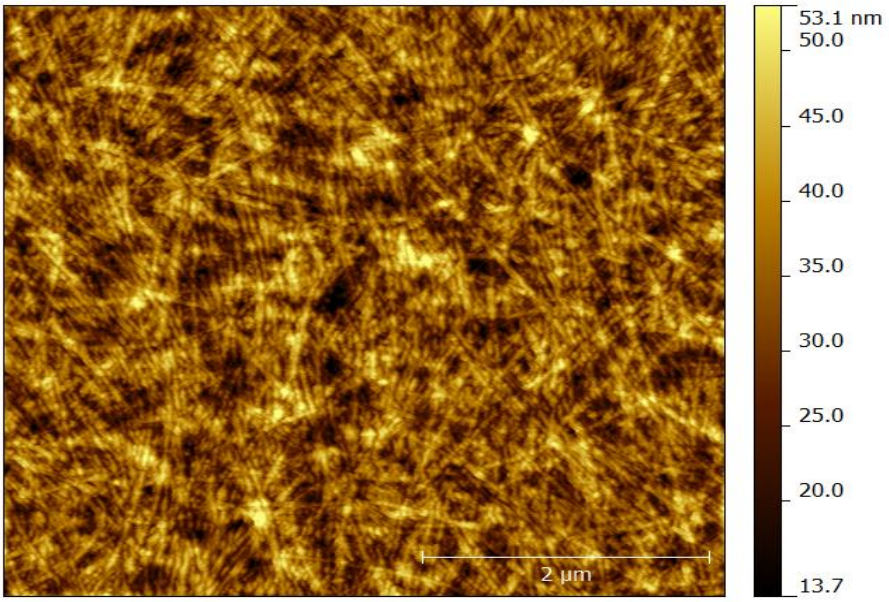

Figure 83: AFM of 1 month old 10mg/ml P3HT in chlorobenzene, drop cast onto clean silicon then placed in closed petri dish to dry.

Figure 82 and Figure 83 show that drop casting produces highly dense films but with large amorphous areas surrounding the nanowires, a lot denser and a lot more amorphous material than previous spin cast layers. Also, open to air drying and contained drying seemed to produce very little differences in the two samples.

The final deposition method tested was the spin casting; this was done with the 5 mg/ml 1 month old P3HT solution in chlorobenzene.

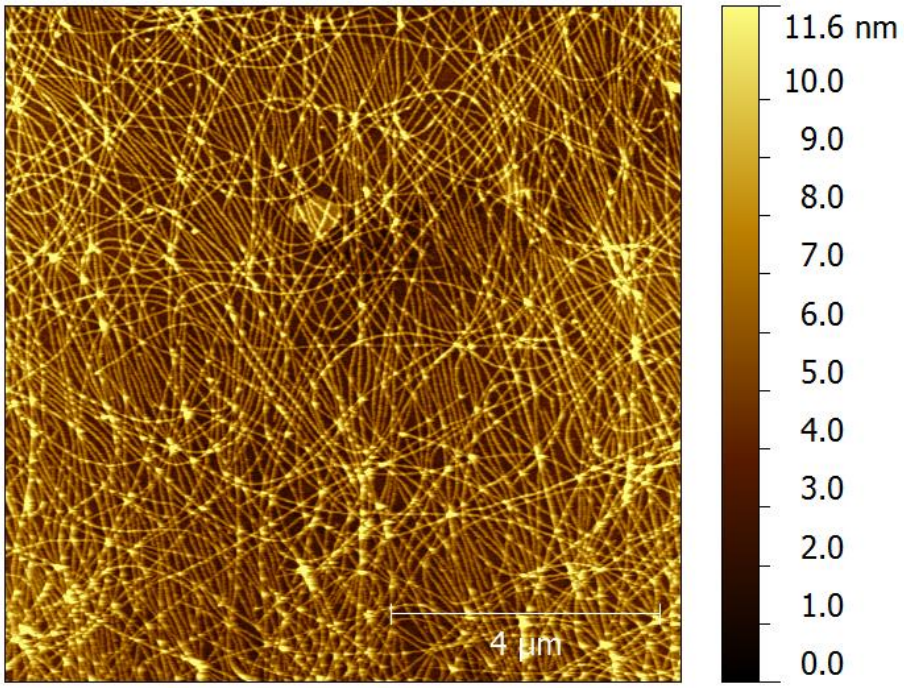

Figure 84: 5 mg/ml P3HT in chlorobenzene, 1 month old and spun onto clean silicon at 4000rpm.

This method produced the highest concentration of fibrils with least amorphous areas. This also came into play for alignment purposes as mentioned in the next section.

4.3.3. Alignment methods

As the preliminary alignment techniques on the trough failed as mentioned in section 0 due to large amounts of amorphous material or the nanowires being too densely packed it was decided to first try an approach which combined the spin coating and Langmuir methods.

To combine the methods, a spin coated sample (1 month old 5mg/ml P3HT in chlorobenzene, spin cast at 2000rpm for 1 minute) was “floated off” in that a scalpel was used to cut the edges of the film which allowed it to float away from the silicon substrate when submersed in the water subphase. It was hoped that this would allow the nanowires (due to less amorphous material than the initial Langmuir films) to be mobile and to align when compressed/vibrated.

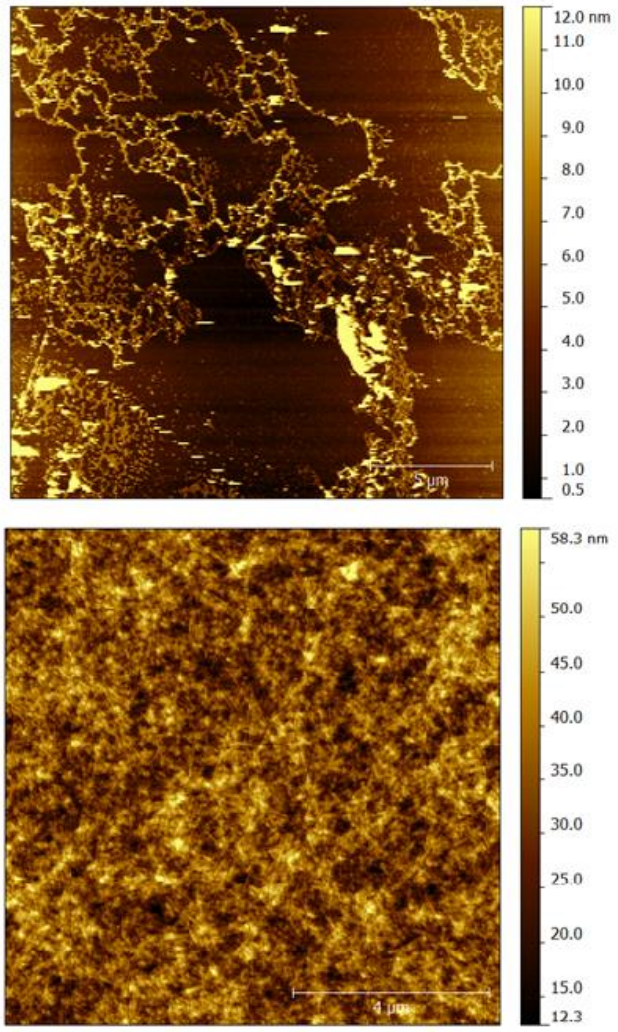

Figure 85:AFM image of 5 mg/ml P3HT in chlorobenzene (1 month old) spun at 2000 rpm onto clean silicon, floated off onto water subphase, vibrated for 10 minutes, compressed 10 times then LS dipped onto clean silicon.

From these images (Figure 85) we can see that vibrating and compression has had no effect on the nanowires. It seems the problem is the same as before in that once the nanowires have dried they are too attached to each other and so densely packed that they cannot move into alignment. Also, from the top image in Figure 85 we also see problems with trying to re-dip a densely packed film as the silicon as only removed parts of the film.

The alignment method that was optimal and produced high alignment films was found when re-investigating previous AFM images of spin cast films. It was found that after spinning at high speeds the nanowires seemed to align themselves radially

outwards from the centre of rotation. In order to test this, the same solution (1 month old, 5 mg/ml P3HT in chlorobenzene) was spun at 1000, 2000, 4000 and 5000 rpm in order to test if there was any correlation between alignment and spin speed.

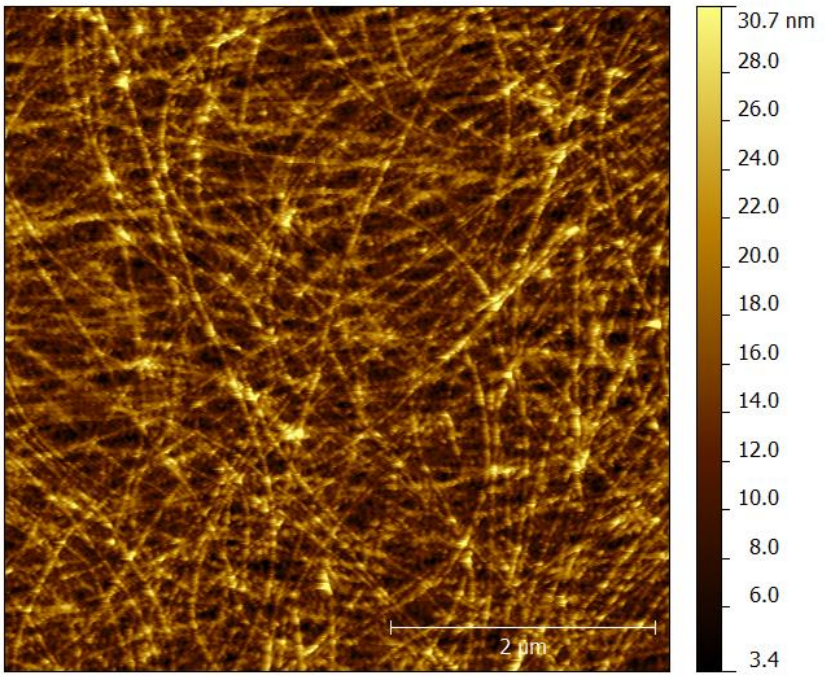

Figure 86: AFM of 1 month old 5mg/ml P3HT in chlorobenzene, spun at 1000 rpm onto clean silicon.

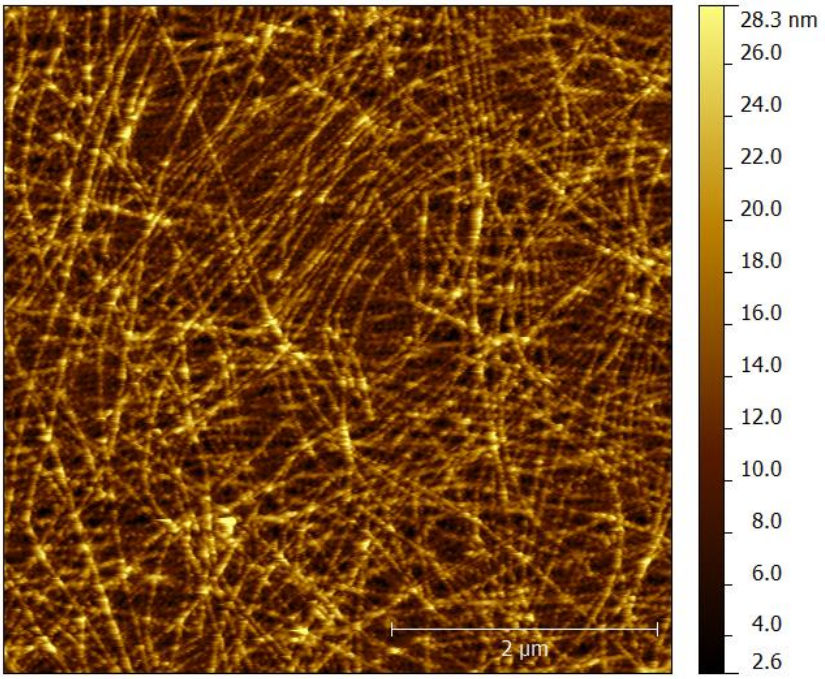

Figure 87: AFM of 1 month old 5mg/ml P3HT in chlorobenzene, spun at 2000 rpm onto clean silicon.

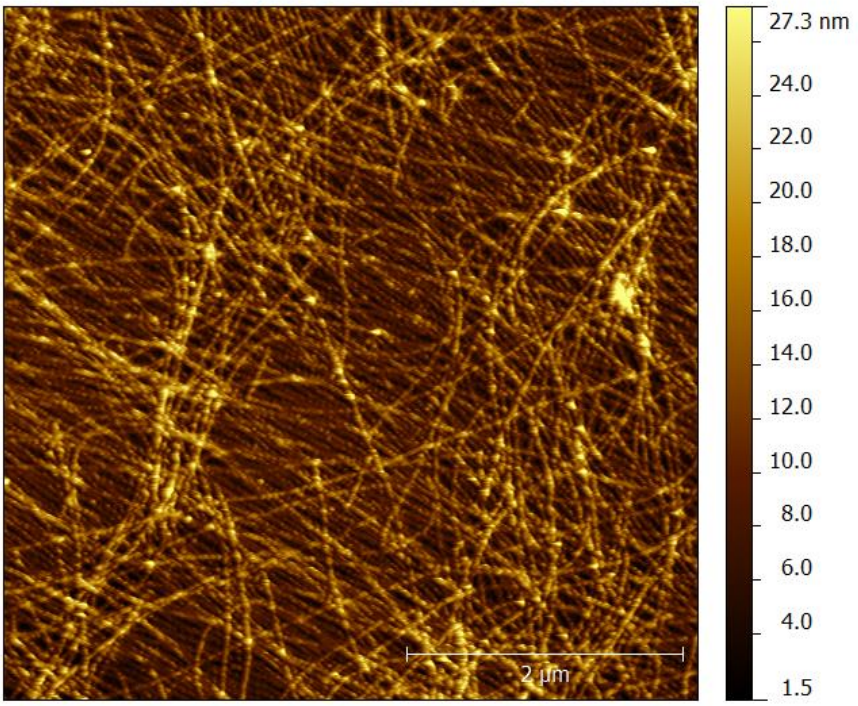

Figure 88: AFM of 1 month old 5mg/ml P3HT in chlorobenzene, spun at 4000 rpm onto clean silicon.

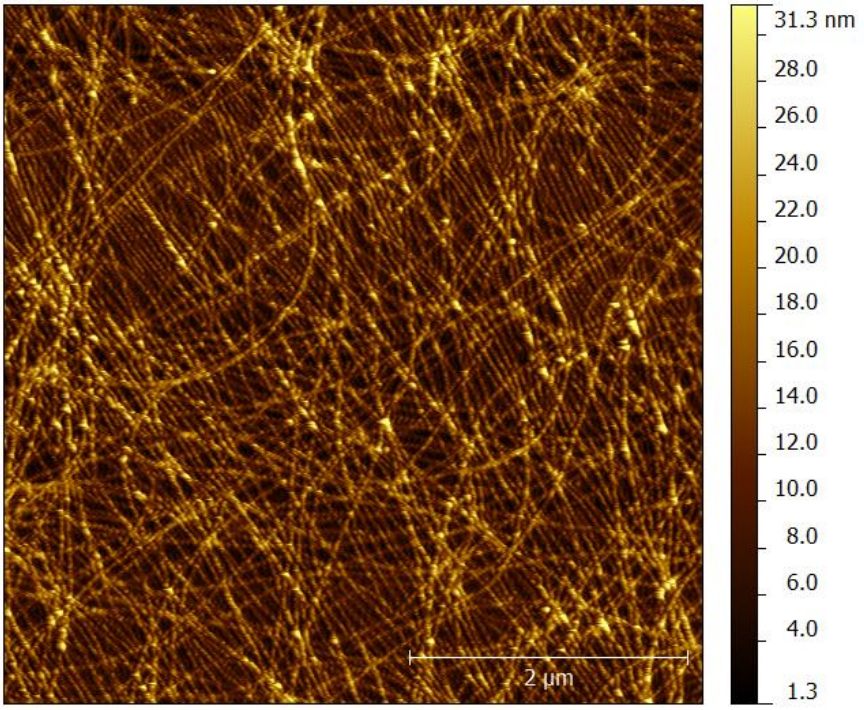

Figure 89: AFM of 1 month old 5mg/ml P3HT in chlorobenzene, spun at 5000 rpm onto clean silicon.

As we can see from figures Figure 86 to Figure 89, the alignment of the nanowires increases the higher the spin speed. The nanowires are partially aligned in the 1000 and 2000 rpm AFM, mainly in the background with random nanowires laid on top. In the 4000 and 5000 rpm AFM images the nanowires are much more aligned, the 5750 rpm being the best speed for high alignment of both underlying nanowires and the ones laying on top.

It was also important to test if the nanowires were running parallel to the radial direction or perpendicular to it, in order to be able to prepare nanowires on pre prepared electrode samples. In order to test this, larger silicon wafers were used with marked areas taken and imaged as shown in Figure 90, Figure 91 and Figure 92.

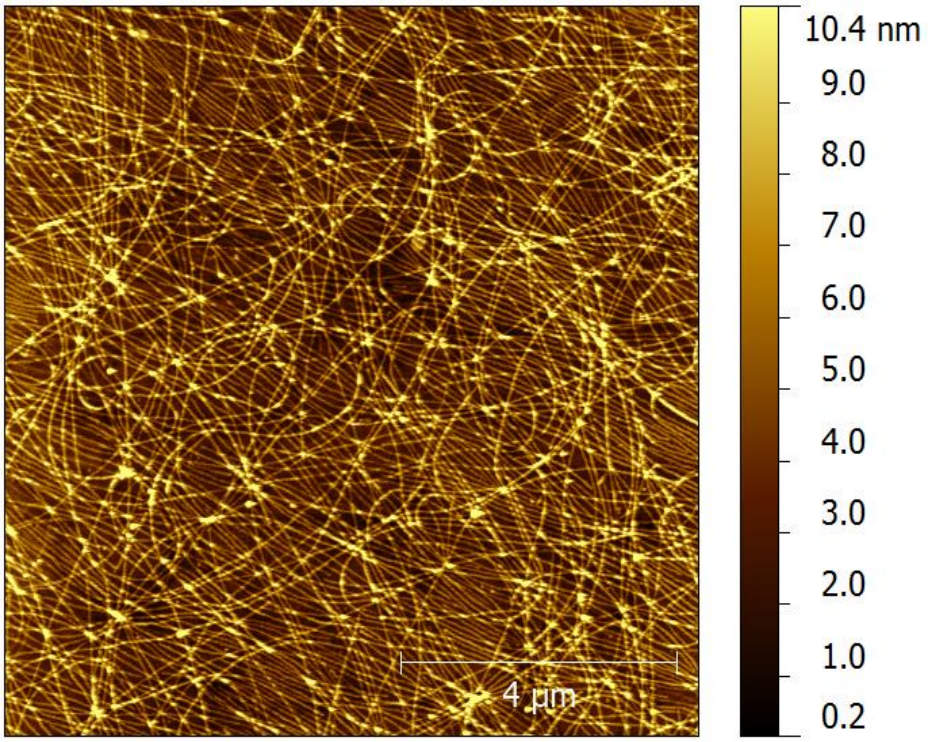

Figure 90: AFM of 1 month old 5mg/ml P3HT in chlorobenzene, spun at 5000 rpm onto clean silicon. Right of centre.

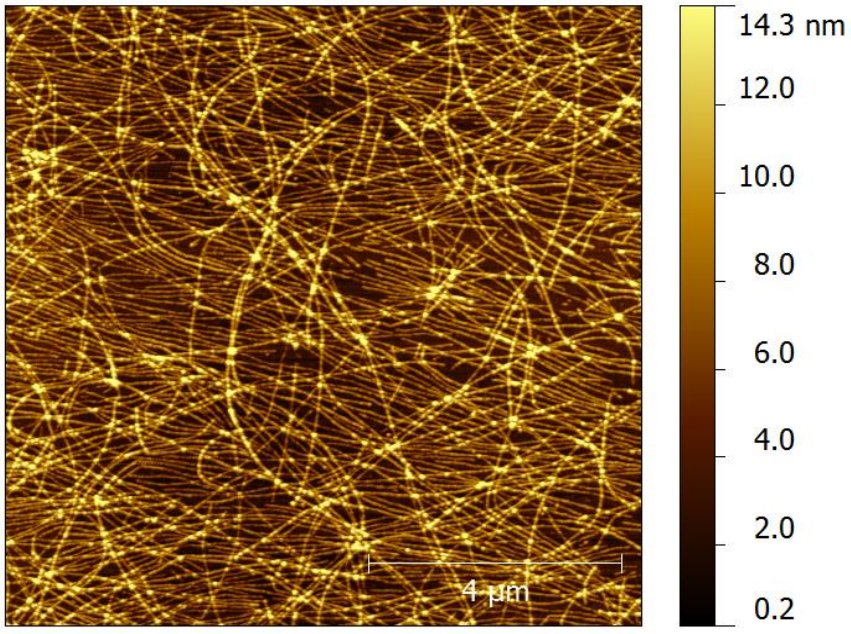

Figure 91: AFM of 1 month old 5mg/ml P3HT in chlorobenzene, spun at 5000 rpm onto clean silicon. Left of centre.

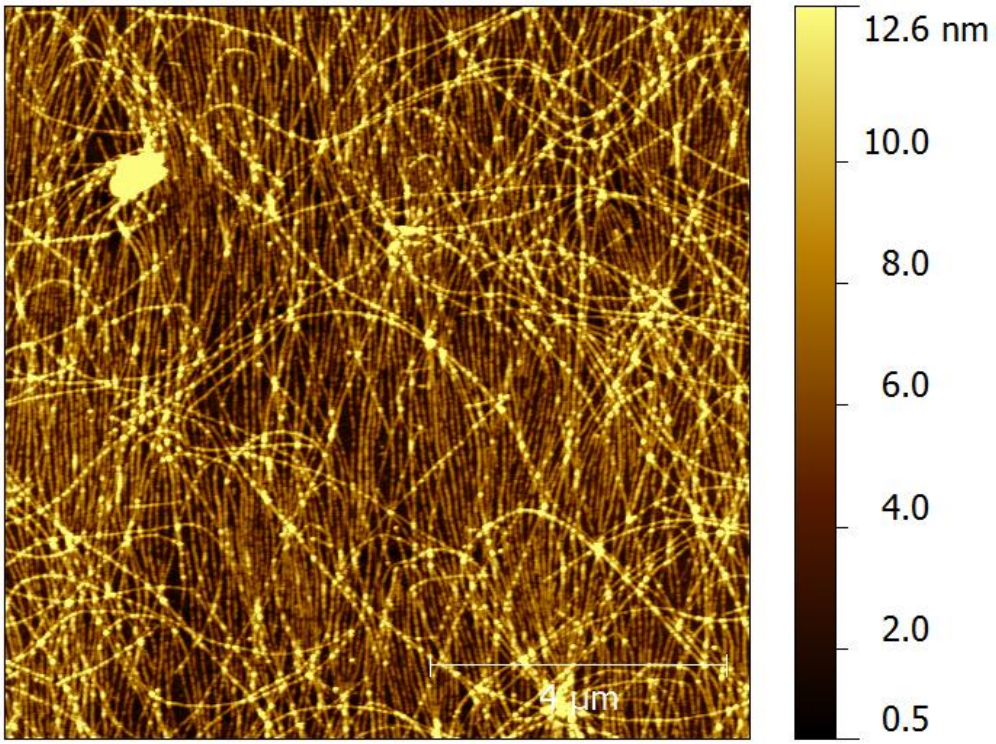

Figure 92: AFM of 1 month old 5mg/ml P3HT in chlorobenzene, spun at 5000 rpm onto clean silicon. Below centre.

The samples were spun at 5000 rpm using the 1 month old 5mg/ml P3HT in chlorobenzene. The AFM images were taken 2cm away from the centre of the sample.

From these images it is clear that the nanowires align themselves radially outwards from the centre of the sample, which can be used to align nanowires as needed on pre positioned electrodes.

4.3.4. Cleaning methods

Once the optimal concentration and concentration were found, as well as the best dipping method to get the best alignment and high density films and investigation into the possibility of getting “cleaner” films was performed. This was mainly to remove as much amorphous material as possible from the nanowire films to give pure nanowires.

In order to do with two methods were tested in four different combinations, each of which was spun at 5000rpm for 1 minute onto clean silicon. A control test of the 1 month old 5mg/ml P3HT in chlorobenzene with no cleaning performed, dilution of a 1 month old 10mg/ml P3HT in chlorobenzene solution in order to dissolve some amorphous P3HT and have it be washed away during the spin process, spin rinsing a sample (1 month old 5mg/ml spun onto silicon) which involved spinning the sample with chlorobenzene in order to dissolve and wash away any residual amorphous P3HT. The final method was to combine the two methods and dilute the 10mg/ml P3HT to 5mg/ml and then spin rinsing with chlorobenzene. The results are shown in figures Figure 93 to Figure 96.

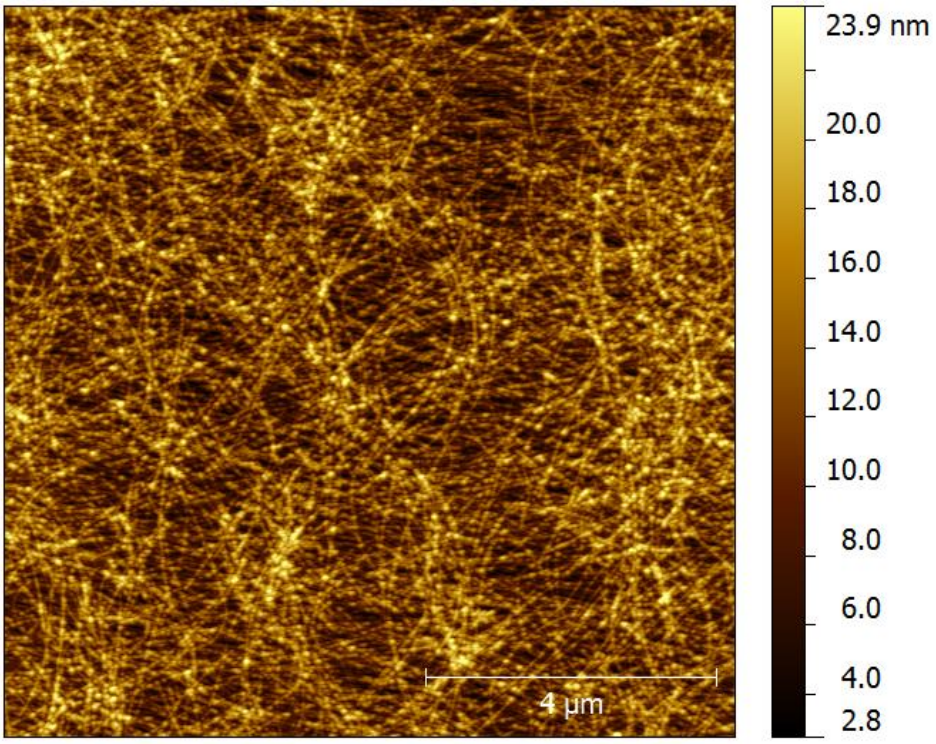

Figure 93: AFM of 1 month old 10mg/ml P3HT in chlorobenzene, diluted to 5mg/ml then spun at 5000rpm onto clean silicon.

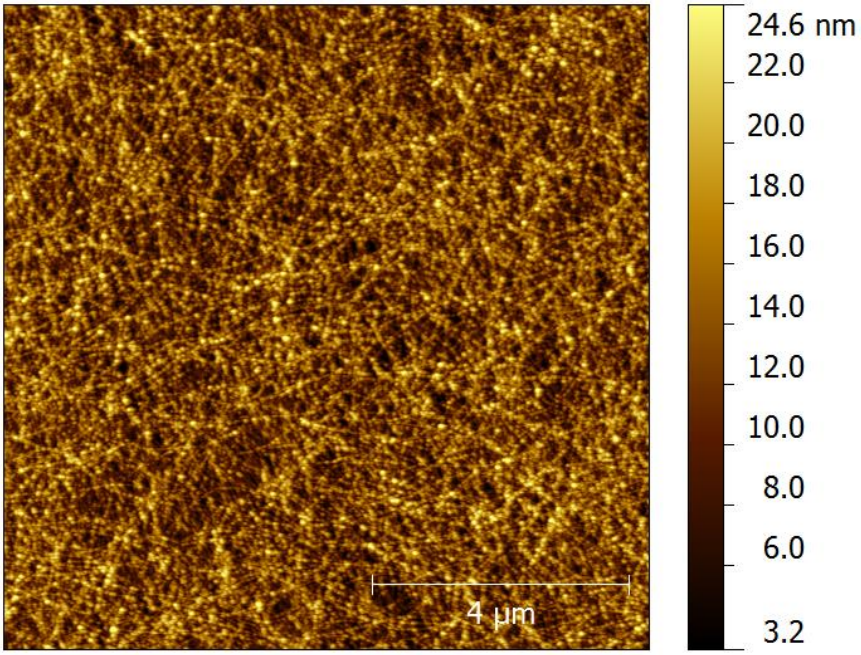

Figure 94: AFM of 1 month old 10mg/ml P3HT in chlorobenzene, diluted to 5mg/ml then spun at 5000rpm onto clean silicon. Afterwards spin rinsed in chlorobenzene for 1 minute.

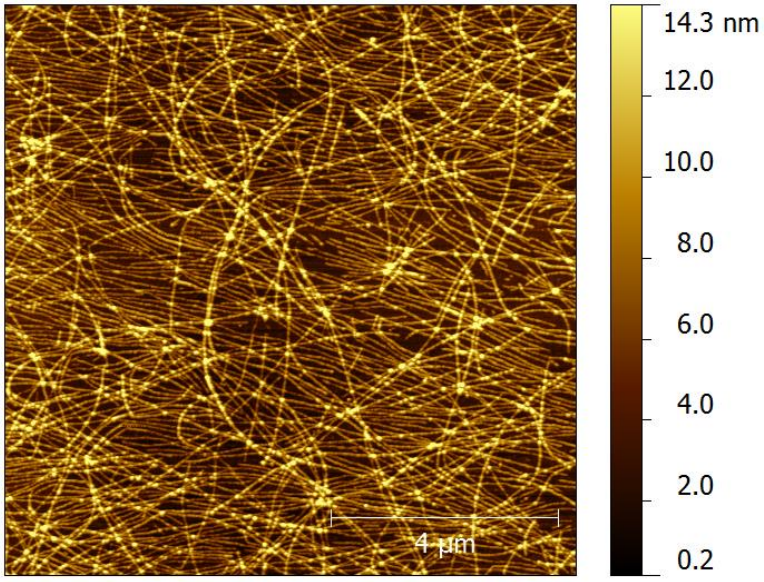

Figure 95: AFM of 1 month old 5mg/ml P3HT in chlorobenzene, spun at 5000rpm onto clean silicon.

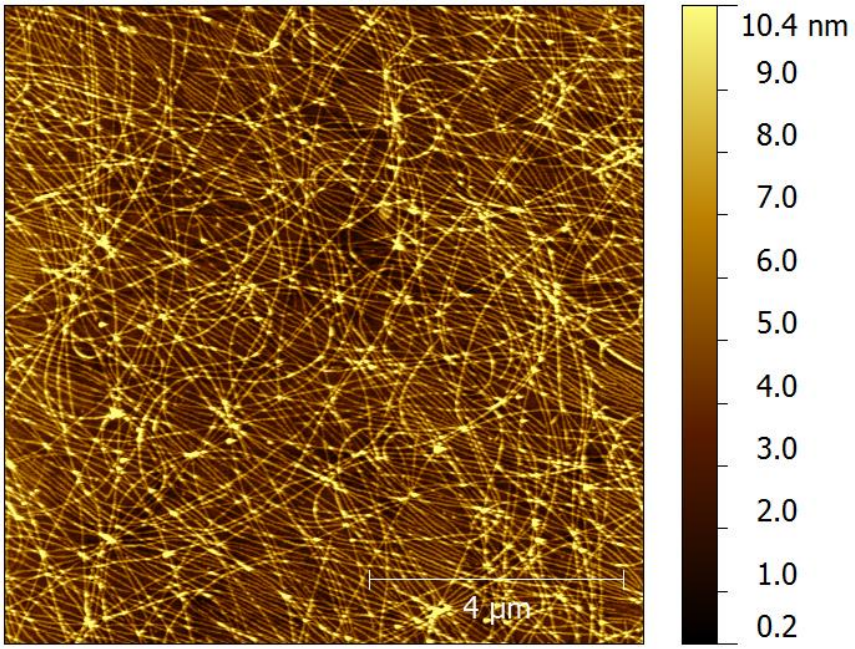

Figure 96: AFM of 1 month old 5mg/ml P3HT in chlorobenzene, spun at 5000rpm onto clean silicon then spin rinsed in chlorobenzene for 1 minute.

From these images we can see that dilution actually produces more amorphous P3HT around the nanowires, and spin rinsing this makes it worse, with more amorphous P3HT. Comparing the two 5mg/ml samples, both original and spin rinsed it is hard to have a decision regarding which is best as both seem to have dense nanowires, highly aligned with very little amorphous P3HT. As such it was preferred to simply use 5mg/ml and not spin rinse if the rinsing would produce little to no improvements to the film.

4.3.5. Nanowire optimisation summary

To summarise the optimal nanowire preparation investigation, the first optimisation to be made was the solvent and solution concentration. It was found that using chlorobenzene produced large amounts of nanowires in around 30 days (although smaller amounts of time did produce nanowires, 30 days was chosen as it represented a time where enough nanowires had formed to have little to no amorphous material when spin casting under optimal conditions). It was also found that the optimal concentration for densely packed nanowires with lengths greater than 1μm but with the least amount of amorphous P3HT was 5mg/ml; any less and the nanowires were sparse and short and any higher and the nanowires had large amounts of amorphous material packed between them.

The best deposition method and alignment method was found to be spin casting as Langmuir dipping produced either a large amount of amorphous material or did not allow alignment to occur either on the water surface or afterwards. Spin casting allowed very high density films to be made with low amorphous P3HT content and at speeds higher than 4000rpm (5000rpm was the most optimal, and the limitation of the spin coater) the nanowires aligned themselves radially outwards from the centre of rotation.

Finally it was found that compared to dilution of the solution or spin rinsing, simply using the optimal 5mg/ml and not performing any “cleaning” to remove amorphous P3HT was the most optimal solution.

4.4. Characterisation of P3HT nanowires in solution and thin films

4.4.1. UV-Vis characterisation

One of the first methods used in this research to characterise the P3HT nanowires was Ultraviolet-Visible spectroscopy. The characterisation was undertaken on two types of samples, thin films on mica and glass, and solution based characterisation where the solution had to be diluted before spectroscopy, in order to allow enough light through for an accurate reading.

For the thin film characterisation, two samples were compared. The first was spun onto mica from a 9 month old 10mg/ml M101 rrP3HT in chlorobenzene solution. The second, the same solution but LS dipped onto glass. These two sets of data are compared in Figure 97.

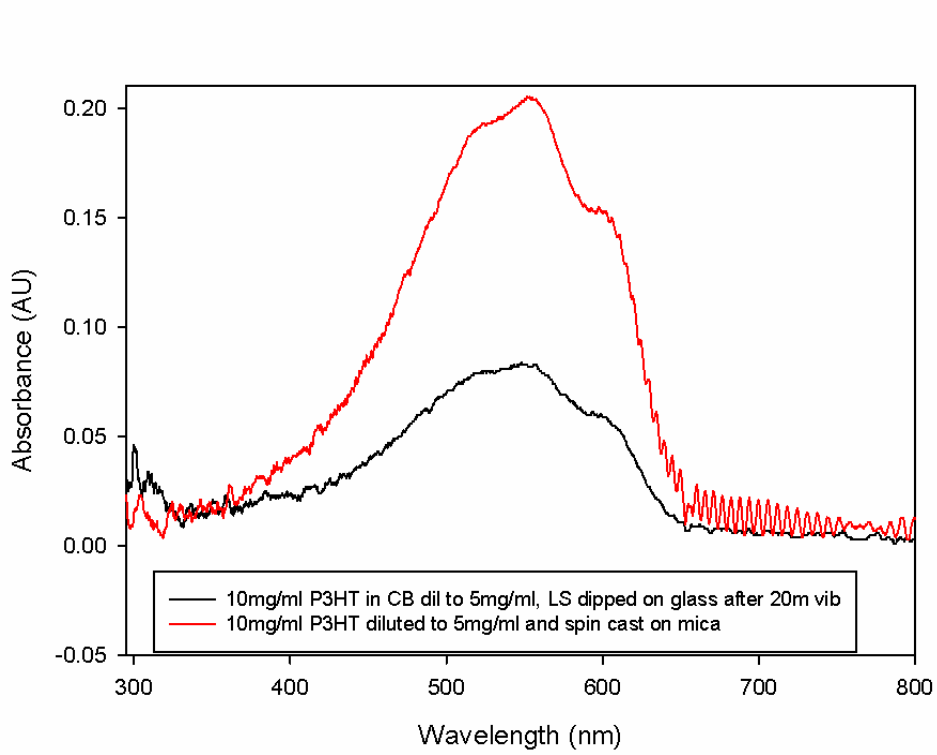

Figure 97: A UV-Vis plot showing a comparison between the absorbance spectra of 10mg/ml M101 rrP3HT spun onto mica and LS dipped onto glass after 20 minutes sonic vibration on the trough.

As can be seen from these data, both exhibit a moderate peak at the given 450nm wavelength which corresponds to molecularly dissolved P3HT [39], however much larger peaks are present in both at the 550nm and 600nm wavelengths which show that on both of these substrates there is a large contribution towards the absorbance spectrum coming from P3HT nanowires[39].

For the solution based characterisation, two solutions were compared. The first was a new 10 mg/ml solution of the M101 rrP3HT in chlorobenzene. This was diluted to 0.025 mg/ml in order for the spectroscopy to work. The second solution was a 13 day old 10mg/ml rrP3HT in chlorobenzene solution which was also diluted to 0.025 mg/ml for optimal spectroscopy. These two data sets are shown, compared with the thin film characterisation in Figure 98.

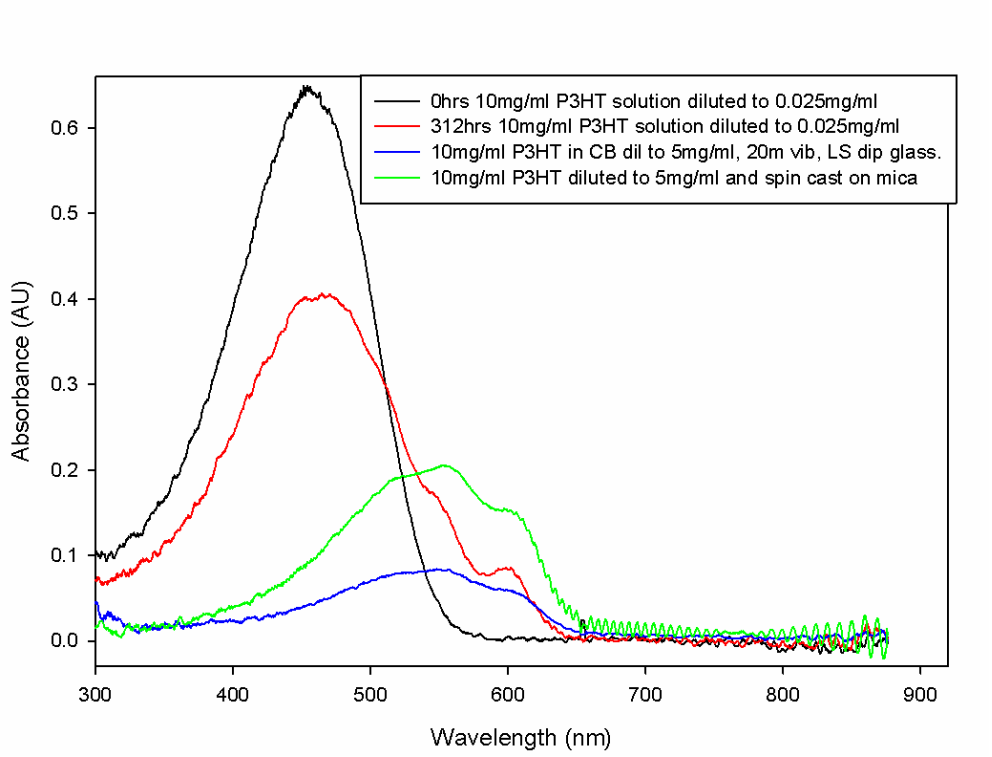

Figure 98: A UV-Vis plot showing a comparison between the previously shown absorbance spectra of 10mg/ml M101 rrP3HT spun onto mica and LS dipped onto glass, with a new 10 mg/ml solution of the same rrP3HT in chlorobenzene, diluted to 0025 mg/ml for solution spectroscopy, and 13 day old 10mg/ml M101 rrP3HT in chlorobenzene solution which was also diluted to 0.025 mg/ml for solution spectroscopy.

From this graph we can see that compared to the thin film samples, the solution based samples have a much larger contribution to the spectrum via the 450nm molecularly dissolved P3HT peak than the solid samples. However it can still be seen that after 13 weeks, although there is still a large, albeit smaller molecularly dissolved 450nm peak, the 550nm and 600nm peaks corresponding to P3HT nanowires are clearly present.

The large molecularly dissolved P3HT contribution to the spectrum of the solution based samples could be explained due to the fact that by diluting the solution by a large amount for spectroscopy, we are dissolving a large amount of nanowires, thus turning it back into molecularly dissolved P3HT. It does also show however, that

after 13 days, even after a large dilution, there is still clear evidence of significant P3HT nanowires in the solution.

4.4.2. AFM characterisation

The characterisation of the nanowires via AFM continued after the initial experiments which allowed us to both determine the time scale for efficient nanowire growth in chlorobenzene, as well as outlining the best deposition techniques and "cleaning" methods.

Once these optimal nanowire films were created, on silicon via spin casting at 4000rpm, from the 9 month old 5 mg/ml M101 rrP3HT in chlorobenzene. AFM data was used in order to determine the average size of the nanowires in comparison to literature.

A few preliminary tests were done on low area nanowires that were only 12 days old (5mg/ml M101 rrP3HT in chlorobenzene) width and height profiles were taken to get an estimate to the size of the nanowires.

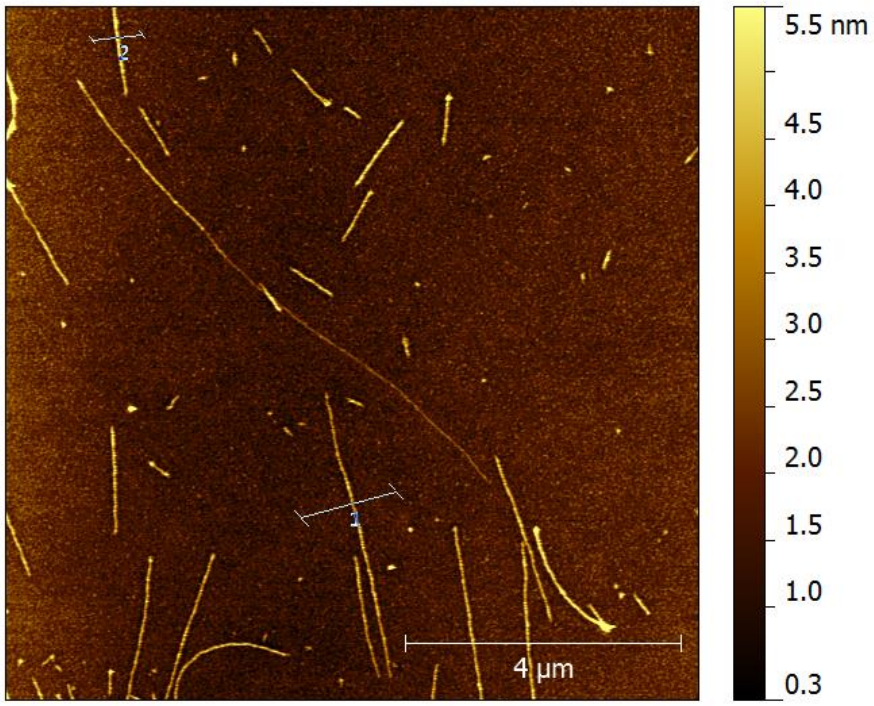

Figure 99: An AFM with profile lines to determine the height and width of P3HT nanowires.

Figure 99 shows the profile of the nanowires with figures Figure 100 and Figure 101 showing the height profile graphs. From these graphs and averaging results we get an average height of 3.08nm, the same graphs were then used to get a width profile which, when average gave an average width of 57.2 nm. These values were within the right order of magnitude from literature [13].

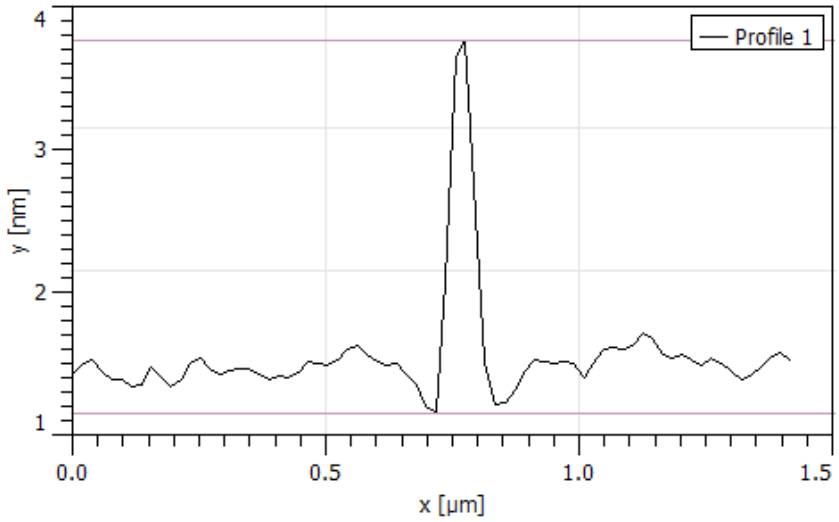

Figure 100: A graph of the height profile of the P3HT nanowires.

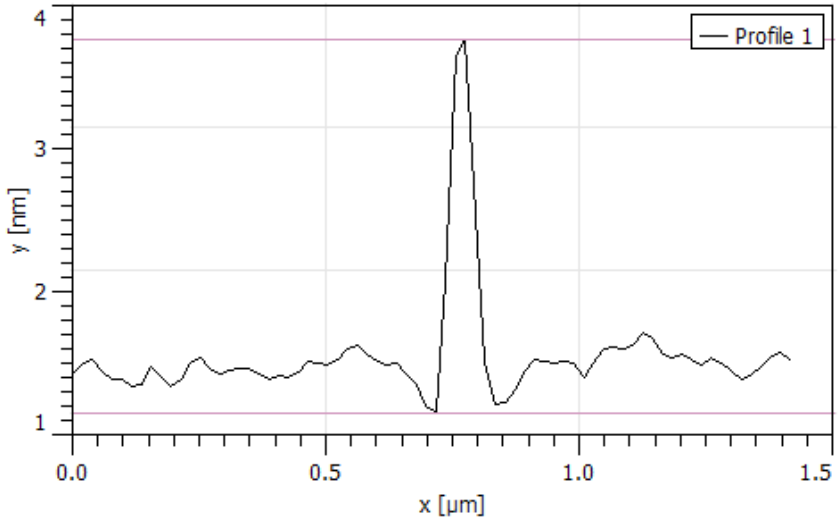

Figure 101: A graph of the height profile of the P3HT nanowires.

This process was repeated on a different sample made from the same 12 day old solution. Figure 102 shows the AFM image used for the height and width profiles of this second sample

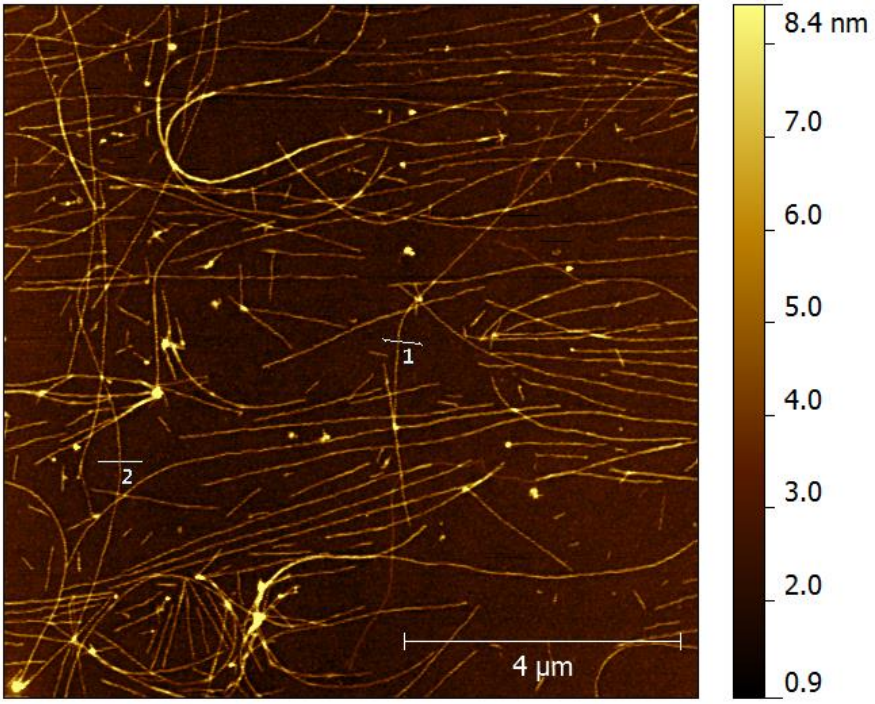

Figure 102: An image showing cross sections of P3HT nanowires used for height and width analysis of the nanowires.

The profile graphs are shown in Figure 103 and Figure 104.

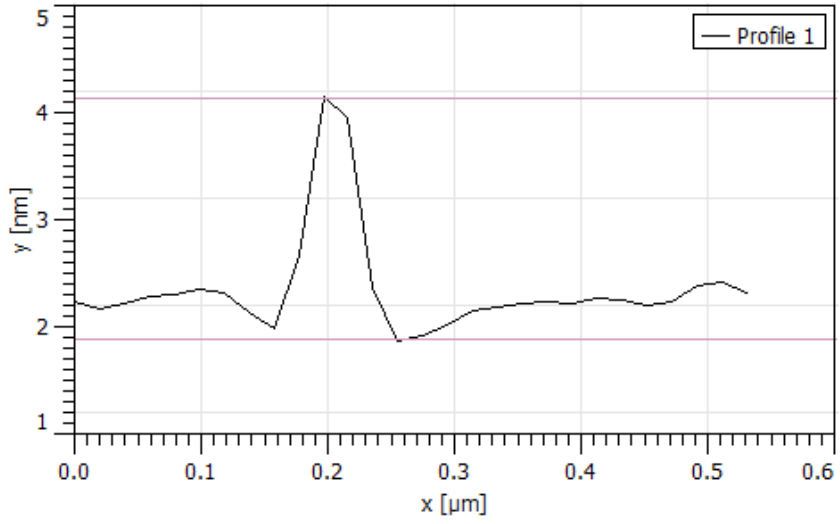

Figure 103: A graph of the height profile of the P3HT nanowires, new sample.

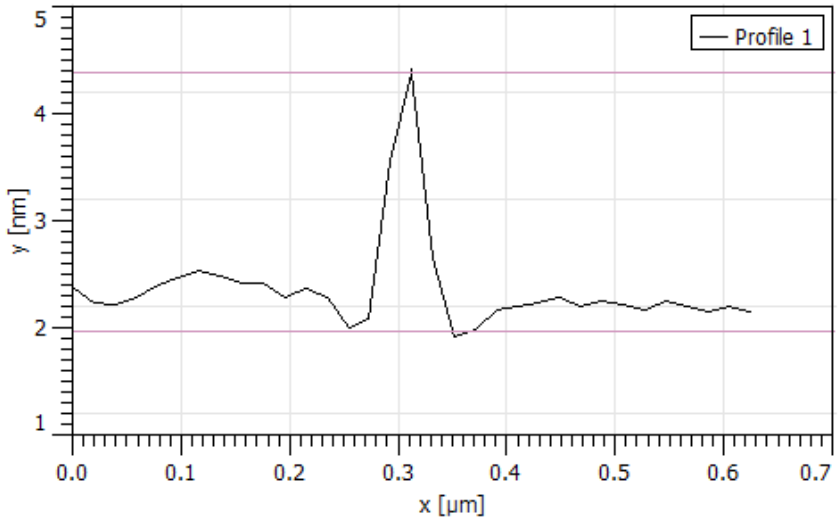

Figure 104: A graph of the height profile of the P3HT nanowires, new sample.

From these figures it would found by averaging the height profiles that the average height of the nanowires was found to be 2.55nm and average width of 42.95nm. This is again within the right order of magnitude but a more comprehensive study was needed in order to get a more precise value for the height and width of the P3HT nanowires.

A more in depth review was undertaken, averaging from 5 months old and 12 days old 5mg/ml M101 rrP3HT in chlorobenzene, spun onto multiple samples of silicon at 5000rpm. Two samples were tested, each with a large number of cross sections taken. The figures Figure 105 and Figure 106 show the two AFM images that were analysed.

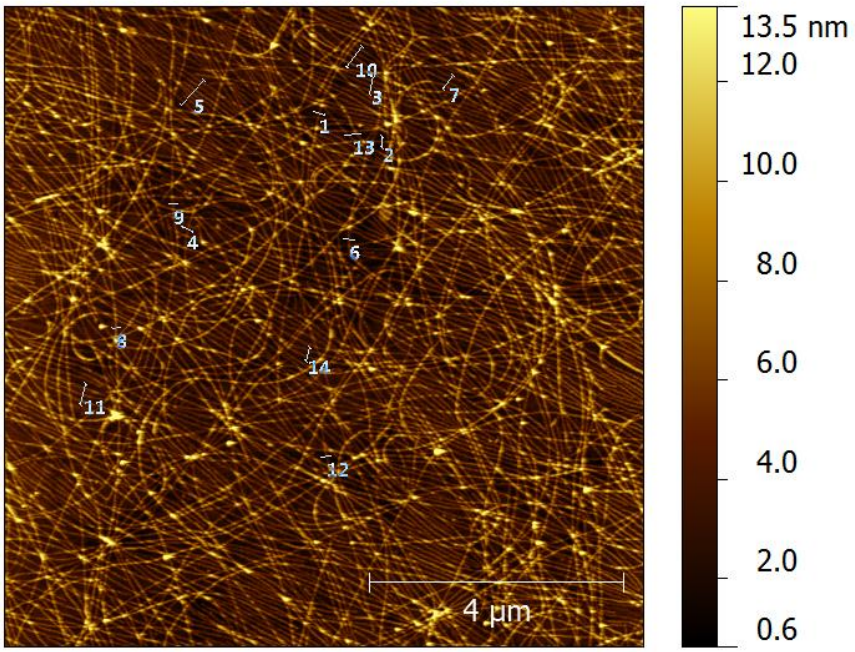

Figure 105: AFM image of various height profiles of 5 month old rrP3HT in chlorobenzene. Height profiles taken and averaged to get average nanowire height and width.

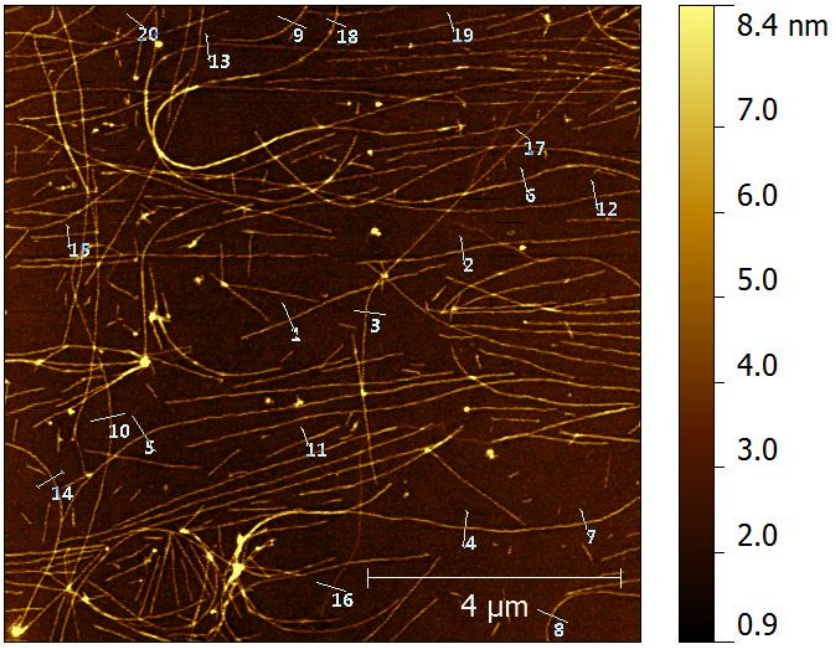

Figure 106: AFM image of various height profiles of 12 days old rrP3HT in chlorobenzene. Height profiles taken and averaged to get average nanowire height and width.

By taking these two images and averaging the nanowire widths and heights via profiles, the average nanowire height was found to be 2.39±0.21 nm and average width of 42.87±0.17 nm. These correspond well with the given heights of nanowires reported in literature, and match well also with the widths, if the width of the nanowire is proportional to M_w and thus the chain length [47].

Scratch tests were also performed and height profiles taken in order to determine the average thickness of the P3HT nanowire film, on the silicon substrate. The sample was the standard 5mg/ml M101 rrP3HT in chlorobenzene, 5 months old and spun onto clean silicon at 5000rpm. The sample was scratched by a scalpel and then tapping mode AFM was performed on it in order to get a step height of the scratch and thus determine the height of the nanowire film.

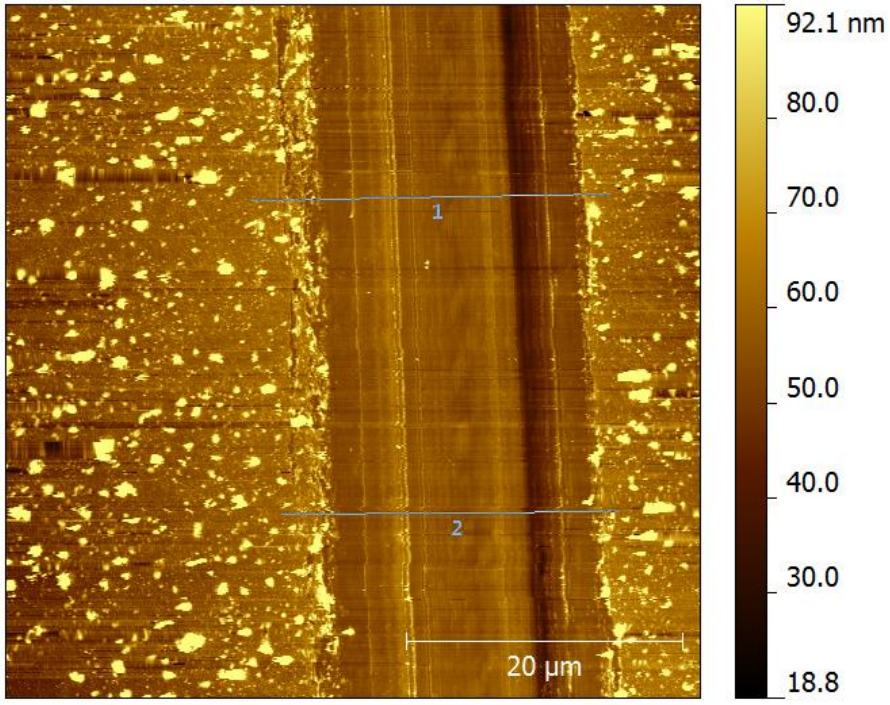

Figure 107: AFM images of a 5mg/ml M101 rrP3HT solution in chlorobenzene, aged 5 months then spread on clean silicon. Scratched with scalpel to perform thickness scratch test.

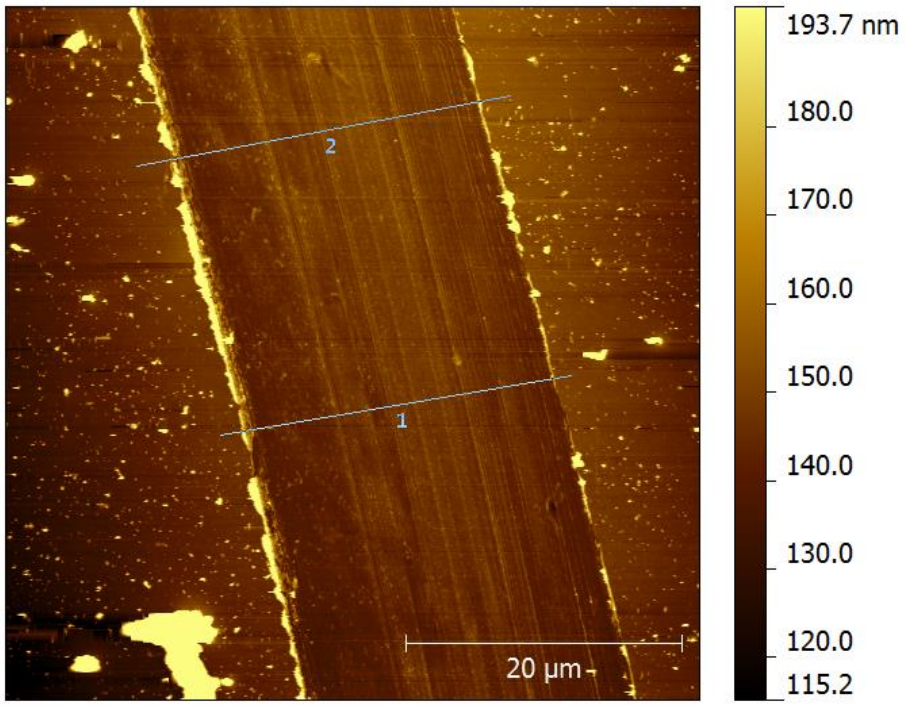

Figure 108: AFM images of a 5mg/ml M101 rrP3HT solution in chlorobenzene, aged 5 months then spread on clean silicon. Scratched with scalpel to perform thickness scratch test.

Figure 107 and Figure 108 show the two samples which were scratched and the two areas on each where height profiles across the scratches were performed. In Figure 109 and Figure 110 the height profiles of each sample is shown respectively, allowing the average thickness of the scratch to be found.

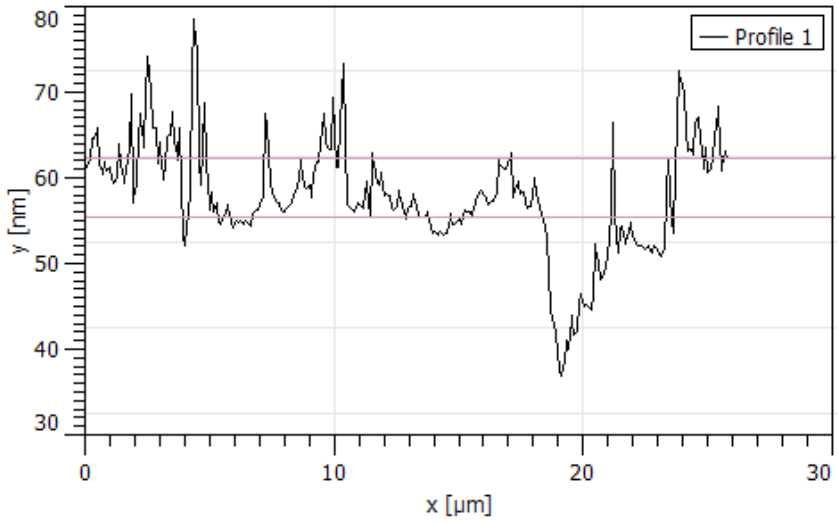

Figure 109: Height profile of the AFM scratch test through a P3HT nanowire film spun on clean silicon.

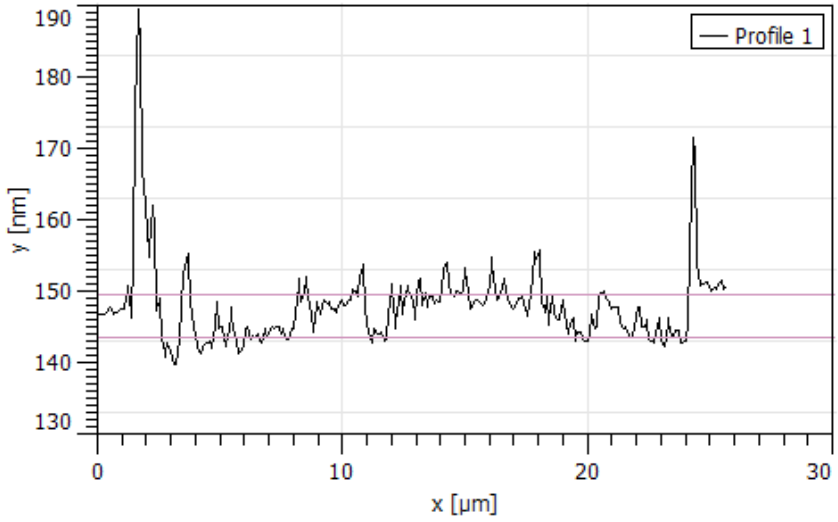

Figure 110: Height profile of the AFM scratch test through a P3HT nanowire film spun on clean silicon.

From these two samples an average thickness of 5.14±0.23nm was found, which corresponds to the nanowires resting ontop of a thin later of amorphous material, or possible another layer of nanowires underneath.

4.4.3. Electrical Characterisation

The electrical characterisation took place on samples of P3HT in chlorobenzene that were spun onto substrates which were comprised of glass with gold contacts evaporated onto them, in general a 5μm channel length was used and therefore will be assumed unless explicitly mentioned.

These glass substrates were placed on a long glass slide which allowed the nanowires to be spun perpendicular or parallel to the channel, depending on which direction the electrodes were affixed to the slide. This means it was possible to compare conductivity across nanowires and across the bulk.

The two orientations of P3HT nanowires are shown in Figure 111 and Figure 112.

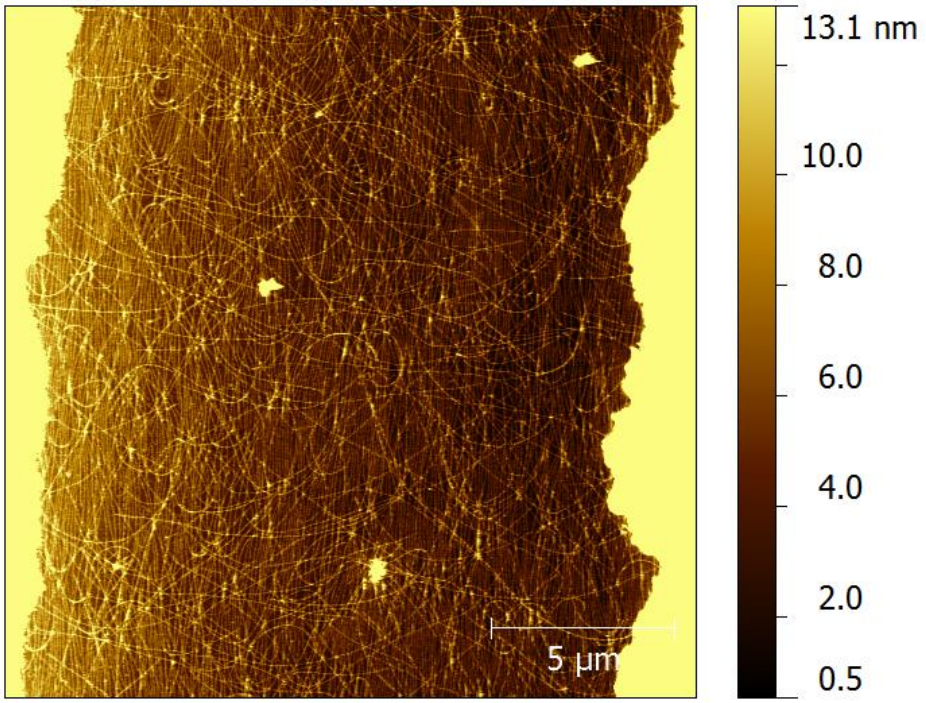

Figure 111: AFM images of P3HT nanowires running parallel (down) the channel.

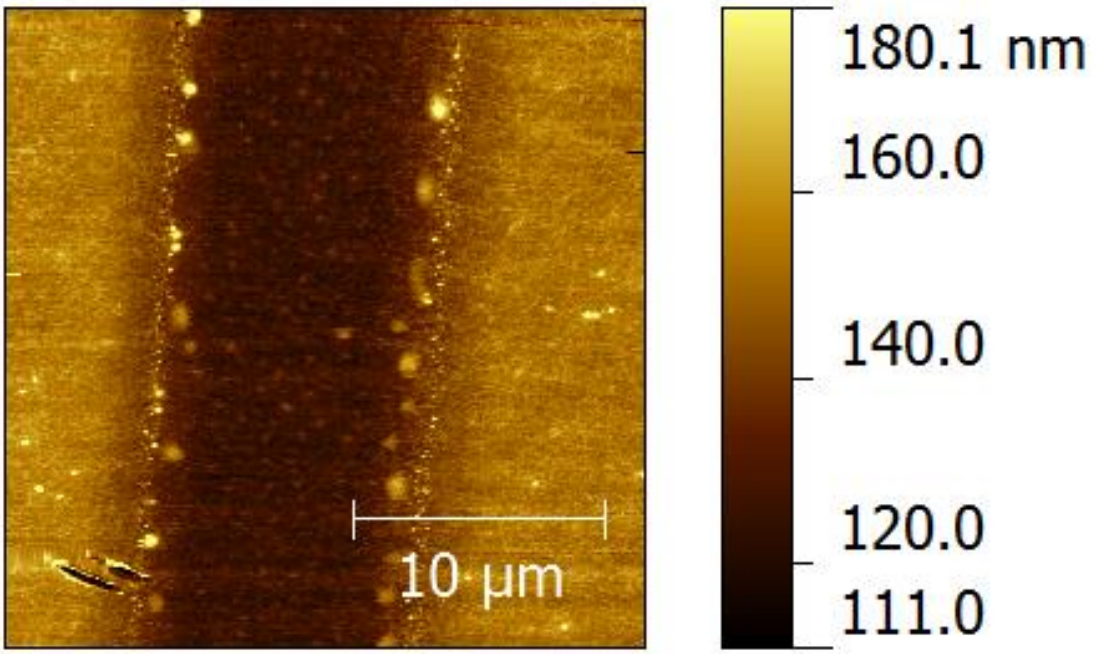

Figure 112: AFM Image showing P3HT nanowires running perpendicular (across) the channel.

The P3HT used was 5 mg/ml M101 rrP3HT and was spun at 4000 rpm onto the substrate, as per the methods discovered in the initial experiments. The voltage sweep was run between 0V to 1V, to -1V to 0V as per the method section and was run over around 10 different samples, 5 of which the nanowires were aligned perpendicular (across the channel) and 5 were aligned parallel (along the channel). These were then averaged and the averages of the currents are shown in Figure 113.

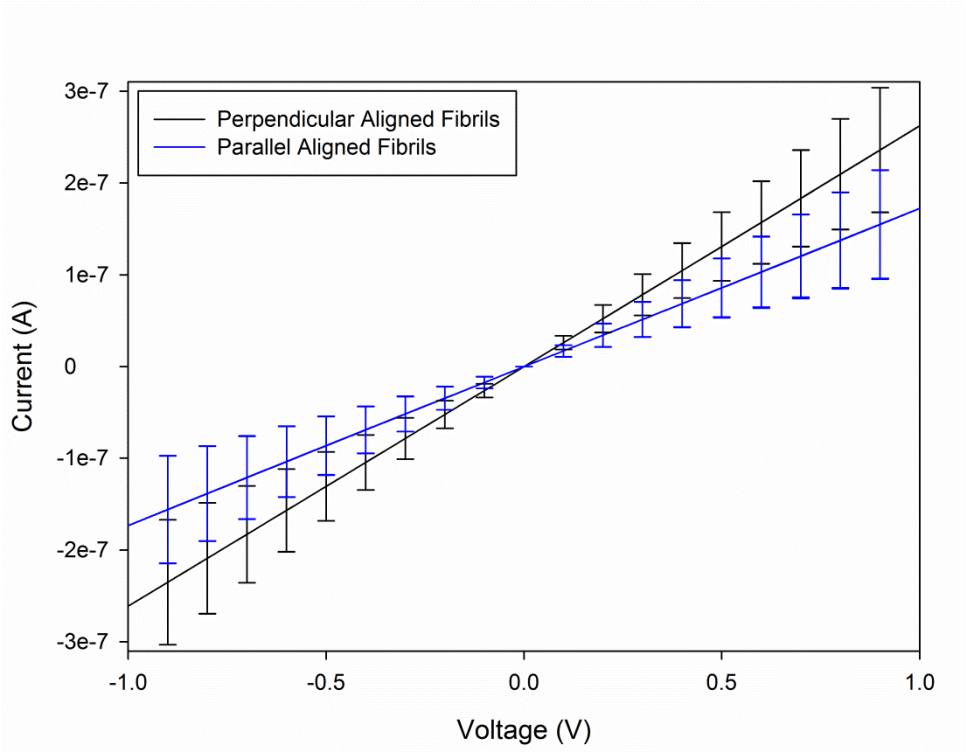

Figure 113: A current voltage graph of 10 averaged measurements of parallel versus perpendicularly aligned nanowires on 5 micron wide channel electrodes.

From this graph we can clearly see that when nanowires run along the channel, they help increase the conductivity of the device, no doubt due to the high mobility along the wire itself, for the nanowires running along the channel, the holes have to "jump" across more nanowire connections and thus the conductivity overall will be lower. This is also supported by the transistor measurements shown later in this thesis.

5. Water-gated organic nanowire transistors

5.1. Introduction

For this research collaboration took place between two research groups in order to investigate utilizing the P3HT nanowires in water-gated transistors. The aim was to gate both p and n-type transistors with an aqueous electric double layer. Both P-type and N-type transistors were tested, however since the scope of this research is using the P3HT nanowires, the P-type transistors only will be mentioned. For these experiments, two different sets of nanowires were used. The ones spun from chlorobenzene that were used in the majority of this thesis, and P3HT nanowires spun from anisole which were provided by the Cardiff soft matter research group.

The use of nanowires rather than a thin film allows for the creation of transistors with lower threshold voltages than the standard thin film design. This has been proven using standard gating techniques and needed to be proved for this aqueous technique. The advantages of using a water based medium rather than the tradition dielectric include the fact that these devices can be used as sensors for detecting waterborne analytes. When exposed to a gate voltage, the liquid analte has mobile ions which form the electric double layer stated above at the region connecting the gate liquid and the semiconductor. This has a very large capacitance which creates a large electric field near the interface, meaning it makes a good gate medium. Any change in the water due to addition of Analytes makes for a large change in output compared to the change in the gate medium.

The nanowires also improve the surface area in comparison to a thin film which in turn should increase the sensitivity to analytes as they have done for similar chemiresistor devices in the past.

For the n-type nanowires, “nanobelts” were grown using poly(benzimidazobenzophenanthroline) (BBL) by utilising a solvent/non-solvent

mixing route, then displacement of the solvent and dispersion in a non-solvent. This will be mentioned briefly as the only part relevant to this thesis was the AFM images taken of the nanobelts, the other research group tested and provided these nanobelts.

5.2. Solution preparation

For the P3HT nanowires used for the majority of this thesis, the nanowires were grown in the standard chlorobenzene solvent at 5mg/mL, the solution was mixed using a magnetic stirrer pip and heated to 80 degrees for 15 minutes to allow the solution to form. The solution was then filtered through a 0.45μm PTFE filter to remove any large non-dissolved P3HT and left in the dark at 18 degrees for one month to allow nanowires to form.

The anisole based nanowires created by the Cardiff group used the whisker method [48]. This method involved 5mg or rrP3HT (sourced from ADS dyes) being dissolved in 1mgk of Anisole. This was then heated to 90 degrees until fully dissolved then left to cool at ambient room temperature for an hour, and left to mature for 3 days.

The BBL nanobelts were formed from poly (benzimidazobenzophenanthroline) (sourced from Sigma Aldrich) which was dissolved at 0.2mg/ml methane sulfonic acid. The growth was not like the P3HT nanowires in that the wires do not self assemble, growth was forced by slowly adding a non-solvent mixture of chloroform and methanol (at a ratio of 4 to 1 respectively) to the BBL solution whilst mixing.

The methane sulfonic acid has to be removed via centrifugation of the solution for 10 minutes at 910g as the acid is not volatile like chloroform and chlorobenzene and thus would re-dissolve the nanowires upon deposition. After centrifugation the nanobelts would settle at the bottom of the vial and the excess solvent ontop was pipette off and replaced with either methanol, ethanol or IPA. It was later shown that either of these alcohols are identical for casting purposes as the nanobelts

disperse well in them. The centrifugation was repeated three times which resulted in the nanobelts suspended in clear solvent which had very little acid.

5.3. Transistor preparation

The nanowires and nanobelts were deposited onto gold electrode pairs as shown in Figure 114. The dimensions are shown in the figure with the main points of a channel widrth 2mm and length 10 μm for the P3HT samples and 20 μm for the larger BBL nanobelts. The gold contacts are 100 nm thick and were prepared via photolithography on top of a 10nm adhesion layer of chrome. This design of contacts with wires extending to the channel meant the overlap between contacts and the water/solvent droplet was minimal in order to reduce parasitic currents across the droplet. The chlorobenzene nanowires were spun ontop of the substrates at 5000 rpm. The anisole nanowires were spun onto the substrates at 2000 rpm and the BBL nanobelts were drop cast with repeat applications of 2 μL droplets of solution onto the substrates and allowed to evaporate until the contacts were covered in BBL nanobelts.

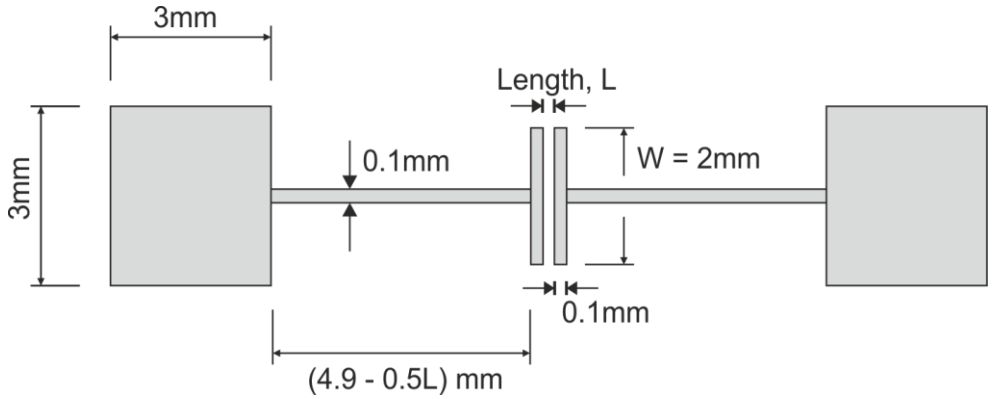

Figure 114: Contact layout for water/solvent gated thin film transistors. Channel length 10 or 20 μm. Width 2mm. The channels are linked to contacts by thin 0.1mm wires, the contacts are 3mm by 3mm square and 100 nm thick and were deposited via photolithography onto insulating Silocon dioxide substrate ontop of a 10 nm chrome adhesion layer (Reprinted from [49] with permission from Elsevier).

5.4. Electrical characterisation setup

The electrical characterisation was performed by collaborating researchers and thus will not be mentioned in a large amount of detail. The testing rig consists of two Tungsten needles being pressed onto the gold contacts using Karl Süss probe heads which allowed them to be the source and drain for the transistor. The gate liquid was deionised water or acetonitrile and was applied (approx 2 μL) dropwise onto the channel. The gate needle was bent into an L shape and placed into the liquid gate material with the L overlapping the channel to act as a gate contact.

The transistor was driven by a sine drive voltage and was connected to a current/voltage converter, this setup is shown in Figure 115. The peak voltage used was 0.8V for the water gate material and 1.1V for the acetonitrile. A frequency of 1HZ was chosen as the electric double layer was slow to form. The output voltages of the samples were recorded on a storage oscilloscope. The setup utilises two Keithley source measure units to measure source/drain and gate voltages.

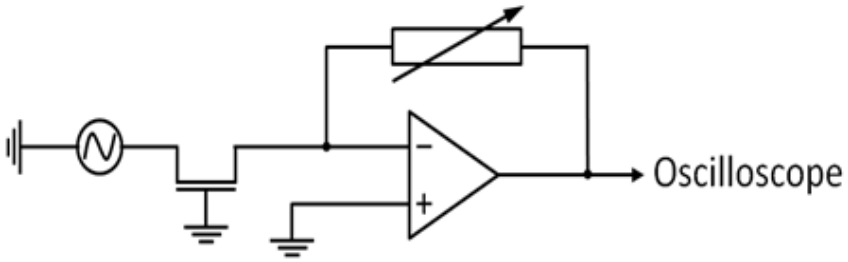

Figure 115: The electrical diagram for the characterisation of the transistor samples. The device was driven by a sine wave source voltage, with a grounded gate and a drain on the virtual ground input of the current voltage converter (Reprinted from [49] with permission from Elsevier).

5.5. AFM Analysis of nanowire samples

For the AFM analysis, a Veeco Dimension 3100 was used to get images of the spun P3HT nanowires on the substrates. The controller used was a Nanoscope IIIa controller with basic extender. The standard tapping mode tips were also used, as mentioned in the experimental methods section.

Figure 116 shows the morphologies of the two P3HT based sets of samples. The top image shows a film cast from the P3HT that was grown in chlorobenzene. These nanowires are rigid and bunch together as can be seen in the figure. Then wires spread and align roughly along the radius of rotation. The anisole nanowires from the bottom image are very different in that they are thinner than the chlorobenzene nanowires and grow into a more branch like structure, rather than the long , much more separate chlorobenzene wires.

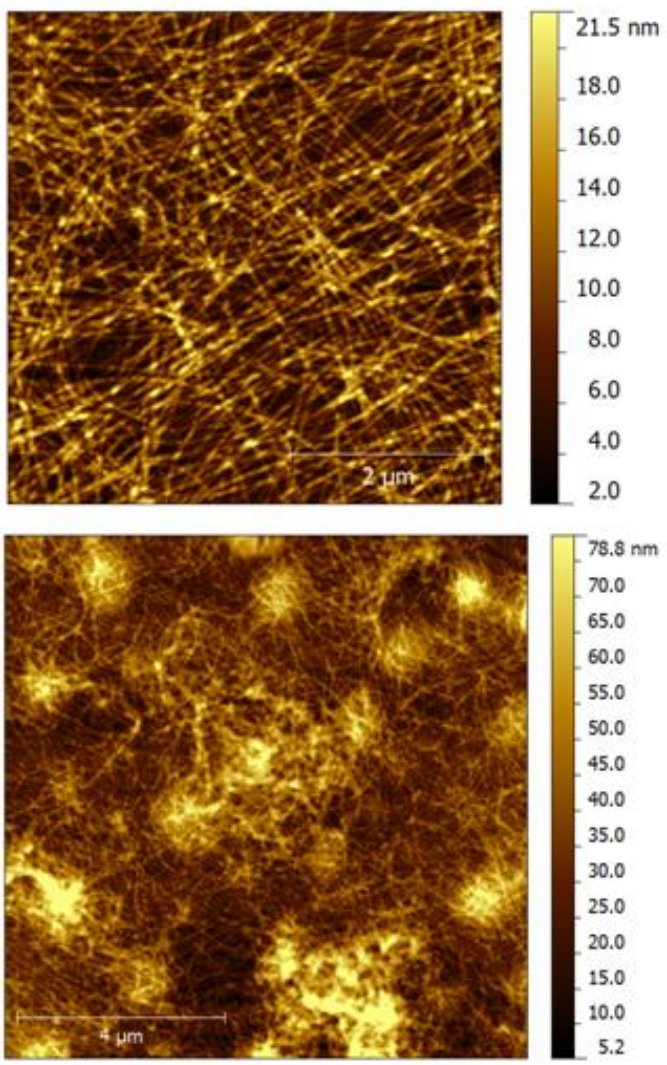

Figure 116: (Top) AFM image of chlorobenzene P3HT nanowires spun onto substrate. 5 mg/ml rrP3HT in chlorobenzene was matured for 1 month then spun at 5000rpm onto the transistor substrate. Image of an area inside the 10µm channel. (Bottom) AFM image of anisole P3HT nanowires spun onto substrate at 2000rpm after aged 3 days (Reprinted from [49] with permission from Elseiver).

Figure 117 shows the morphology of the BBL nanobelts which are more like ribbons than wires. These are larger than nanowires, more densely packed and difficult to AFM and thus microscopy was used as they are easier to image than the much smaller nanowires. From these and similar images it was found that using either of the three alcohols did not produce any morphological differences in the samples.

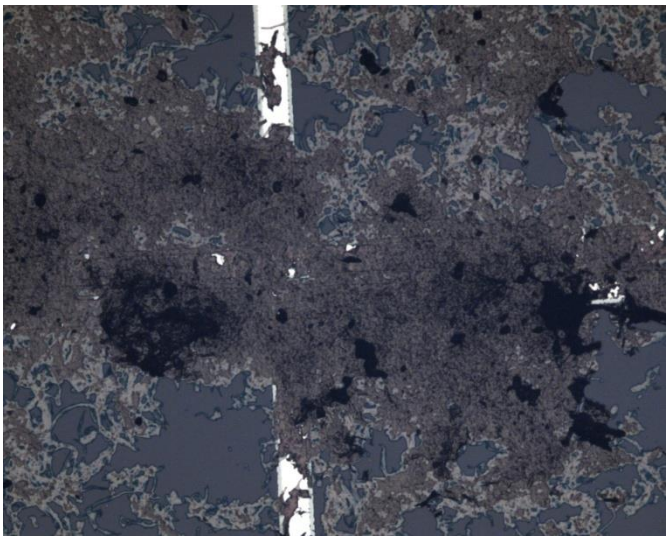

Figure 117: An Optical micrograph of the BBL nanobelts which were cast onto the substrates from IPA. The white line is the channel which is covered completely by the nanobelts (Reprinted from [49] with permission from Elsevier).

5.6. Summary of results obtained

The AFM characterisation clearly shows the differences between morphology based simply on nanowire creation solvent and method. Chlorobenzene produces long, sperate wires that tend to align along a common axis. Whereas anisole nanowires branch out from single "seed points" and do not align due to their branch like nature.

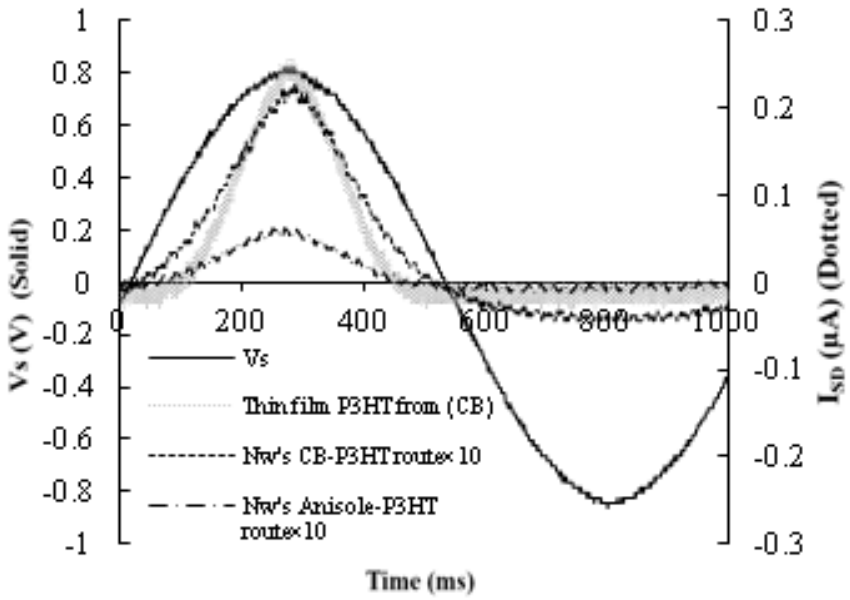

Figure 118: Sinusoidal drive voltage and the resulting source drain current of the water gated chlorobenzene and anisole transistors. The drain current is calculated from the output voltage of the current voltage converter. The source drain current is shown from a standard thin film transistor for comparison and the anisole and chlorobenzene data has been multiplied by 10 for ease of comparison (Reprinted from [49] with permission from Elsevier).

Electrically, comparing the source drain current to a thin film shows the nanowires have a lower saturated drain current overall but comparing the chlorobenzene and anisole nanowires the chlorobenzene based nanowires have a source drain current that is four times as large as the anisole. They both show low threshold voltage transistor characteristics and it can be seen that there is a distinct on cycle for positive voltages and off for negative voltages which is typical for a p-type transistor driven from the source contact.

Both types of P3HT based nanowire thin films can therefore be gated with the electric double layer and work with water gating. The different morphologies did affect the source drain current but both produced transistors with very low threshold voltages (lower than that of the example P3HT thin film transistor). These observations mirror ones found when using conventional gate materials and make water gated transistors viable for use in sensing water borne analytes with as high sensitivities as non water based transistors

6. Final Conclusions and Further Work

The work that has been presented in this thesis covers a large range of experimental methods and techniques as well as numerous different nanoscale materials. It has covered important techniques for analysis of nanoscale materials (namely P3HT nanowires) such as Atomic Force microscopy, which is very useful for studying the length scales on solid substrates at nanoscale. However it can be limited due to the surface only scanning nature of AFM. Neutron scattering also played a large part as it allowed the solutions to be probed to investigate growth of nanowires at smaller length scales. UV-Vis was also useful to confirm the existence of and investigate the growth of nanowires and what happens during deposition. Electrical measurements were also taken in order to investigate the conductivity of nanowires and how the orientation across a channel affected this

Various different deposition and cleaning methods were investigated and an optimal solvent, solvent concentration, cleaning method and deposition method were found for optimal alignment of the P3HT nanowires. Further to this, after finding the optimal production methods the nanowires were analysed through a number of methods to determine growth and size compared to literature.

Finally through collaboration the effects of including P3HT nanowires in transistor water gated sensors was investigated and nanowires were found to increase the sensitivity of said transistors, compared to traditional thin film transistors.

The most important discoveries and innovations are shown below:

a. Length scales of P3HT nanowires correspond to chain length and molecular weight and can be measured well via Atomic force microscopy
b. The optimal solvent for long aligned nanowires was found to be chlorobenzene, at an optimal growth concentration of 5mg/ml.
c. In chlorobenzene, at least a couple of days is needed for sufficient nanowire growth for AFM. However the longer left, the more nanowires grow, to a large mesh at

months. This is limited by the amount of material however but studies show that at least a month will still cause nanowires to grow.

d. The optimal deposition method is spin coating for P3HT nanowires in solution, as it removes the amorphous molecularly dissolved P3HT and at distances greater than a few cm away from the centre of rotation, also aligns the nanowires.
e. Neutron scattering is a very important and useful tool which has allowed the nanowire growth at very small length scales to be probed in solution, where it was not possible with conventional light scattering methods. Neutron scattering confirmed some early predictions about nanowire growth, in that seeding or cooling nanowires will promote growth and heating to high temperatures causes a large portion of the nanowires to re-dissolve back into molecularly dissolved P3HT.
f. P3HT nanowires enhance the properties of water gated transistors if spun across the channel, in comparison to standard thin films of P3HT.

In addition to these conclusions, further work done on this research area are proposed below:

i. Further study into the electrical properties of the nanowires with regards to vapour sensing, as the additional surface area of the nanowires should help increase sensitivity to vapours.
ii. Expanded neutron scattering study into P3HT nanowire growth in different solvents. As there is a difference between nanowires grown in chlorobenzene to those grown in a solvent such as chloroform.
iii. Possible applications into solar cells if nanowires could be combined with PCBM or another similar material. This would mean a mix of amorphous P3HT and nanowires could be mixed to give the best mixing and thus potentially improve devices.

References

1. Ma, W., et al., *Thermally Stable, Efficient Polymer Solar Cells with Nanoscale Control of the Interpenetrating Network Morphology.* Advanced Functional Materials, 2005. **15**: p. 1617-1622.
2. Ellis, D.L., et al., *Conductive Polymer Films as Ultrasensative Chemical Sensors for Hydrazine and Monomethylhydrazine Vapor.* Analytical Chemistry, 1996. **68**(5): p. 817-822.
3. Li, B., et al., *Volatile Organic Compound Detection Using Nanostructured Copolymers.* Nano Letters, 2006. **6**(8): p. 1598-1602.
4. Clayden, T., et al., *Organic Chemistry*, ed. O.U. Press. 2001.
5. Kim, J.S., et al., *Poly(3-hexylthiophene) Nanorods with Aligned Chain Orientation for Organic Photovoltaics.* Advanced Functional Materials, 2010. **20**(4): p. 540-545.
6. Grell, M., *Masters Courses in Nano Technology: Organic Semiconductors (Phy6007)*. 2010, University of Sheffield: Sheffield.
7. *Hybridised Carbon Bonds*. Available from: www.nyu.edu.
8. *Illustration of Carbon Hybrid Orbitals*. Available from: http://www.chem.umass.edu/.
9. Roncali, J., *Conjugated Poly(thiophenes): Synthesis, Functionalization, and Applications.* Chemical Reviews, 1992. **92**(4): p. 711-738.
10. Dag, S. and L.-W. Wang, *Packing Structure of Poly(3-hexylthiophene) Crystal: Ab Initio and Molecular Dynamics Studies.* Journal of Physical Chemistry B, 2010. **114**: p. 5997-6000.
11. Suzuki, Y., K. Tajima, and S.-J. Kang. *Regioregularity Control in Semiconducting Polymers*. 2007; Available from: http://www.light.t.u-tokyo.ac.jp/english/photovoltaic/Regioregular_Polymers.html.
12. Watanabe, S.-i., et al., *Direct determination of interfacial molecular orientations in field-effect devices of P3HT/PCBM composites by electron spin resonance.* Organic Electronics, 2011. **12**(4): p. 716-723.
13. Merlo, J.A. and C.D. Frisbie, *Field Effect Transport and Trapping in Regioregular Polythiophene Nanofibers.* Journal of Physical Chemistry B, 2004. **108**: p. 19169-19179.
14. Savenije, T., et al., *The formation of crystalline P3HT fibrils upon annealing of a PCBM:P3HT bulk heterojunction.* Thin Solid Films, 2006. **511-512**: p. 2-6.
15. Paul Scherrer Institute, M.G. *Spin Coating*. Available from: http://materials.web.psi.ch/Research/Thin_Films/Methods/Spin.htm.
16. Richardson, T., *Langmuir-Blodgett Films*, in *Introduction to Molecular Electronics*, M.C. Petty, M.R. Bryce, and D. Bloor, Editors. 1995, Edward Arnold: London. p. 220-242.
17. Brittle, S.A., *Selective Vapour Sensing Using Nanoscale Porphyrin Films*, in *Physics and Astronomy*. 2009, University of Sheffield: Sheffield.

18. Im, J., et al., *A hybrid chemiresistive sensor system for the detection of organic vapors.* Sensors and Actuators B: Chemical, 2011. **156**(2): p. 715-722.
19. Saxena, V., et al., *Enhanced NO 2 selectivity of hybrid poly(3-hexylthiophene): ZnO-nanowire thin films.* Applied Physics Letters, 2007. **90**(4).
20. He, M., et al., *Fabricating polythiophene into highly aligned microwire film by fast evaporation of its whisker solution.* Polymer, 2010. **51**(10): p. 2236-2243.
21. Scavia, G., et al., *Micro-contact printing of poly(3-hexylthiophene) on silicon oxide: Effect of stamp stretching.* European Polymer Journal, 2010. **46**(8): p. 1660-1670.
22. Kim, S.-S., et al., *Annealing-free fabrication of P3HT:PCBM solar cells via simple brush painting.* Solar Energy Materials and Solar Cells, 2010. **94**(2): p. 171-175.
23. Greifswald. Available from: www3.physik.uni-greifswald.de.
24. *Atomic Force Microscopy- A guide to understanding and using the AFM.* Galloway Group, 2004.
25. Bullen, H.A. *Introduction to Scanning Probe Microscopy*. Available from: http://physwiki.ucdavis.edu/Wikitexts/UCD_BPH241/AFM_on_Membranes.
26. Wilson, R.A. and H.A. Bullen, *Introduction to Scanning Probe Microscopy (SPM) - Basic Theory: Atomic Force Microscopy (AFM).* Department of Chemistry, Northern Kentucky University.
27. Knoll, A., R. Magerle, and G. Krausch, *Tapping Mode Atomic Force Microscopy on Polymers: Where Is the True Sample Surface?* Macromolecules, 2001. **34**: p. 4159-4165.
28. Blanchard, C.R., *Atomic Force Microscopy.* The Chemical Educator, 1996. **1**(5): p. 1-8.
29. García, R. and R. Pérez, *Dynamic atomic force microscopy methods.* Surface Science Reports, 2002. **47**: p. 197-301.
30. Rogers, D.S. *Sans2d information page*. Available from: http://www.isis.stfc.ac.uk/instruments/sans2d/sans2d3000.html.
31. Sivia, D.S., *Elementary Scattering Theory, For X-ray and Neutron Users*. 2011, Oxford: Oxford University Press.
32. ISIS. *Small Angle Neutron Scattering*. Available from: http://www.isis.stfc.ac.uk/instruments/small-angle-scattering2573.html.
33. King, S.M., *Small Angle Neutron Scattering.* Large-Scale Structures, 1995.
34. Hammouda, B., *A new Guinier-Porod Model.* Journal of Applied Crystallography, 2010. **43**: p. 716-719.
35. Heenan, R.K., *SASView Help File*.
36. *Introduction to Ultra-Violet Visible Spectroscopy (UV)*. 2009; Available from: http://www.le.ac.uk/spectraschool/sias/Introduction%20to%20UV-Vis%20Spectroscopy.pdf.

37. Jemmis, E.D., et al., *Bond length and bond multiplicity: [sigma]-bond prevents short [small pi]-bonds.* Chemical Communications, 2006(20): p. 2164-2166.
38. *Basic UV-Vis Theory, Concepts and Applications*. Structural Biology Initative; Available from: http://sbio.uct.ac.za/Sbio/documentation/spectrophotometer.pdf.
39. Zhao, K., et al., *A New Method to Improve Poly(3-hexyl thiophene) (P3HT) Crystalline Behavior: Decreasing Chains Entanglement To Promote Order−Disorder Transformation in Solution.* Langmuir, 2010. **26**(1): p. 471-477.
40. Kingsley, J., *Ossila*.
41. Nanofab, *Veeco Dimension 3100 operating manual*.
42. Heenan, R.K., et al., *Small Angle Neutron Scattering Using Sans2d.* Neutron News, 2011. **22**(2): p. 19-21.
43. *ISIS Website*. Available from: http://www.isis.stfc.ac.uk.
44. *Mantid Project*. Available from: http://www.mantidproject.org.
45. Wignall, G.D. and F.S. Bates, *Neutrons in Soft Matter.* Journal of Applied Crystallography, 1987. **20**: p. 28.
46. Hague, L., *The Vapour Sensing Capabilities of Organic Field-Effect Transistors*, in *Physics and Astronomy*. 2012, University of Sheffield: Sheffield.
47. Oosterbaan, W.D., et al., *Efficient formation, isolation and characterization of poly(3-alkylthiophene) nanofibres: probing order as a function of side-chain length.* Journal of Materials Chemistry, 2009. **19**(30): p. 5424.
48. Chen, C.-Y., et al., *Formation and Thermally-Induced Disruption of Nanowhiskers in Poly(3-hexylthiophene)/Xylene Gel Studied by Small-Angle X-ray Scattering.* Macromolecules, 2010. **43**(17): p. 7305-7311.
49. Al Naim, A., et al., *Water-gated organic nanowire transistors.* Organic Electronics, 2013. **14**: p. 1057-1063.

Acknowledgements

The author would like to acknowledge a great number of people for the support and assistance in completing this thesis. He would first and foremost like to thank his late supervisor, Dr Tim Richardson, without whom he would not have undertaken his PhD. The author would also like to acknowledge his current supervisors, Dr Alan Dunbar and Dr Martin Grell, who have shown an enormous amount of patience [throughout the author's degree and again, the author is certain he would not be in the position he is in without the help, support and guidance of both of them.

The author would also like to thank all the PhD students in the D44 office, there are too many to mention but each and every one of you have helped get the author through the PhD, whether it be a friendly chat, help with experiments, or simply getting a cup of coffee when thinks get rough.

The author would also like to thank his partner, Paolo Cattaneo for the constant support, love and patience throughout the course of the PhD, especially during the stressful thesis writing period. He would also like to thank his family for the understanding, support and guidance. Especially on the worst days when things looked bleak, my mother, father and sister would pick me up and get me back on track.

The author would also like to thank any collaborators from the past such as Dr Sarah Rodgers from ISIS, Dr Andy Parnell, the whole technician staff and porters at the Hicks building, Dr Jamie Hobbs for allowing unprecedented access to the AFM suite in the Hicks building. To anyone else I may have missed, I thank you all for the help and support on my journey through research.